Spring 5-14-2016

Combinatorial Growth Factor Signaling Controls Nephron Progenitor Renewal and Differentiation

Sree Deepthi Muthukrishnan
MMCRI, muthus@mmc.org

COMBINATORIAL GROWTH FACTOR SIGNALING CONTROLS NEPHRON PROGENITOR RENEWAL AND DIFFERENTIATION

By

Sree Deepthi Muthukrishnan

M.S. University of Madras, 2009

A DISSERTATION

Submitted in Partial Fulfillment of the

Requirements for the Degree of

Doctor of Philosophy

(in Biomedical Sciences)

The Graduate School

The University of Maine

May 2016

Advisory Committee:

Dr. Leif Oxburgh, Scientist III, Maine Medical Center Research Institute, Advisor

Dr. Robert Friesel, Director, Center for Molecular Medicine, Maine Medical Center Research Institute

Dr. Calvin Vary, Scientist III, Maine Medical Center Research Institute

Dr. Jeong Yoon, Scientist II, Maine Medical Center Research Institute

Dr. Todd Valerius, Scientist, Brigham and Women's Hospital

DISSERTATION ACCEPTANCE STATEMENT

On behalf of the Graduate Committee for Sree Deepthi Muthukrishnan, I affirm that this manuscript is the final and accepted dissertation. Signatures of all committee members are on file with the Graduate School at the University of Maine, 42 Stodder Hall, Orono, Maine.

Dr. Leif Oxburgh, Scientist III, Maine Medical Center Date:

LIBRARY RIGHTS STATEMENT

In presenting this thesis in partial fulfillment of the requirements for an advanced degree at The University of Maine, I agree that the Library shall make it freely available for inspection. I further agree that permission for "fair use" copying of this thesis for scholarly purposes may be granted by the Librarian. It is understood that any copying or publication of this thesis for financial gain shall not be allowed without my written permission.

Signature:

Date:

COMBINATORIAL GROWTH FACTOR SIGNALING CONTROLS NEPHRON PROGENITOR RENEWAL AND DIFFERENTIATION

By Sree Deepthi Muthukrishnan

Dissertation Advisor: Dr. Leif Oxburgh

An Abstract of the Dissertation Presented
in Partial Fulfillment of the Requirements for the
Degree of Doctor of Philosophy
(in Biomedical Sciences)
May 2016

Self-renewal and differentiation of nephron progenitor cells (NPCs) in the developing kidney is governed by three major growth factor pathways: BMP, FGF and WNT. Mechanisms underlying the cross-talk between these pathways at the molecular level are largely unknown.

In this study, we demonstrate that BMP7 activates SMAD1/5 signaling in the distal region of the cap mesenchyme (CM) to promote the transition of early CITED1+ NPCs into the SIX2-only compartment. BMP7-mediated SMAD1/5 signaling synergizes with WNT9b-β-catenin signaling in SIX2-only cells to induce the pro-differentiation program via *Wnt4* activation. We show that the pharmacological inhibition of SMAD1/5 signaling retains the NPCs in the CITED1+ progenitor state, delays cessation of nephrogenesis and increases nephron endowment in mice.

We also delineate the pathway through which the proliferative BMP7 signal is transduced in CITED1+ NPCs. BMP7 activates the MAPKs TAK1 and JNK to phosphorylate the transcription factor JUN, which in turn governs the transcription of an AP-1 element containing G1 phase cell cycle regulators such as *Myc* and *Ccnd1* to promote NPC proliferation. Conditional inactivation of *Tak1* or *Jun* in the cap mesenchyme causes identical phenotypes characterized by premature depletion of NPCs. While JUN is regulated by BMP7, we find that its partner FOS is regulated by FGF9. We demonstrate that BMP7 and FGF9 coordinately regulate AP-1 transcription to promote G1-S cell cycle progression and NPC proliferation. Our findings identify a molecular mechanism explaining the important cooperation between two major NPC self-renewal pathways.

ACKNOWLEDGMENTS

I would like to thank my mentor Dr. Leif Oxburgh for his guidance, motivation and encouragement to pursue my research interests and for providing a nurturing environment to help me grow as a scientist.

All the members of the Oxburgh laboratory for aiding in my growth with their valuable suggestions and inputs on experiments and presentations, and for making the lab a fun place to work.

My thesis advisory committee for their support and guidance with grants, publications, and feedback on my dissertation work.

Dr. Robert Friesel and Dr. Xuehui Yang for sharing reagents and mice, which greatly helped me in completing my thesis work.

The Graduate School of Biomedical Sciences and Engineering for providing me the opportunity to pursue a PhD in a diverse and stimulating research environment.

The Maine Medical Center Research Institute for creating a warm, friendly and collaborative atmosphere for graduate students and offering a unique training program that enhances research skills and helps in professional development.

TABLE OF CONTENTS

LIST OF TABLES

LIST OF FIGURES

LIST OF ABBREVIATIONS

CKD - Chronic Kidney Disease

UB - Ureteric Bud

MM - Metanephric Mesenchyme

CD - Collecting Duct

CM - Cap Mesenchyme

NZC - Nephrogenic Zone Cell

NPC - Nephron Progenitor Cell

PTA - Pre-Tubular Aggregate

RV - Renal Vesicle

MET - Mesenchymal-to-Epithelial Transition

CI - Cortical Interstitium

PAX2 - Paired-box homeotic transcription factors 2

SIX2 - Sine-Oculis homeobox homolog 2

CITED1 - Cbp/p300-interacting transactivator 1

WT1 - Wilm's tumor suppressor 1

LEF1 - Lymphoid Enhancer-Binding Factor 1

WNT4 - Wingless -Type MMTV Integration Site Family member 4

FOXD1 - Forkhead Domain Transcription factor 1

BMP4 - Bone Morphogenetic Protein 4

RA - Retinoic Acid

FAT4 - FAT Atypical Cadherin 4

FLK - Fetal Liver Kinase 1

VEGF - Vascular Endothelial Growth Factor

BMP7 - Bone Morphogenetic Protein 7

FGF9 - Fibroblast Growth Factor family member 9

FGF20 - Fibroblast Growth Factor family member 20

WNT9b - Wingless -Type MMTV Integration Site Family member 9B

TGF-β - Transforming Growth Factor-beta

MAPK - Mitogen- Activated Protein Kinase

MAP3K7 - Mitogen-Activated Protein Kinase Kinase Kinase 7

SMAD - Mothers against DPP homolog 1

R-SMAD - Receptor-regulated SMAD

Co-SMAD - Common-mediator SMAD

TAK1 - TGFβ-activated kinase 1

JNK - c-JUN N-Terminal Kinase 1

GS - Glycine-Serine Rich domain

ALK2/3/6 - Activin Receptor-Like Kinase 2, 3 and 6

ACVR2A - Activin A Receptor Type II A

ACVRB - Activin A Receptor Type II B

BMPR2 - Bone Morphogenetic Protein Receptor, Type II

BMPER - BMP Binding Endothelial Regulator

CV2 - Cross Veinless 2

TWSG - Twisted Gastrulation

ATF2 - Activating Transcription Factor 2

FGF2 - Fibroblast Growth Factor family member 2

FGF8 - Fibroblast Growth Factor family member 8

FGFR - Fibroblast Growth Factor Receptors

PI3K - Phosphoinositide -3 (PI3) kinase

PKB - Protein Kinase B

FRS2 - Fibroblast Growth Factor Receptor Substrate 2

HSPG - Heparan Sulfate Proteoglycan

HS2ST1 - Heparan Sulfate 2-O-Sulfotransferase 1

ERK - Extracellular signal-regulated Kinase

CASK - Calcium/Calmodulin dependent serine protein kinase 1

DLG1 - Discs-Large homolog 1

SPRY1 - Sprouty Homolog 1

MEK2 - MAPK/ERK kinase 2

GSK3β - Glycogen Synthase Kinase 3-beta

TCF - T-cell Factor 1

LRP - Low Density Lipoprotein Receptor-Related Protein

DVL - Dishevelled

ROR2 - Receptor Tyrosine Kinase-Like Orphan Receptor 2

RYK - Receptor-Like Tyrosine Kinase

NLK - Nemo-Like Kinase

NFAT - Nuclear Factor of Activated T-Cells

pHH3 - Phospho-Histone H3

GUDMAP - Genitourinary Development Molecular Anatomy Project

AP-1 - Activating Protein 1

FOS - FBJ murine osteosarcoma gene

FRK - Fos-Related Kinase

TRE - TPA- Responsive Element

SRE - Serum Response Element

SRF - Serum Response Factor

ELK - ETS domain containing protein

MYC - V-Myc Avian Myelocytomatosis Viral Oncogene Homolog

BCL2 - B-cell Lymphoma 2

BIM - Binding of Microtubules

CCND1/2/3 - Cyclins D1, D2 and D3

CCNE1 - Cyclin E1

PCNA - Proliferating Cell Nuclear Antigen

EdU - 5’-Ethynyl-2’deoxy-uridine

DPF3 - D4, Zinc and Double PHD Fingers, Family 3

MEOX1 - Mesenchyme Homeobox 1

SFRP1 - Secreted Frizzled Related protein 1

CDC25A - Cell Division Cycle 25a

CCNA2 - Cyclin A2

CDKN1A/ P21 - Cyclin-Dependent Kinase Inhibitor 1A

CDKN1B /P27 - Cyclin-Dependent Kinase Inhibitor 1B

EGFP - Enhanced Green Fluorescent Protein

DM - Dorsomorphin

BSA - Bovine Serum Albumin

DAPI - 4',6-diamidino-2-phenylindole

KSFM - Keratinocyte Serum Free Media

DMSO - Dimethyl Sulfoxide

MOI - Multiplicity of Infection

TUNEL - Terminal deoxynucleotidyl transferase (TdT)-mediated dUTP nick end labeling

H&E - Hematoxylin and Eosin

CHAPTER 1

INTRODUCTION

1.1. Overview of mammalian kidney development

1.1.1. Kidney structure and function

Kidneys are bean-shaped, bilateral organs composed of three different layers: an outer fibrous layer called the renal capsule, a peripheral layer called the cortex, and an inner layer called the medulla. Nephrons, the structural and functional units of the kidney, are localized within the cortex and the medulla. A typical nephron contains two major components: the glomerulus and the tubular epithelium (Figure 1.1)[1,2]. The major functions of the kidney include excretion of waste from blood in the form of urine, regulating blood pressure, electrolyte balance and red blood cell production.

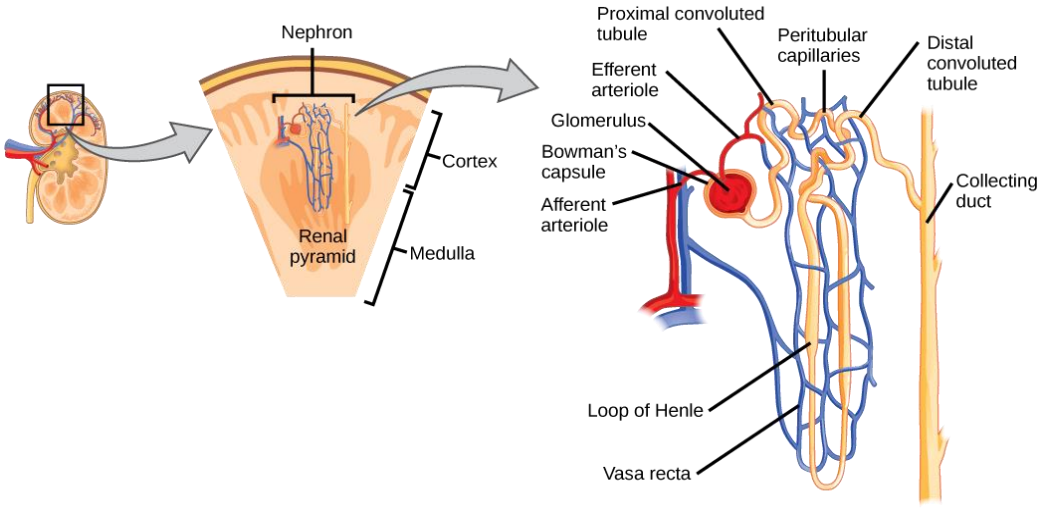

Figure 1.1: Anatomy of an adult kidney: Cross-section of a kidney showing the localization of nephrons in the cortex and medulla and the structural components of a nephron[3].

A human kidney has anywhere between 200,000 and 2 million nephrons, displaying a 10-fold variability in number[4]. A reduced nephron number is associated with hypertension and chronic kidney disease (CKD) in adult life. The final nephron number is determined during the embryonic period by two key factors: the growth and branching of the collecting duct (CD) and the supply of nephron progenitor cells (NPCs) that give rise to the tubular epithelial system of the nephrons[5-7]. Nephrogenesis ceases at 36th week of pregnancy in humans and shortly after birth in mice, with no evidence of *de novo* nephron formation in the adult kidney. Therefore, the final complement of nephrons is established during embryonic development[8]. Determining the molecular underpinnings governing NPC renewal and differentiation in the embryonic kidney will be essential for our understanding of renal organogenesis and disease.

1.1.2. Metanephric kidney development

In mice, the formation of a permanent metanephric kidney begins at embryonic day 10.5 (E10.5), when a subset of metanephric mesenchyme (MM) cells is induced by a permissive signal from the invading ureteric bud (UB) to condense and form a 4-5 cell layer thick, morphologically distinguishable structure from the more peripheral MM, called the capping or cap mesenchyme (CM)[9-11]. Genetic ablation experiments revealed that *Wnt9b* secreted from the UB acts as an inducer of the condensation of the MM[12]. The UB induces the NPCs within the CM to undergo mesenchymal to epithelial transition (MET) to form the epithelial components of the nephron[13]. Reciprocally, CM signals promote iterative branching of the UB to form the CD system, and thus the formation of the permanent metanephric kidney is initiated at E11.5 (Figure 1.2)[9-14].

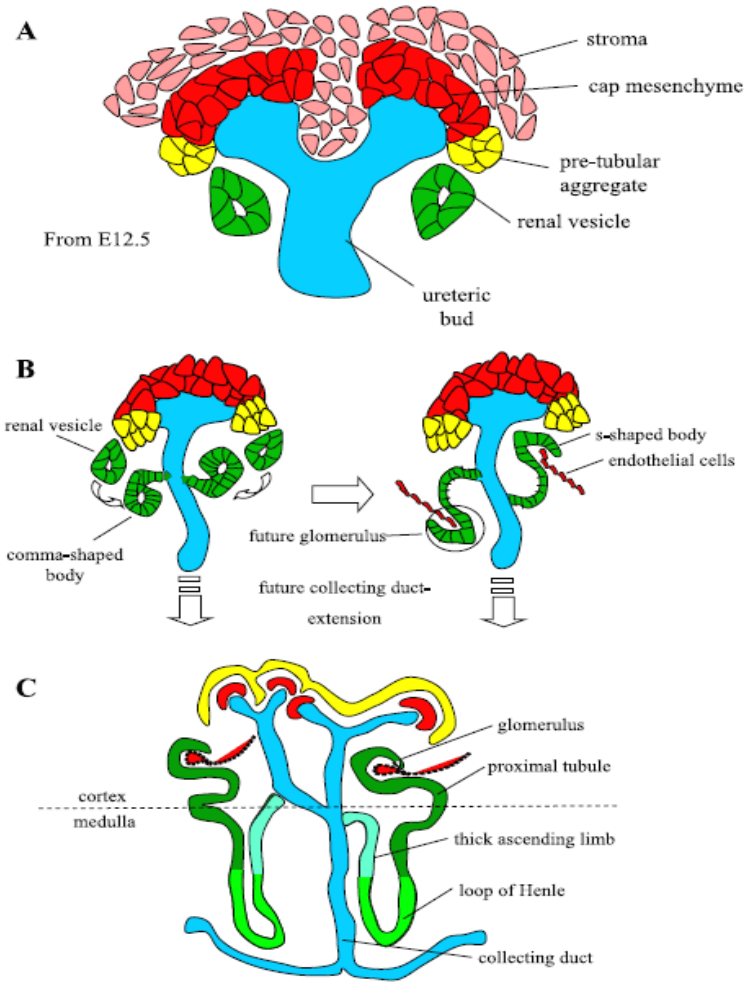

Figure 1.2: Stages of metanephric kidney development: A) At E11.5, the cap mesenchyme (CM) cells condense around the ureteric bud (UB) tip and become distinct from the surrounding cortical stromal mesenchyme. Signals from the UB induce the CM cells to differentiate, resulting in the appearance of the first pre-tubular aggregate underneath the tips. B) The renal vesicle (RV) is evident as polarized columnar epithelial cells at E12.5, following which it elongates to form the comma- and S-shaped bodies. The distal segment of the RV fuses with the UB epithelium, and the endothelial cells invade the glomerular cleft of the S-shaped body. *C)* After E16.5*,* there is increased growth and patterning of nephron segments associated with expansion of the renal cortex and patterning of the medullary region of the kidney[14].

1.1.3. Compartmentalization of cap mesenchyme

Within the CM, the transcription factor *Six2* (Sine-oculus homeobox homolog 2) is strongly expressed in the undifferentiated NPCs and becomes down-regulated upon differentiation[15]. *Six2*-deficient kidneys exhibit precocious differentiation leading to ectopic nephrogenesis and premature depletion of NPCs, indicating that *Six2* is essential for maintaining the "stemness" or progenitor state and self-renewal of NPCs[15,16]. *Cited1* (Cbp/p300-interacting transactivator 1), a transcriptional regulator is also expressed in the early undifferentiated NPCs[17]. Inactivation of *Cited1* has no effect on kidney development, suggesting that *Cited1* is not essential for the maintenance or self-renewal of NPCs[26]. Fate mapping studies have established that the population of CM cells expressing *Cited1* and *Six2* marks the undifferentiated multipotent and self-renewing NPCs that generate all of the epithelial components of the nephron (tubular epithelium, podocytes) and do not contribute to non-epithelial lineages within the adult kidney[16,18].

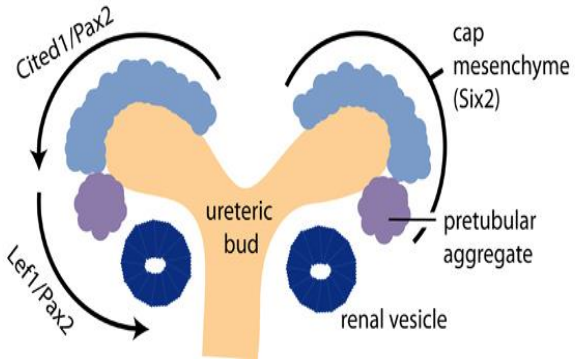

Figure 1.3: Cap mesenchyme sub-compartments: The early progenitor compartment within the cap mesenchyme express CITED1, PAX2 and SIX2 (light blue). The pre-tubular aggregate (purple) compartment continues to express PAX2 and low level SIX2, and acquires expression of LEF1. Epithelialized renal vesicles (dark blue) express LEF1 and PAX2[21].

Microanatomical and gene expression studies have demonstrated that the CM can be sub-divided into the capping or un-induced mesenchyme (*Six2*+, *Cited1*+), which is spatially restricted to the cortical aspect of the collecting duct tips and the induced mesenchyme or pre-tubular aggregates (PTA) (*Six2*+, *Cited1*- *Lef1*+) localized to the distal or medullary region under the CD tips[19,20]. PTAs subsequently undergo MET to form a single epithelial renal vesicle (RV, *Wnt4*+), an early precursor of the nephron (Figure 1.3)[19-21]. Although these structures can be identified as morphologically distinct entities in histological sections, the transition from the un-induced CM to the induced PTA and RV represents a continuum of differentiation states[9-13]. The functional epithelial nephrons form via the elongation, segmentation and patterning of the RV to the comma and S-shaped body stages, after which the distinct tubule segments arise, separated by the loop of Henle[9-13].

The non-condensed mesenchymal cells of the MM express the forkhead transcription factor *Foxd1* and represent the metanephric stromal progenitor population. *Foxd1*+ cortical stromal progenitors are molecularly distinct from the *Six2*-expressing NPCs[22-24]. Lineage tracing analyses have shown that *Foxd1*-expressing stromal cells represent a multipotent, self-renewing progenitor pool that give rise to the non-epithelial vascular smooth muscle cells, mesangial cells and mature stromal interstitial cell types in the kidney[25,26]. Stromal progenitor-derived signals (Retinoic acid, FGFs, BMP4, and FAT4) are crucial for UB branching, NPC maintenance and differentiation[27].

In addition to the CM and stroma, a population of *Flk1*-expressing angioblasts/vascular precursors is present within the early MM. *Flk*+ angioblasts cluster around the UB, and VEGF signaling from these cells is integral to the development of the glomerular tuft[27,28].

Coordinated development and reciprocal signaling interactions between the UB, CM, stroma and endothelial precursors ensures that a full complement of functional nephrons is established before the cessation of nephrogenesis at postnatal day 3 (P3). Between P2 and P3, the CM markers SIX2 and CITED1 disappear, and the NPCs are terminally exhausted. With this, the kidney loses the capacity for *de novo* nephrogenesis[8]. The signaling mechanisms involved in the alteration of the balance between NPC self-renewal and commitment to differentiation during the cessation of nephrogenesis is poorly understood.

1.2. Molecular regulation of NPC self-renewal and differentiation

The self-renewal and differentiation of NPCs are combinatorially regulated by multiple growth factor signaling pathways, including Bone Morphogenetic Protein 7 (BMP7), Fibroblast Growth Factor (FGF) 9/20, and Wingless-Type MMTV Integration Site Family member 9b (WNT9b).

1.2.1. BMP7 signaling

BMP7 belongs to the transforming growth factor-β (TGF-β) superfamily and binds to type I and type II transmembrane serine-threonine kinase receptors to activate the canonical SMAD and non-canonical MAPK signaling pathways (Figure 1.4)[29,30].

Although several BMP ligands (BMPs 2, 4, 6 and 7) are expressed in the embryonic kidney, *Bmp7* is exclusively expressed in the CM and CD cells[32-34]. *Bmp7* null mice display premature arrest in kidney development by E16.5 due to cell death and the early

depletion of CM, suggesting that BMP7 is required for the maintenance and self-renewal of NPCs[33,34]. Organ explant experiments also demonstrated that BMP7 acts as a survival factor for the maintenance of the CM[45]. UB-MM separation experiments suggested that CD signaling is necessary to maintain the CM expression of *Bmp7,* and WNT9b secreted from the UB may be involved in this function[36,37]. Global conditional inactivation of *Bmp7* at E12.5, after the onset of metanephric kidney development, recapitulated the *Bmp7* null phenotype, confirming that BMP7 is required during metanephrogenesis[38].

The BMP signal is transduced by the type I BMP receptors ALK2, ALK3 and ALK6[29,30]. Conditional inactivation of *Alk3* in the early MM using *Rarb2-cre* results in hypomorphic kidneys[39]. However, cell death and premature depletion of NPCs, which are characteristic of the *Bmp7* null phenotype, are not features of this mutation, indicating that ALK3 acts redundantly with the other type I receptors ALK2 and ALK6 and may not serve as the cognate type I receptor for BMP7 in NPCs. Type II BMP receptors include BMPR2, ACVR2A and ACVR2B[40]. Compound inactivation of *Acvr2a* and *Acvr2b* causes kidney agenesis. However, their specific effects on CM survival and self-renewal remain to be elucidated[40]. The roles of ALK2, ALK6 and BMPR2 in kidney development have not yet been explored.

BMP7-mediated SMAD and MAPK signaling occurs in the CM[41-45]. Previous studies have reported that CITED1+ NPCs within the CM have low levels of activated SMAD1/5[43-45]. Binding of activated SMAD1/5 transcription factors to co-SMAD4 is essential for translocation and accumulation in the nucleus[46,47]. Inactivation of *Smad4* in the CM only partially recapitulates the *Bmp7* null phenotype, with premature cessation of nephrogenesis and cell death in the nephrogenic zone[41].

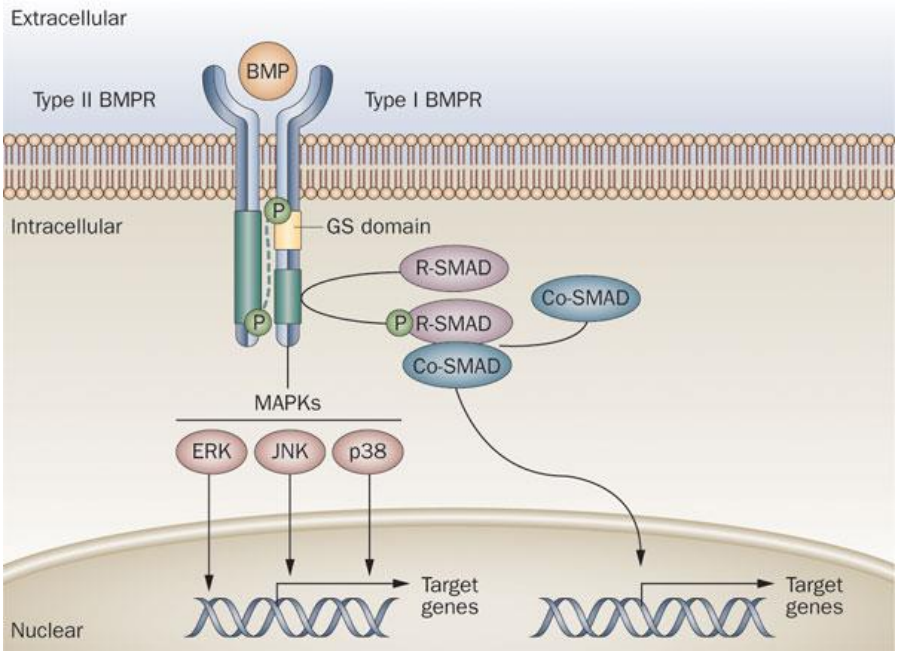

Figure 1.4: BMP-mediated signaling pathways: Extracellular BMP ligands bind to the type I and type II BMP receptors on the cell membrane. Ligand binding induces hetero-tetrameric receptor complex formation and activates signaling through type II-receptor-mediated phosphorylation of the type I receptor on the GS domain. Activated type I receptors phosphorylate cytoplasmic signal transduction proteins such as R-SMADs and MAPKs (including JNK, ERK and p38), which in turn regulate the transcription of target genes in the nucleus[31].

Progenitor marker analysis showed that substantial numbers of NPCs remained in the mutant kidneys but lacked cap-like organization and were interspersed with the surrounding cortical interstitial (CI) cells[41]. An extracellular modifier of BMP signaling, *Cv2* (*Bmper*), is expressed in the CM, and its inactivation results in reduced activation of the SMAD1/5 transcription factors[45]. Compound inactivation of *Cv2* and *Bmp7* results in the mixing of NPCs with CI cells, recapitulating the *Smad4* mutant phenotype and strongly suggesting that SMAD4-dependent BMP7 signaling is essential for the proper segregation of NPCs from the CI[45]. Interestingly, the suppression of SMAD1/5 activation in

NPCs in the *Cv2* null and the associated hypomorphic phenotype is reversed by compound inactivation of another BMP modulator, *Twsg* (Twisted gastrulation)[45]. This interaction suggests that a network of extracellular modifiers control BMP7-mediated SMAD signaling in the CM.

Previous studies from our laboratory have demonstrated that the inhibition of MAP3K7 (TAK1) and JNK in BMP7-treated NZC cultures *in vitro* blocked the proliferative response of cells to BMP7, providing an explanation for the reduced proliferation of NPCs in the *Bmp7* null[43]. Activation of the downstream transcription factors JUN and ATF2 is also reduced in the *Bmp7* null, indicating that the proliferative signal is mediated through a BMP7-TAK1-JNK-JUN pathway[43]. However, the molecular mechanism by which BMP7 activates TAK1-JNK-JUN signaling to regulate NPC proliferation is yet to be determined.

One aim of the current study is to map the TAK1-JNK-JUN signaling pathway components *in vivo* and to determine the underlying molecular mechanism by which BMP7 controls NPC self-renewal.

1.2.2. FGF9/20 signaling

FGF signaling is initiated by the binding of the FGF ligands to tyrosine-kinase fibroblast growth factor receptors (FGFRs), resulting in the activation of the RAS-MAPK, PI3K/AKT and PLC-γ pathways (Figure 1.5)[48]. Early studies of the roles of FGFs in the developing kidney revealed that FGF2 promotes CM survival and maintenance[49,50]. Inhibition of FGF receptor activity by transgenic expression of soluble dominant negative

receptors or conditional gene inactivation in the MM causes severe renal dysplasia due to a failure of MM growth, demonstrating an essential role for FGF-mediated signaling in NPC maintenance[51,52].

Overexpression of the RTK signaling inhibitor *Spry1* specifically in CM cells using the *Cited1-creER* strain resulted in the apoptosis of CITED1+ cells, confirming the requirement for FGF- and RTK-mediated signaling in NPC survival and maintenance[21]. Because the MM fails to survive once the UB is removed from explant cultures, FGFs produced by the UB are primary candidates for the natural signal to the CM.

Of the FGFs expressed in the UB, FGF2 and FGF9 efficiently promote the survival and proliferation of NPCs *in vitro*[21]. *Fgf9* is also expressed in the CM. However, mice lacking these genes exhibit normal kidney development, suggesting that they may act redundantly[54,55]. FGF20, which is exclusively expressed in the CM, is essential for the maintenance of NPCs[55].

Compound inactivation of *Fgf9* and *Fgf20* results in NPC apoptosis and loss of the MM, similar to the effect of conditionally inactivating FGF receptors 1 and 2[52,55]. *Fgf9* in the CM is activated by WNT9b, but a mechanism for the control of *Fgf20* in these cells is yet to be elucidated[56]. Compound inactivation of *Fgf2* with *Fgf9* or *Fgf20* has not yet been reported, and the *in vivo* contribution of FGF2 remains unknown. Genetic inactivation studies also revealed that NPC survival is dependent on *Fgf8*, which is expressed in the epithelializing PTA[57,58].

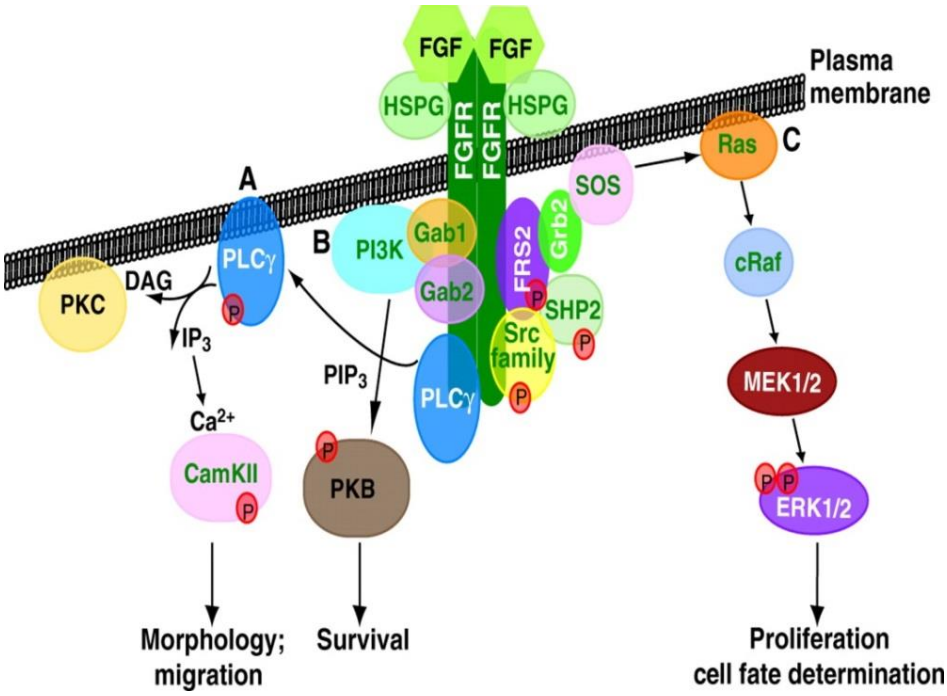

Figure 1.5: FGF signaling cascades: FGF signaling is initiated by the ligand-dependent dimerization of the tyrosine-kinase FGF receptors, which leads to the cross-phosphorylation (P) of tyrosine residues in the intracellular domain of the receptors. The phosphorylated residues are specifically bound by several intracellular signal transduction proteins, including PLC-γ, FRS2 and Src family members. These initiate several intracellular signaling pathways, including the (A) PLC-γ pathway, (B) PI3K/PKB pathway and (C) the Ras/ERK pathway, which regulate key cellular processes such as survival, proliferation, differentiation and migration[48].

The tyrosine-kinase receptors involved in the transduction of FGF9 and FGF20 signals in NPCs are not fully understood. Conditional inactivation of genes encoding either FGFR1 or FGFR2 in the MM has no major effect on metanephric development, whereas compound conditional inactivation of both genes completely arrests kidney development at E10.5[62]. CITED1+ NPCs exclusively express the c forms of FGFRs 1 and 2, and compound inactivation of the *Fgfr2IIIc* splice form with *Fgfr1* in the MM results in a phenotype resembling the *Fgfr1*;*Fgfr2* compound mutation[59]. However, neither *Fgfr3* nor *Fgfr4* appear to play a role in signal transduction in NPCs, as kidney development is unperturbed in the *Fgfr3*;*Fgfr4* compound mutants[60].

In addition to the specific high-affinity FGF receptors, FGF signal transduction is also dependent on the presence of low-affinity heparin sulfate proteoglycan (HSPG) receptors[61]. *Hs2st1* (heparan sulfate 2-O-sulfotransferase 1) is expressed throughout the E11.5 MM and in the CM, but not in the UB or CD. A gene trap mutation in *Hst2st1* causes premature arrest of metanephric development by E11.5, with the formation of a small MM and the absence of UB branching[62]. Failure of MM growth at this developmental stage suggests that *Hs2st1* may operate in the FGF pathway.

Intracellular signal transduction mechanisms utilized by FGF ligands in NPCs remain incompletely understood, but essential roles for RAS and PI3K pathways have been identified. *In vitro* observations in primary cells stimulated with FGF2 support a requirement for RAS activation in the maintenance of CITED1 expression in NPCs and demonstrate a requirement for PI3K signaling but not ERK for NPC proliferation[21].

A recent study reported that the scaffolding proteins CASK and DLG1 may be required to establish the FGF signaling complex in NPCs[63]. *Cask*;*Dlg1* inactivation in the CM causes a reduction in the activation of RAS/RAF/ERK, p38 and JUN, with premature depletion of the CM. CASK interacts with the HSPG Syndecan 2, and DLG1 interacts with MEK2, potentially forming a signaling complex[64-66]. Several distinct signaling pathways are perturbed in the *Six2-cre*;*Cask*;*Dlg1* mutants, and further studies will be needed to understand if expression of these scaffolding proteins in NPCs is essential for the transduction of multiple growth factor signals.

In summary, FGF9/20 signaling is essential for the survival, proliferation and maintenance of CITED1+ NPCs.

1.2.3. WNT9b signaling

Secreted WNT ligands bind to cell surface receptors of the frizzled and LRP families and activate canonical β-catenin/TCF/LEF signaling and non-canonical Ca^{2+}-dependent and Rho/JNK pathways (Figure 1.6)[67].

In the embryonic kidney, *Wnt9b* secreted from the UB is essential for the inductive response of the CM[12,56]. In *Wnt9b* null mutants, the CM fails to aggregate and undergo MET to form renal vesicles[12]. *Wnt9b* promotes the expression of *Wnt4* and *Fgf8* in the PTA but not in the CITED1+/SIX2+ compartment of the CM. Despite the graded expression pattern of *Wnt9b* in the CD tip, some level of signaling occurs in the undifferentiated CITED1+ SIX2+ compartment within the CM[12]. Recent studies revealed that β-catenin signaling is indeed activated in the SIX2+ cells of the CM in response to WNT9b[68,69]. Although the CM is correctly specified in *Wnt9b* mutants, proliferation is reduced in CITED1+ cells compared with wild type, indicating that WNT9b signaling is also involved in the regulation of NPC proliferation[56].

More recent studies have suggested that the switch between the pro-proliferative function and the pro-differentiation function of WNT9b/β-catenin signaling in the CM could be determined by the amplitude of β-catenin signaling relative to expression of the anti-differentiation transcription factor SIX2[47].

The cell surface receptors through which WNT9b signals are transduced in NPCs remain to be identified. Transcriptome data from the GUDMAP database shows the expression of several frizzled and LRP receptors in the CM, indicating redundant functions of these receptors[70].

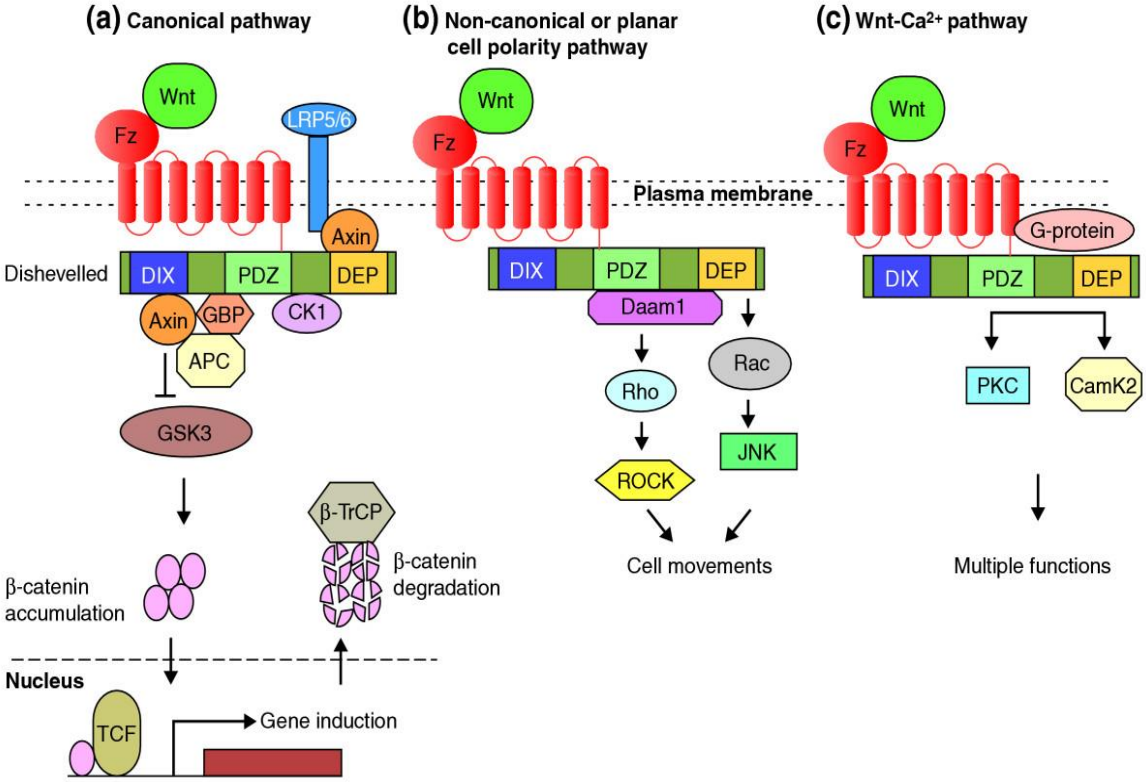

Figure 1.6: Canonical and non-canonical WNT signaling pathways: WNT signals are transduced through canonical and non-canonical pathways to control cell fate, cell movement and tissue polarity. Canonical WNT signals are transduced through Frizzled family receptors and LRP5/LRP6 co-receptors to the β-catenin signaling cascade. Non-canonical WNT signals are transduced through Frizzled family receptors and ROR2/RYK co-receptors to the DVL-dependent (Rho family GTPases and JNK) or the Ca^{2+}-dependent (NLK and NFAT) signaling cascades[67].

Wnt4 is activated by WNT9b/β-catenin signaling and is essential for CM differentiation into the renal vesicle[12,71]. Sustained activation of β-catenin blocks the epithelial differentiation of CM cells, indicating that β-catenin activation needs to be down-regulated once *Wnt4* expression has been acquired. WNT4 induces calcium influx in primary MM cells, and treatment with the ionophore ionomycin to raise intracellular calcium causes epithelialization[72,73]. The calcium influx following WNT signaling may regulate the calcineurin-activated NFAT transcription factors that are expressed in the developing kidney.

Increasing intracellular calcium partially rescues the loss of epithelial differentiation in the *Wnt4* null, and calcineurin inhibition with cyclosporine A arrests the epithelial differentiation of NPCs[73]. Whether WNT4 signals in an autocrine or paracrine manner is unknown. The receptors used to transduce the non-canonical WNT4 signal in the PTA are also undetermined. Further studies are required to elucidate the molecular mechanisms underlying the pro-proliferative and pro-differentiation functions of WNT9b signaling in NPCs.

1.3. Signaling cross-talk between BMP, FGF, WNT pathways

NPCs within the CM are subject to multiple signaling inputs from the nephrogenic niche that includes signals from the CD cells, cortical stromal progenitors and endothelial precursors. BMP7, FGF9/20 and WNT9b signaling control NPC maintenance, self-renewal and differentiation, and previous studies have reported important interactions between these growth factors. Examples include BMP7 and FGF2 interaction in the synergistic maintenance of the CM in organ explant cultures and the activation of common targets by FGF and WNT9b/β-catenin signaling in the CM[21,35,55]. These studies strongly suggest a potential convergence and cross-talk among these signaling pathways. A plethora of candidate mechanisms for the molecular cross-talk between these pathways can be found in the literature. However, the mechanistic bases for these interactions in NPCs in the context of kidney development remain unknown. We are only now beginning to uncover the intracellular signal transduction mechanisms utilized by these distinct pathways.

Previous findings indicate that BMP7 activates the TAK1-JNK-JUN signaling cascade to promote NPC proliferation, and FGF-dependent RAS signaling is essential for the maintenance of NPCs[21,43]. FGF-mediated RAS/MAPK and WNT-activated β-catenin signaling regulate JUN activation and the transcription of AP-1 target genes in other cellular contexts[74-76]. Therefore, regulation of JUN/AP-1 transcriptional activity could be a potential mechanism by which these distinct NPC self-renewal pathways collaboratively regulate NPC self-renewal.

1.4. AP-1 transcription factors and targets in NPCs

The activating protein 1 (AP-1) transcription factor family consists mainly of JUN, FOS and ATF protein dimers[77]. Members of the AP-1 transcription factor family are involved in the regulation of many cellular processes including survival, proliferation and differentiation in normal development and cancer[78,79]. A prototypical AP-1 dimer chiefly consists of a JUN and FOS heterodimer (Figure 1.7)[80].

While JUN can form homodimers and bind to AP-1 sites in the promoters of early response genes, FOS proteins cannot homodimerize but form stable, heterodimeric complexes with JUN, enhancing its DNA-binding activity[80].

JUN-FOS heterodimers act as stronger transactivators of AP-1 transcription than JUN-JUN homodimers, and the composition of AP-1 dimers strongly determines the amplitude of AP-1 activity[80].

AP-1 activity is also determined by the phosphorylation status and transcriptional activation of its individual components. JUN proteins are phosphorylated by JNK on the residues Ser63 and Ser73 within the N-terminal transactivation domain[78-80].

The specific kinases that regulate FOS activation are not clear, but FRK (Fos-related kinase) and ERK phosphorylate FOS in a RAS-MAPK dependent manner (Figure 1.8)[80].

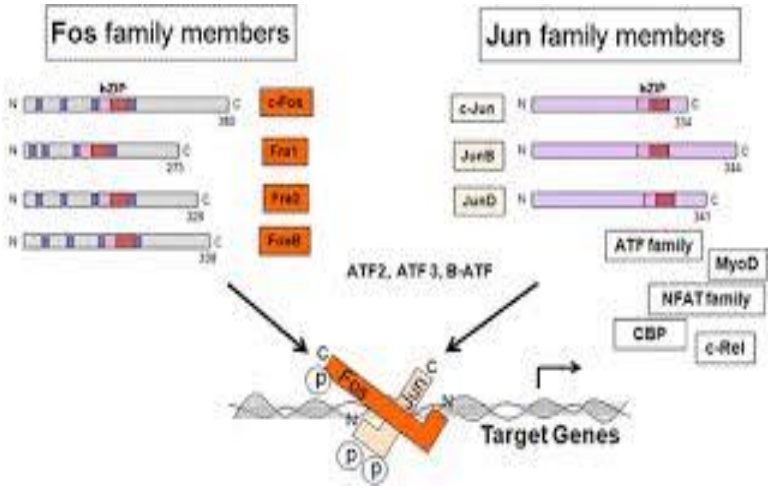

Figure 1.7: AP-1 transcription factor families: AP-1 transcription factor family consists of FOS, JUN, ATF, and MAF sub-family members that form homo or heterodimers to activate target transcription[80].

The *Jun* promoter contains the AP-1 sites/TRE-sequences. Therefore, *Jun* is auto-regulated by its protein product[81]. Transcription of *Fos* is regulated by ERK/Elk/SRF transcription factors binding to SRE sequences in its promoter (Figure 1.8)[80].

Binding of the AP-1 complexes to canonical AP-1 target sites (consensus sequence 5'-TGAG/CTCA-3', TRE sequence) on genes results in their transcriptional activation. Some of the well-characterized AP-1 transcriptional targets include apoptotic and cell cycle regulatory genes such as *Ccnd1*, *p53*, *Myc*, *Bim*, *Bcl-2*, *p21*[82,83]. Of these targets, *Myc* has been demonstrated to be important for NPC self-renewal[84].

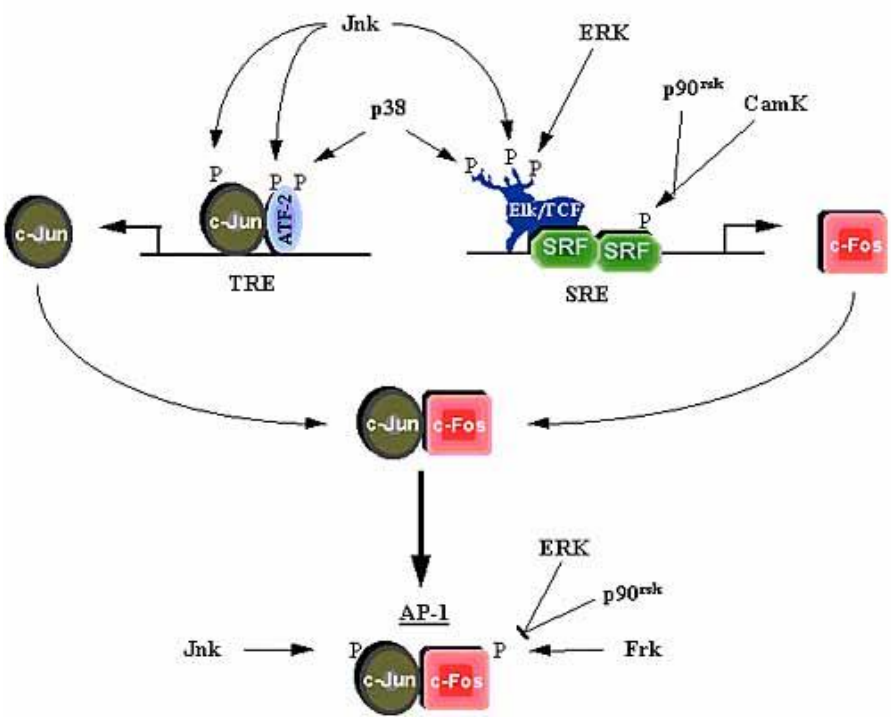

Figure 1.8: Phosphorylation and transcriptional activation of the AP-1 factors: JNK potentiates the activation of c-*jun*. Frk and ERK phosphorylate c-*fos*[80].

Interestingly, inactivation of *Myc* in the CM results in the reduced proliferation of NPCs specifically in the later stages of nephrogenesis from E15-E18[84]. In contrast, *N-Myc* is required for CM maintenance and renewal during early stages (E11-E14) of nephrogenesis, indicating differential regulation and activation of *Myc* genes during different phases of nephrogenesis[85].

The anti-apoptotic regulator *Bcl-2* is also highly expressed in NPCs and is essential for metanephric kidney development. *Bcl-2* null kidneys display normal MM specification until E12 but undergo apoptosis after E12.5, resulting in severely hypoplastic kidneys by P0[86]. More recent studies have delineated a role for p53 in the regulation of *Pax2* expression in the CM, and inactivation of *p53* in the NPCs results in kidney hypoplasia[87]. These studies strongly suggest a potential role for AP-1 function in NPCs.

A major aim of this study is to determine if BMP7 and FGF9 cooperatively control AP-1 transcriptional activity, which will potentially provide an explanation for their combinatorial regulation of NPC self-renewal.

CHAPTER 2

MATERIALS AND METHODS

2.1. Mouse strains and treatments

Cited1-creER^{T2} mice, *R26RlacZ* mice and *Spry1-Tg* mice were maintained on an FVB/NJ background[18,88, 89]. *Bmp7*$^{+/cre}$ mice were maintained on an ICR background. *Six2-cre-EGFP* mice, *Tak1*$^{c/c}$ mice, *Tak1*$^{+/c}$ mice, and *Jun*$^{c/c}$ mice were maintained on a C57BL/6 background[16, 90,91].

For tamoxifen-inducible Cre mice, pregnant dams were injected with 3 mg tamoxifen in corn oil per 40 g mouse weight at the indicated time points.

LDN-193189 (3mg/kg) in 20 ml of DMSO/PBS was administered intraperitoneally into newborn pups (P0) at 12 hour internals daily for two days (P2)[98].

Animal care was in accordance with the National Research Council Guide for the Care and Use of Laboratory Animals, and protocols were approved by the Institutional Animal Care and Use Committee of Maine Medical Center.

2.2. Histology, immunohistochemistry and morphometrics

Dissected whole kidneys were fixed in 4% paraformaldehyde for 30 minutes (E14.5 and E17.5) to 1 hour (P0) at room temperature. Paraffin embedded sections were incubated with blocking solution containing phosphate buffered saline (PBS), 1% bovine serum albumin (BSA), 5% serum of the secondary antibody species (Jackson ImmunoResearch) and 0.05% hydrogen peroxide (Sigma) for 1 hour at room temperature. The following

primary antibodies were diluted in PBS and incubated at 4°C overnight: anti-SIX2 (1:200, Proteintech), anti-CITED1 (1:200, Neomarkers), anti-GFP (1:100, Abcam), anti-pHH3 (1:100, Cell Signaling), anti-Ki67 (1:100, Abcam), anti-PAX2 (1:100, Invitrogen), anti-pSMAD1/5 (1:50, Cell Signaling), anti-Caspase3 (1:100, Cell Signaling), anti-Cytokeratin8/TROMA-I (1:100, DSHB), anti-DBA Lectin (1:500, Vector Laboratories), anti-JUN and anti-pJUN (1:200, 1:1,000, Cell Signaling), anti-FOS and anti-pFOS (1:400, Cell Signaling), anti-CCND1 (1:100, Cell Signaling), anti-CCND3 (1:100, Cell Signaling), anti-MYC (1:100, Abcam), anti-CCNE1 (1:250, Santa Cruz), and anti-PCNA (1:200, Santa Cruz).

Alexa Fluor-488/568/647 conjugated secondary antibodies were used at 1:250 to detect labeled cells. Nuclei were stained using DAPI (Molecular Probes) for immunofluorescence and hematoxylin for immunohistochemistry. Sections were mounted using Vectashield (Vector Laboratories).

TUNEL staining was performed using ApopTagPlus peroxidase in situ apoptosis detection kit according to the manufacturer's instructions (EMD Millipore).

2.2.1. Quantification of NPCs, collecting duct tips and glomeruli

Quantification of NPC number and NPC proliferation was performed manually on E14.5, E17.5 and P0 whole kidney sections stained with CITED1 or SIX2 (NPC markers) and a proliferation marker (Ki67 or pHH3). A minimum of five serial sections 100 μM apart per kidney per genotype was scored to determine the total number of CITED1+ or SIX2+ NPCs and SIX2+Ki67+, CITED1+ pHH3+ and CITED1-SIX2+PHH3+ proliferating NPCs.

For collecting duct (CD) tip quantification, E14.5 whole kidney sections were stained with Cytokeratin8 to label the CD tips. A minimum of 5-10 serial sections 100 μM apart per kidney per genotype was scored to calculate the number of CD tips per group. Whole kidneys from mice were serially sectioned and stained with hematoxylin and eosin (H&E). The relative number of glomeruli per kidney section was counted in sections every 100 μM. Seven mice per group were analyzed, and the number of glomeruli scored was represented as the glomerular index per experimental group.

2.2.2. Whole mount immunostaining

Dissected kidneys were fixed in 4% paraformaldehyde for 10 minutes at room temperature and washed with 1X PBS for 5 minutes at 4ºC. Kidneys were permeabilized with 1X PBS containing 0.1% Triton-X for 10 minutes at 4ºC, followed by a wash in 1X PBS containing 0.01% Tween. Kidneys were incubated with blocking solution of 1X PBS containing 0.01% Tween with serum of secondary antibody species for 8 hours. Primary antibodies to anti-SIX2 (1:200, Proteintech) and anti-Cytokeratin8 (1:100, DSHB) were diluted in blocking solution, added to the wells containing the kidneys and incubated for 24 hours at 4ºC. Alexa-Fluor 488/568 secondary antibodies (Molecular Probes) were used at 1:250 and incubated for 24 hours to detect staining in the kidneys.

2.2.3. Body weight, kidney weight, kidney size

Kidney weight measurements were normalized to body weight to account for differences in body size. Data are represented in grams (g) for body weight and milligrams (mg) for kidney weight for each experimental animal analyzed. For kidney size measurements, images of dissected whole kidneys were taken on a stereomicroscope, and the pole-to-

pole distance of each kidney was calculated using Spot 5.1 Imaging software. The cross-sectional area per kidney is depicted in the scatter plots.

2.3. Cell culture: isolation, purification and monolayer culture of NPCs

Total NZCs were isolated from the dissected kidneys of E14.5 and E17.5 ICR mice by enzymatic digestion with a collagenase A/pancreatin enzyme mix[43]. For isolation of NZCs from E14.5, E17.5 and P0 conditional mutants, control and mutant kidneys were sorted based on size and GFP expression (*Six2-cre-EGFP* and *Cited1-creER^{T2}-EGFP*) and confirmed by genotyping.

NZCs were isolated from E13.5 to P1 kidneys and cultured in monolayer in keratinocyte serum-free medium (Thermo Fisher Scientific) supplemented with FGF2 (50 ng/ml, R&D Systems). Cultures were treated with 50 ng/mL BMP7 (R&DSystems), 50 nM TAK1 inhibitor (Analyticon Discovery), and 2.5 μM dorsomorphin (DM, Sigma).

Enrichment for CITED1+ NPCs was performed by negative depletion with magnetic activated cell sorting (MACS), phycoerythrin (PE)–conjugated antibodies and anti-PE microbeads following the manufacturer's protocol (Miltenyi Biotec). NPCs were purified by passing PE-labeled NZCs through an autoMACS separator using the "Deplete S" program setting.

Purified NPCs were cultured in monolayer under serum-free conditions in KSFM supplemented with FGF2 (50 ng/ml, R&D Systems) and 100 U/ml penicillin-streptomycin in plates coated with human plasma fibronectin (100 μg/ml, EMD Millipore). The identity of purified NPCs from ICR and conditional mutant mice was verified by immunostaining

using anti-CITED1 (1:200, Cell Signaling), anti-SIX2 (1:200, Proteintech), and anti-LEF1 (1:100, Cell Signaling) antibodies and RT-qPCR analysis of cap mesenchyme and cortical interstitium markers before and after growth factor/inhibitor treatments.

2.4. Plasmid constructs:

Wild type and kinase-defective TAK1 (K63W) plasmids were procured from Dr. Jun Ninomiya-Tsuji[92]. The pCX-EGFP construct was a gift from Dr. Andreas Nagy[93]. FLAG-JUNWT-Myc and FLAG-JUN4A-MYC were gifts from Dr. Axel Behrens (Addgene # 47443, 47444)[94]. FOS-DD was a gift from Dr. John Blenis (Addgene # 8698)[95].

3xAP1-pGL3 was a gift from Dr. Alexander Dent (Addgene # 40342)[96]. pGL3Basic-962 CCND1 promoter luciferase and the pGL3Basic-962 CCND1 promoter AP-1 site mutant (Addgene #32727 and # 32728) were gifts from Dr. Frank McCormick[97]. pRL-CMV (Renilla-Luciferase) was obtained from Promega.

2.5. Adeno-viral vectors and transduction:

E17.5 NPCs harvested from *Tak1*$^{c/c}$ and *Jun*$^{c/c}$ were cultured in monolayer in KSFM (Gibco) supplemented with FGF2 (50 ng/ml, R&D Systems) overnight. Adeno-viral vectors (Ad-Cre and Ad-GFP) were transduced at a multiplicity of infection (MOI) of 500 or 1,000 for 40 hours.

GFP expression was used to estimate transduction efficiency. RNA was harvested to analyze the reduction in *Tak1* and *Jun* transcripts in Ad-Cre transduced NPCs.

2.6. Growth curve analysis of NPCs:

Freshly isolated E17.5 NPCs plated in monolayer in KSFM with FGF2 (50 ng/ml) were treated with TAK1 and JNK inhibitors for 1 hour, after which BMP7 (50 ng/ml, R&D Systems) was added and cells were incubated overnight at 37*c. Fresh media was added to cells every day, and cell proliferation over 3 days was measured by counting cells with a hemocytometer. A minimum of 3-5 biological replicates per condition from three independent experiments was analyzed.

2.7. Lipofectamine mediated transfection in NPCs:

E17.5 NPCs cultured in KSFM media with rh-FGF2 (50 ng/ml) were transfected for 24 hours using Lipofectamine® 2000 (Life Technologies). Plasmid DNA (2 µg) and lipid (2 µl) were mixed in a 1:1 ratio in Opti-MEM (Life Technologies), added to NPCs in KSFM without antibiotics and incubated for 1 hour at 37ºC. Media was replaced with fresh KSFM with FGF2 1 hour after transfection to minimize cytotoxicity. Transfection efficiency was estimated using a pCX-EGFP construct at 24 and 48 hours after transfection and by RT-qPCR for transcript levels of over-expressed genes.

2.8. Dual-luciferase reporter assays in NPCs:

Between 50,000 and 100,000 NPCs from E17.5 ICR mice and conditional mutants were plated in monolayer culture containing KSFM with FGF2 for 2 hours. The 3XAP1-Luc and Renilla-Luc constructs were transfected with Lipofectamine in KSFM media without antibiotics and incubated at 37ºC for 1 hour. Media was replaced with fresh KSFM with antibiotics and FGF2, and cells were allowed to grow overnight.

The next day, transfected cells were stimulated with vehicle, FGF9 and BMP7 for 24 hours. Cells were lysed, and luciferase activity was measured using the Dual-Luciferase Reporter Assay Kit (Promega). Relative luciferase activity was normalized to Renilla-luciferase. The average fold changes relative to vehicle treatment from four biological replicates and two independent experiments are presented in the graphs.

2.9. Immunoblotting:

E17.5 NZCs and NPCs were cultured in monolayer for 2 hours in KSFM with rh-FGF2. For inhibitor treatments, TAK1i (0.5 μM, Analyticon Discovery) and JNKi (10 μM, Calbiochem) were added to cells and incubated for 1 hour. BMP7 or FGF9 (50 and 100 ng/ml, R&D systems) were added and incubated for 15 minutes. Total protein was extracted using SDS lysis buffer containing protease inhibitors. Antibodies used were: anti-pSMAD1/5 (Ser 463/465), anti-pTAK1 (Thr184/187), anti-pJNK (Thr183/Tyr185), anti-pJUN (S73), anti-JNK1/2, anti-pFOS (S32) (1:1,000, Cell Signaling), anti-β-tubulin (1:5,000, Santa Cruz), anti-JUN (1:1,000, sc-45 Santa Cruz), and anti-TAK1 (1:500, Upstate). Protein levels were quantified using ImageJ software by measuring the integrated density of the indicated proteins and normalizing to β-tubulin, the loading control.

2.10. Quantitative RT-PCR:

RNA extraction from E14.5 and E17.5 NPCs was performed using the RNeasy Microkit (Qiagen). The RNA concentration was measured using a NanoDrop 2000 Spectrophotometer (Thermo Fisher Scientific), and a final concentration of 100-250 ng/μl of RNA was used for cDNA synthesis by iScript^{TM} Reverse Transcription Super Mix (BioRad). Quantitative RT-PCR was performed using iQ-SYBR Green Super Mix (BioRad). Primer

sequences used in the study are listed in Table 1. Fold changes were normalized to the housekeeping gene β-actin, and average values (mean ± SD) of three technical replicates and from 2 to 3 independent experiments (n = 2 or 3) are shown in the figures. *P*-values were calculated using a two-tailed Student's t-test, and $P<0.05$ was considered significant.

Table 1.1: Primer Sequences I

Gene	Primer Sequence (Forward)	Primer Sequence (Reverse)
Actin	CGTGCGTGACATTAAAGAGAAG	TGGATGCCACAGCATTCCATA
Tak1	CGGATGAGCCGTTACAGTATC	ACTCCAAGCGTTTAATAGTGTCG
Jun	CAGTCCAGCAATGGGCACATCA	GGAAGCGTGTTCTGGCTATGCA
Myc	TCGCTGCTGTCCTCCGAGTCC	GGTTTGCCTCTTCTCCACAGAC
Cited1	CCACTAGCTCCTCTGGATCG	AGCCCCTTGGTACTGGCTAT
Six2	CACCTCCACAAGAATGAAAGCG	CTCCGCCTCGATGTAGTGC
Dpf3	CCTCTCAGGAAGACCACGACAA	CCAGGTGAGTATGAGCGTAGTG
Meox1	GGAGGATTGCATGGTACTTGGG	CTTTGCTGCTGCCTTCTGGCTT
Foxd1	CCTACTCGTACATCGCGCTCAT	TAAGGGAAGCGGCTGCTGATGA
Sfrp1	CAATACCACGGAAGCCTCTAAGC	GCAAACTCGCTTGCACAGAGATG
Ccnd1	GCAGAAGGAGATTGTGCCATCC	AGGAAGCGGTCCAGGTAGTTCA
Ccnd3	CGAGCCTCCTACTTCCAGTG	GGACAGGTAGCGATCCAGGT
p21	TCGCTGTCTTGCACTCTGGTGT	CCAATCTGCGCTTGGAGTGATAG
p27	TCAAACGTGAGAGTGTCTAACG	CCGGGCCGAAGAGATTTCTG

Table 1.2: Primer sequences II

Pea3	CACAGACTTCGCCTACGACTCA	GCAGACATCATCTGGGAATGGTC
Cv2	CCTGCTGTGAACGATGCAAAGG	ACCTCAGACTCTGTCACCACAC
Id1	TTGGTCTGTCGGAGCAAAGCGT	CGTGAGTAGCAGCCGTTCATGT
Id3	GCGTGTCATAGACTACATCCTCG	GTCCTTGGAGATCACAAGTTCCG
Id4	AGTGCGATATGAACGACTGCTAC	AGCAAAGCAGGGTGAGTCTCCA
Hoxb7	GCCGCAAGTTCGGTTTTCG	GCAAAGGCGAAGAAGTTTGT
Wnt4	GAGAACTGGAGAAGTGTGGCTG	CTGTGAGAAGGCTACGCCATAG
Sp5	TCGCACCGATACCAGTTGTCTC	AGGTGATCGCTTCGCATGAAGC
Cdc25a	ACAGCAGTCTACAGAGAATGGG	GATGAGGTGAAAGGTGTCTTGG
Ccne1	GTGGCTCCGACCTTTCAGTC	CACAGTCTTGTCAATCTTGGCA
Fos	GGGAATGGTGAAGACCGTGTCA	GCAGCCATCTTATTCCGTTCCC
Spry1	ATGGATTCCCCAAGTCAGCAT	CCTGTCATAGTCTAACCTCTGCC

2.11. 5'-Ethynyl-2'deoxy-uridine (EdU) labeling of NPCs:

E17.5 NPCs were cultured in monolayer with BMP7 and FGF9 (50 and 100ng/ml, R&D systems) in KSFM. Cultures were incubated with 20 μM EdU (Click-iT® EdU Alexa Fluor® 488 Imaging Kit, Life Technologies) 4 hours after growth factor stimulation and pulse-chased for 20 hours. Fixation, permeabilization and Click-iT reaction were performed according to the manufacturer's instructions. Cultures were incubated with anti-pHH3 (1:100, Cell Signaling) antibody for 1 hour, and AlexaFluor-568 secondary antibody was used to visualize the staining. Nuclei were stained with Hoechst 33342 (Life Technologies). Between 5-10 images were taken per well for each condition, with a min-

imum of three biological replicates from two independent experiments (n = 2). Pooled images were analyzed by ImageJ, and the number of EdU+ (S-phase) and/or pHH3+ (Mitosis or M-phase) nuclei were counted and divided by the total number of nuclei to determine the percentage of cells in S- and M-phase. Data are represented as percentage of S- or M- phase cells in each condition.

2.12. Cell cycle marker analysis:

NPCs were cultured in monolayer with BMP7 and/or FGF9 (50 and 100 ng/ml, respectively, R&D systems) in KSFM for 24 hours. Cells were fixed in 4% PFA and blocked in PBS containing serum of the secondary antibody species, after which they were incubated in primary antibodies to CCNE1 and PCNA. AlexaFluor-488 (CCNE1) and AlexaFluor-568 (PCNA) secondary antibodies were used to visualize the staining. Between five and eight images were taken per well for each condition, with a minimum of three biological replicates and three independent experiments. Pooled images were analyzed by ImageJ, and the number of cells positive for G1 (CCNE1+), G1-S (CCNE1+/PCNA+) and S (PCNA+) phases were counted and divided by the total number of nuclei (DAPI+) to determine the percentage of cells representing G1, G1-S or S phase. Data are represented as the percentage of G1 or S phase cells in each condition.

2.13. Statistical analyses:

For statistical analyses, unpaired two-tailed Student's t-tests were performed, and *P*-values of less than 0.05 were deemed significant.

CHAPTER 3

ELUCIDATING THE ROLE OF BMP7-SMAD SIGNALING IN NPC DIFFERENTIATION

3.1. Requirement for BMP7-pSMAD1/5 signaling in the transition from the early CITED1+ to the SIX2-only compartment

NPCs are arranged in distinct compartments within the CM marked by the expression of the transcription factors CITED1, SIX2 and LEF1, representing a continuum of differentiation states[19-21]. To better define the compartments within the CM of the E17.5 kidney from which we derived our nephrogenic zone cell (NZC) cultures, we conducted fluorescent immunostaining in tissue sections. The earliest progenitor cells associated with the cortical aspect of the CD tip expressed CITED1, whereas the slightly more differentiated population associated with the internal or distal aspect of the CD tip lost expression of CITED1 but maintained expression of SIX2 (Figure 3.1A,B). LEF1 expression was limited to the more differentiated PTA compartment that is primed for epithelial conversion (Figure 3.1C).

Triple immunofluorescence staining with CITED1, SIX2 and LEF1 showed that both high (white arrows) and low (gray arrows) expressing sub-populations of “SIX2- only” progenitors reside between the CITED1 and LEF1 compartments (Figure 3.1D). These results indicated an arrangement of distinct cell states or compartments within the CM in which CITED1 expression is lost as cells differentiate to a SIX2-only state before finally entering the LEF1+ PTA and renal vesicle (RV) compartments (Figure 3.1E).

Previously, we demonstrated that CITED1+ progenitors in NZC cultures depend on FGF/RTK signaling for the maintenance of their phenotype[21]. We therefore sought to understand which signals push CITED1+ cells into the SIX2-only and the LEF1+ PTA compartments. To screen for pathways that promote CITED1+ progenitor differentiation, we used the primary NZC culture system. BMP7 treatment of NZC cultures resulted in loss of CITED1 and maintenance of SIX2 expression. However, BMP7 treatment did not promote LEF1 expression, indicating that cells do not differentiate all the way to the PTA compartment but remain in the SIX2-only compartment (Figure 3.1F).

To understand if this pro-differentiative effect of BMP7 is a feature of the culture system or if it occurs *in vivo,* we analyzed CITED1 and SIX2 expression in kidneys from *Bmp7* null mutants. By E17.5, *Bmp7* null kidneys are severely dysplastic, precluding analysis[33,34]. However, at E14.5 *Bmp7* null kidneys are approximately half of the size of their wild type counterparts, and the nephrogenic zone can be studied. As expected, CITED1 immunostaining showed a reduction in the number of CITED1+ cells in the mutant kidneys compared to wild type (Figure 3.1G). CITED1+ progenitors in mutant kidneys were more linearly arranged around the periphery, in contrast to wild type kidneys in which they wrap around CD tips (Figure 3.1G). CITED1 and SIX2 co-staining revealed that loss of *Bmp7* was associated with a more substantial decrease in the SIX2-only population (Figure 3.1H). These results strongly support a role for BMP7 in promoting the transition of undifferentiated NPCs from the CITED1+ compartment to the SIX2-only compartment *in vivo.*

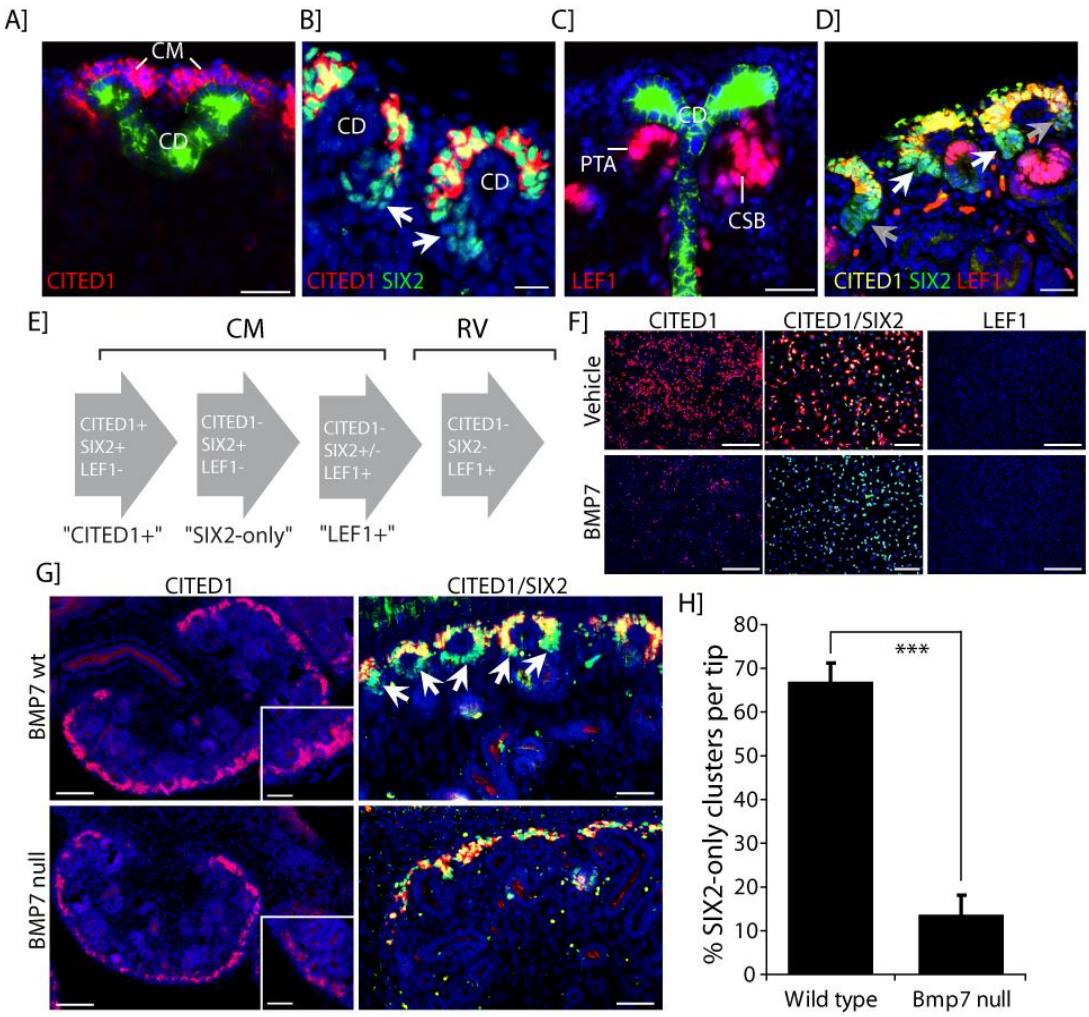

Figure 3.1: BMP7 promotes the transition of CITED1+ NPCs into the SIX2-only compartment: (A) CITED1 (red) localizes to the cortical aspect of the collecting duct (green). Scale bar, 200 μM. (B) Progenitors in the cap lose CITED1 (red) but retain SIX2 (white, arrows). Scale bar, 50 μM. (C) LEF1 (red) is limited to the pre-tubular aggregate and renal vesicles. Scale bar, 100 μM. (D) A "SIX2 only" progenitor population (green, arrows) resides between the CITED1+ (orange/yellow) and LEF1+ compartments (red). Scale bar, 50 μM. (E) Schematic representation of compartments showing loss of CITED1 as cells differentiate to SIX2-only before entering the LEF1+ pretubular aggregate and renal vesicle compartments. (F) BMP7 treatment showing loss of CITED1 (red), maintenance of SIX2 (green), and no LEF1 expression (red, absent). Scale bars, 200 μM. (G) E14.5 *Bmp7* null kidneys display reduced numbers of CITED1+ progenitors (G, H) Reduction in SIX2-only population. Scale bars, 500 μM and 50 μM. (H) Quantification of SIX2-only clusters in E14.5 *Bmp7* null (n = 4, 130 total tips) and wild-type kidneys (n = 6, 510 total tips). Error bars represent S.D. *** $P<0.0001$, Student's t-test.

We previously showed that BMP7 promotes proliferation of NZCs through TAK1-MAPK, explaining the reduction of CITED1+ progenitors seen in E14.5 *Bmp7* null kidneys[43]. However, SMAD signaling is also activated by BMP7 in the CM[42,45]. To confirm that BMP7-mediated SMAD signaling occurs in isolated NZCs, we immunostained BMP7 treated NZC cultures with PAX2 (CM marker) and co-stained with phospho-SMAD1/5. PAX2 expression co-localized with phospho-SMAD1/5, suggesting that BMP7 does indeed activate SMAD1/5 signaling in NPCs (Figure 3.2A).

Furthermore, phospho-SMAD1/5 expression was also observed in PAX2-expressing progenitors in a region of the CM just underneath the CD tip *in vivo* (Figure 3.2B). This was further confirmed by co-staining with CITED1, which revealed that nuclear phospho-SMAD1/5 localized in a subset of progenitors underneath the CD tip at the junction between CITED1+ and CITED1− cells, which represents the SIX2-only compartment (Inset in Figure 3.2B).

To determine which BMP7-initiated signaling branch (MAPK versus SMAD) is responsible for the shift of progenitors from the CITED1+ compartment to the SIX2-only compartment, NZCs were treated with BMP7 with or without addition of dorsomorphin (DM), a small molecule inhibitor of SMAD signaling, or TAK1 inhibitor (Figure 3.2C). BMP7 treatment with DM but not with TAK1 inhibitor blocked the ability of BMP7 to promote transition out of the CITED1+ compartment, showing that SMAD-mediated signaling is essential for this effect (Figure 3.2C).

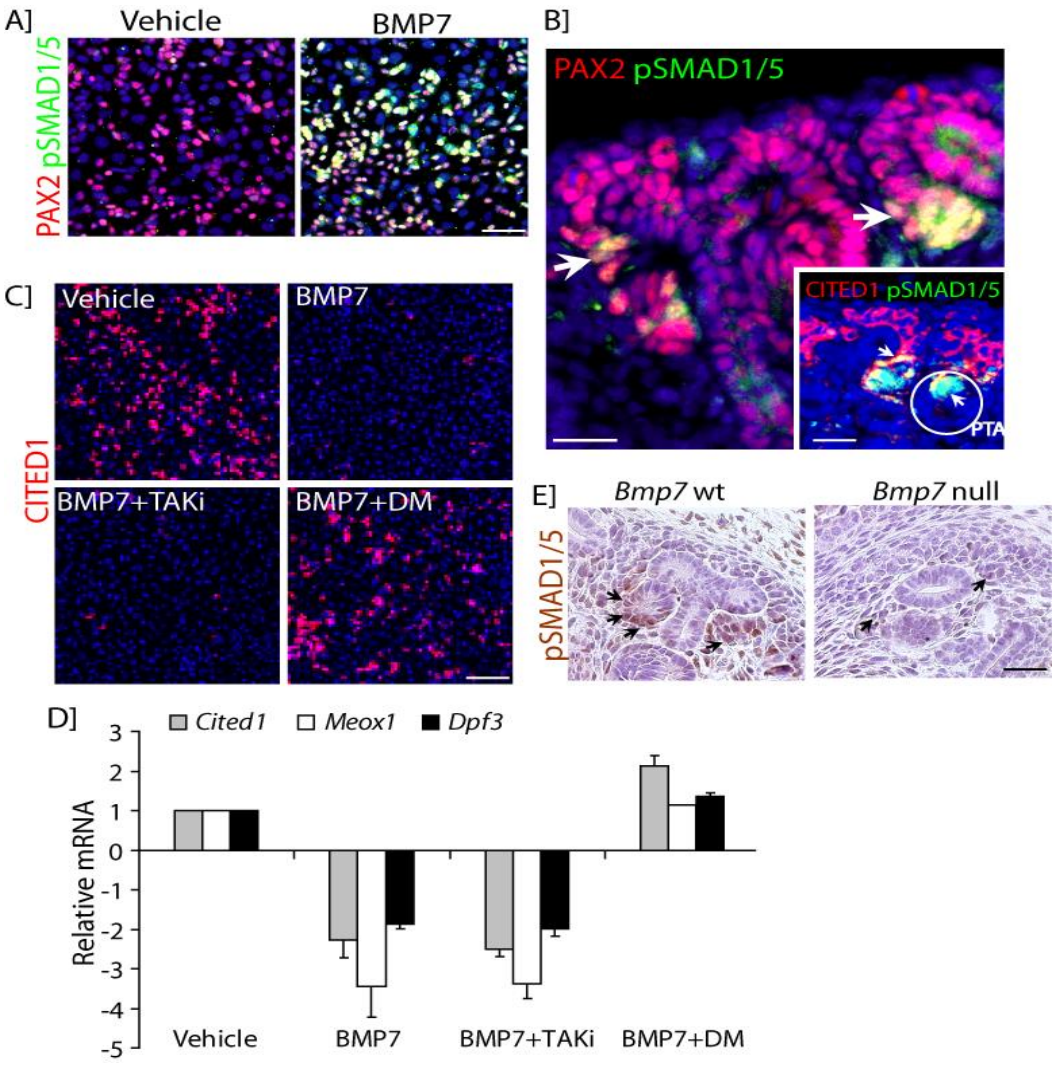

Figure 3.2: BMP7 activates pSMAD1/5 signaling in SIX2-only NPCs: (A) BMP7 treatment results in pSMAD1/5 (green) activation in PAX2 progenitors (red); costaining is yellow. Scale bars, 100 μM (B) Immunofluorescence of E17.5 kidney sections shows nuclear pSMAD1/5 in the distal cap underneath collecting duct tips (arrows). Inset shows CITED1 (red) and pSMAD1/5 (green) at the CITED1+/CITED1− border. Scale bars, 100 μM and 50 μM. (C) CITED1 staining (red) of NZCs pretreated with vehicle, BMP7, BMP7 + dorsomorphin (DM), or BMP7 + TAK1 inhibitor (TAK1i) shows that SMAD1/5 inhibition blocks the ability of BMP7 to reduce CITED1 expression. Scale bars, 100 μ M (D) Quantitative RT-PCR analysis shows that inhibition of SMAD dependent signaling by DM, compared with TAK1i, blocks the ability of BMP7 to reduce transcription (48 hours) of a group of early progenitor markers (*Cited1*, *Meox1*, *Dpf3*). Raw data are normalized to β-actin expression, and fold changes are relative to the vehicle control. (E) pSMAD1/5 (black arrows) in the distal cap mesenchyme is lost in the E14.5 *Bmp7* null kidneys. Scale bars, 100 μM.

To confirm that this transition reflects a change in cellular state rather than simply a reduction of CITED1, we evaluated the expression of *Meox1* and *Dpf3*, which are co-expressed with *Cited1* in the CM. *Meox1* and *Dpf3* were indeed co-regulated with *Cited1* following BMP7 treatment, indicating that the transition out of the CITED1+ compartment represents a change of cellular state (Figure 3.2D).

Tissue staining for phospho-SMAD1/5 in the *Bmp7* null kidney at E14.5 revealed loss of nuclear phospho-SMAD1/5 in the mutants, confirming that SMADs are activated in the distal cap specifically by BMP7 *in vivo* (Figure 3.2E). In summary, these results suggest that BMP7 promotes the transition of progenitors out of the CITED1+ compartment to the SIX2-only compartment in a SMAD-signaling dependent manner.

3.2. Inhibition of phospho-SMAD1/5 signaling *in vivo* retains NPCs in the CITED1+ progenitor state

BMP7-SMAD1/5 signaling is required for undifferentiated CITED1+ NPCs to transition to a CITED1-/SIX2+ state in which they are sensitized to epithelial induction by WNT9b/β-catenin signaling[56] (Figure 3.3A). We reasoned that SMAD1/5 signaling might increase during the terminal phase of nephrogenesis, skewing the renewal versus differentiation balance and depleting the CM. Cessation of nephrogenesis is defined as the final round of new nephron formation in which the last wave of NPCs undergo MET[8]. In mice, this occurs shortly after birth and is accompanied by a reduction in *Cited1*+ CM by P2 (Figure 3.3B).

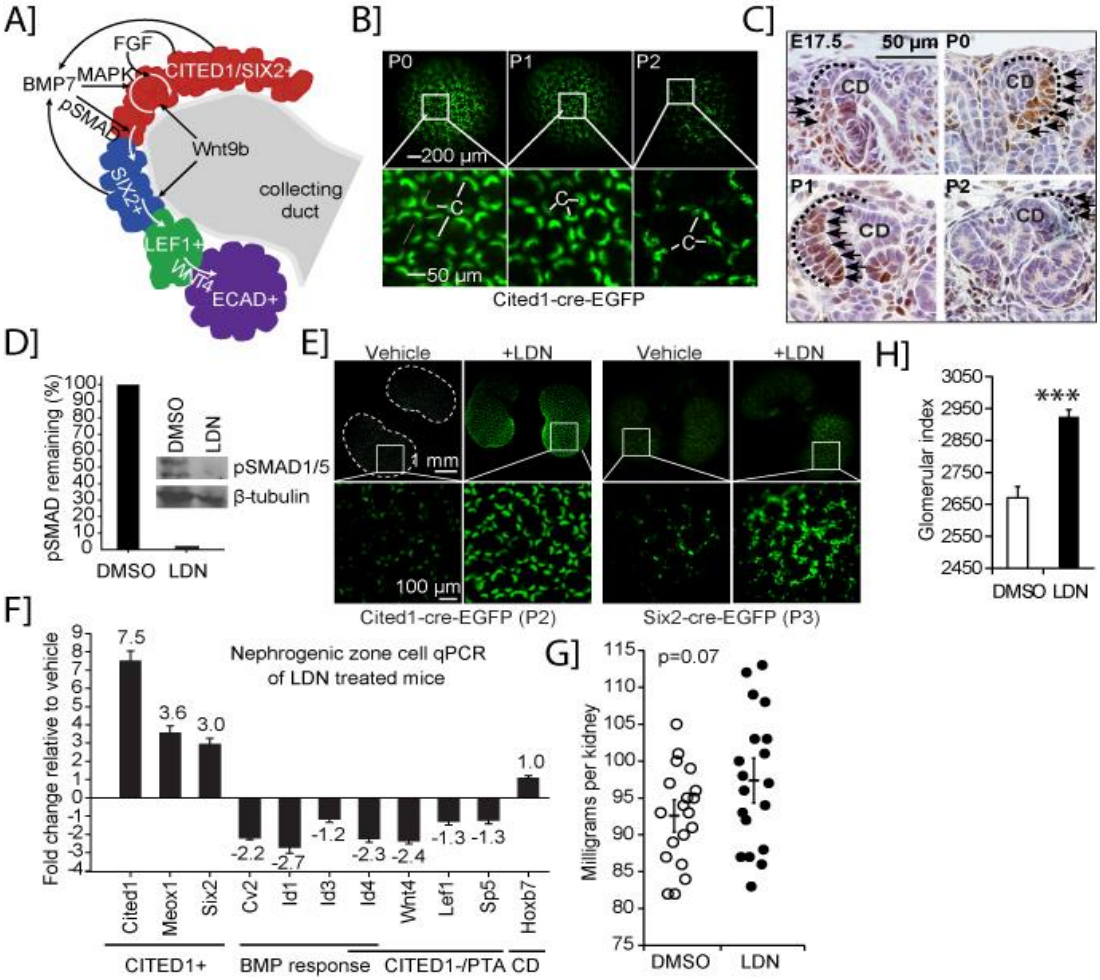

Figure 3.3: Pharmacological SMAD1/5 inhibition retains NPCs in the early CITED1+ compartment: (A) Schematic of cap mesenchyme compartments and key signaling pathways required for their maintenance and differentiation. (B) *Cited1creERT2-EGFP* kidneys harvested at postnatal stages showing GFP expression in cap mesenchymes. (C) Immunostaining of pSMAD1/5 (black arrows) in E17.5 to P1 kidneys. Cap mesenchymes are outlined with dotted black lines. (D) pSMAD1/5 immunoblot of NZCs. Graph shows percent remaining after LDN treatment quantified by densitometry and normalized to β-tubulin. NZCs were isolated from four kidney pairs per treatment group and pooled. (E) Fluorescent imaging of kidneys from *Cited1*- or *Six2-EGFP* mice in vehicle and LDN-treated animals. n = 4. (F) Transcriptional analysis of cap mesenchyme markers in isolated NZCs. Error bars represent s.d from five technical replicates from five (DMSO) and six (LDN) pooled kidney pairs. (G) Distribution of kidney weights from P0 mice treated for 2 days with DMSO or LDN and harvested at 2 weeks. Error bars represent S.E.M. $P = 0.07$, Student's t-test. (H) Relative number of glomeruli counted per kidney (glomerular index). Error bars represent S.E.M. ***$P<0.0001$, Student's t test.

Immunostaining of E17.5 to P2 wild type kidneys for activated phospho-SMAD1/5 (pSMAD1/5) showed that an expanded domain of SMAD1/5 activation in many CMs associates with cessation of nephrogenesis (Figure 3.3C). To understand if CM cells in their natural signaling environment could be prevented from transitioning out of the native CITED1+ progenitor cell state, we treated newborn animals with the SMAD1/5 small molecule inhibitor LDN-193189 (LDN) during the first two postnatal days. LDN is highly specific for SMAD1/5 and has been successfully used *in vivo*[98]. Immunoblot of NZCs isolated from LDN-treated animals showed greater than 95% reduction in SMAD1/5 phosphorylation compared to controls, confirming efficient inhibition of SMAD1/5 signaling (Figure 3.3D).

To measure the differentiation status of NPCs, we used the *Cited1creERT2-EGFP* and *Six2cre-EGFP* mouse strains, which dynamically express fluorescent protein under the control of the *Cited1* and *Six2* promoters[14,16]. While untreated animals lost *Cited1* and *Six2* expression in the CM at P2 and P3, respectively, expression was maintained in LDN-treated pups (Figure 3.3E). RT-qPCR analysis of isolated NZCs with additional marker genes expressed within these two compartments confirmed that the progenitor state was rescued in LDN-treated pups (Figure 3.3F).

We observed the expression of CITED1+/SIX2+ compartment-specific transcripts such as *Cited1*, *Meox1* and *Six2* and loss of markers for the CITED1-/SIX2+ and PTA compartments, including the WNT/β-catenin response genes *Wnt4*, *Lef1* and *Sp5*. Transcription of BMP response genes including *Cv2* and several inhibitors of differentiation (*Ids*)

was also decreased, consistent with suppression of SMAD signaling by LDN (Figure 3.3F).

Kidneys of treated mice aged for two weeks after LDN administration were slightly larger and contained more nephrons than vehicle-treated controls, as determined by counting glomeruli in serial kidney sections spaced 100 µm apart (Figure 3.3G,H). Although less precise than counting all glomeruli using stereology, this index is proportional to the number of glomeruli and nephrons in each kidney.

Taken together, these findings suggest that inhibition of pSMAD1/5 activation retains NPCs in the *Cited1+/Six2+* progenitor cell state within their natural signaling niche and that pharmacological delay of CITED1+ depletion with LDN results in increased nephron endowment.

CHAPTER 4

MAPPING BMP7-MAPK SIGNALING COMPONENTS IN NPCS

4.1. Functional dissection of BMP7-MAPK pathway components in NPCs

Previous work from our laboratory indicated that BMP7 promotes the proliferation of NZCs through MAPK signaling[43]. However, NZC cultures comprise a mixture of cell types: CITED1+ NPCs, FOXD1+ CI cells and CD31+ endothelial cells. To understand if BMP7 activates the MAPK pathway specifically in CITED1+ NPCs and to determine the kinetics of pathway activation, we measured the phosphorylation states of each of the MAPK components TAK1, JNK, and JUN in response to BMP7 in NPCs purified by immunomagnetic separation (Figure 4.1A). Following BMP7 stimulation, we detected a sequence of phosphorylation events with peak activation of pTAK1 at 10 minutes, pJNK at 15 minutes, and pJUN at 20 minutes, suggesting that BMP7 activates the TAK1-JNK-JUN signaling cascade specifically in NPCs (Figures 4.1B,C).

Activated JUN binds to AP-1 elements in target gene promoters, including itself and *Myc*[77-81]. In NPCs, *Jun* and *Myc* were up-regulated 2 hours after BMP7 stimulation, and pre-treatment with TAK1 and JNK inhibitors significantly reduced this response, indicating that they are early transcriptional targets of the pathway in these cells (Figure 4.1D). *Tak1*- and *Jun*-deficient NPCs showed a significant reduction in BMP7 stimulation of *Jun* and *Myc* transcription, corroborating the finding that BMP7 controls the transcription of *Jun* and *Myc* through TAK1-JNK signaling (Figures 4.1E,F). *Myc* is required for the re-

newal of NPCs *in vivo*, and our findings outline one signaling mechanism for the control of *Myc* expression in these cells[84].

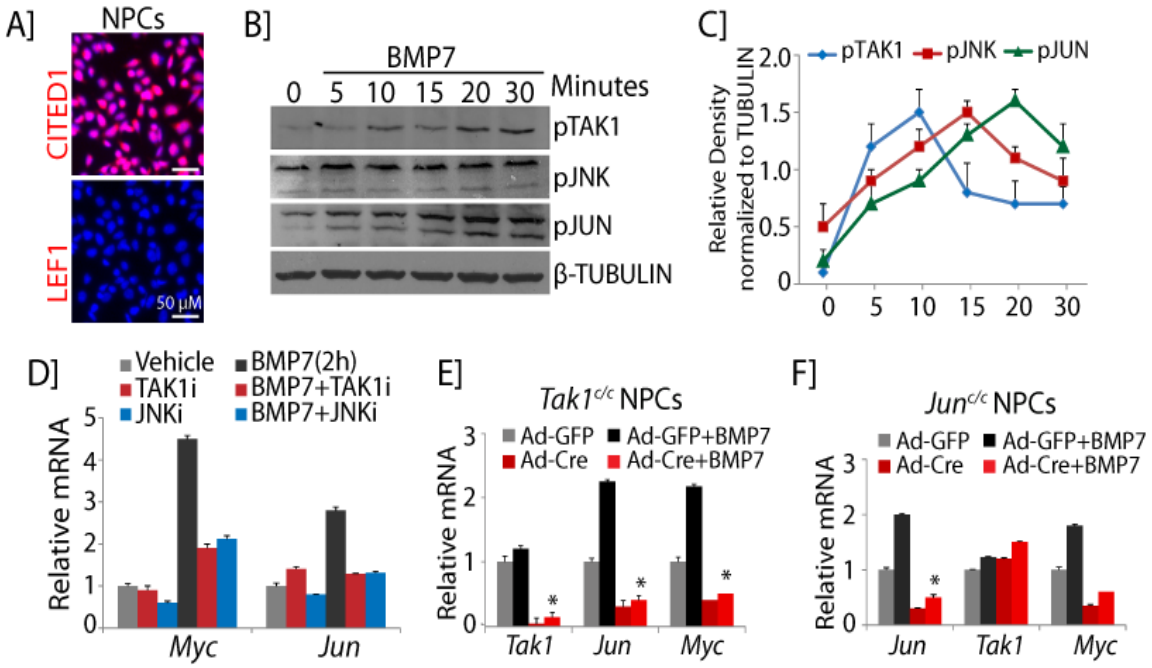

Figure 4.1: BMP7 activates TAK1-JNK-JUN pathway in NPCs: (A) CITED1 and LEF1 immunostaining of freshly purified E17.5 NPCs. Scale bars, 50 µM. (B) Immunoblot shows the time course of activation of pTAK1, pJNK, and pJUN in NPCs stimulated with BMP7. (C) Average protein densities measured at each time point from two independent experiments (n = 2). Error bars represent S.D. (D) RT-qPCR of *Myc* and *Jun* on NPCs treated with vehicle, BMP7, TAK1, and JNK inhibitors for 2 hours. Error bars represent S.D. ***P*<0.005, Student's t-test. Three biological replicates analyzed per condition, n = 3. (E,F) RT-qPCR of *Tak1*, *Jun,* and *Myc* on *Tak1*- and *Jun*-inactivated NPCs stimulated with BMP7 for 2 hours. Error bars represent S.D. ***P*<0.05, Student's t-test. Two biological replicates analyzed per condition, n = 2.

To evaluate the role of the BMP7-TAK1-JNK-JUN pathway in cellular proliferation, we assessed the growth curves of BMP7-stimulated NPCs treated with TAK1 or JNK inhibitors. As expected, BMP7-stimulated proliferation was reversed by TAK1 or JNK inhibition, indicating that BMP7 promotes NPC proliferation in a TAK1- and JNK-dependent manner (Figure 4.2A).

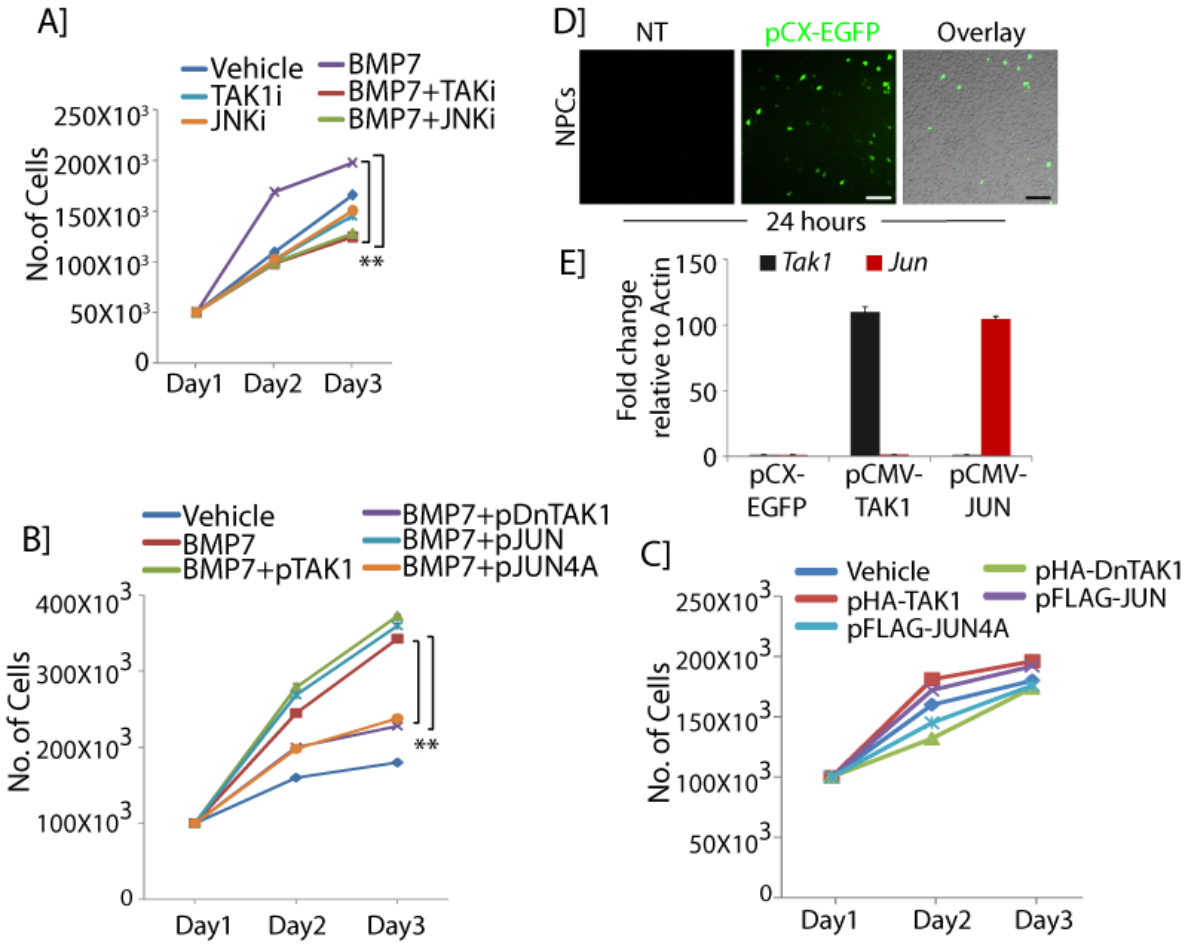

Figure 4.2: BMP7 promotes NPC proliferation through TAK1-JNK-JUN signaling: (A) Growth curve of NPCs treated with vehicle, BMP7, TAK1, and JNK inhibitors. Average numbers are derived from five biological replicates per condition, n = 5. Error bars represent S.D. $^{**}P<0.005$, Student's t-test. (B,C) Growth curve of vehicle or BMP7-treated NPCs transfected with wild type or kinase dead TAK1 and JUN constructs. Average numbers are derived from three biological replicates per condition, n = 3. Error bars represent S.D. $^{**}P<0.009$ and $^{**}P<0.005$, Student's t-test. (D) Panels show GFP expression in isolated NPCs transfected with pCX-EGFP using Lipofectamine for 24 hours. Scale bars, 200 µM. (E) RT-qPCR of *Tak1* and *Jun* expression in NPCs transfected with pCX-EGFP, pCMV-TAK1 and pCMV-JUN for 24 hours. Error bars represent S.D. Two biological replicates per condition, n=2.

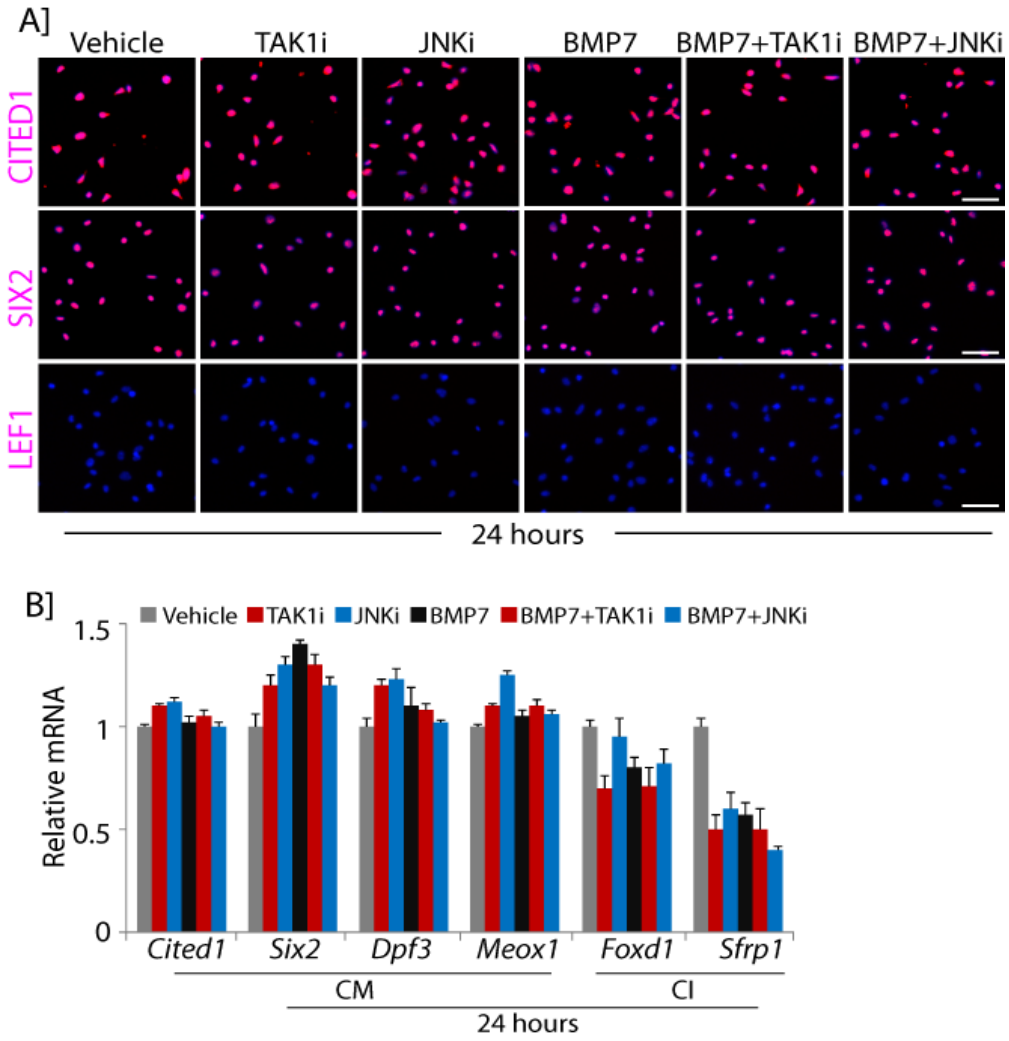

Figure 4.3: Cellular identity of NPCs during growth factor treatments: (A) CITED1, SIX2 and LEF1 immunostaining of NPCs treated with vehicle, BMP7, TAK1i and JNKi for 24 hours. Scale bars, 100 μM. (B) RT-qPCR of cap mesenchyme and cortical interstitium markers in NPCs treated with BMP7 and TAK1 and JNK inhibitors for 24 hours. Error bars indicate S.D. Three biological replicates per condition, n=3.

To confirm that BMP7-stimulated proliferation depends on the kinase activity of pathway components, wild type and kinase dead versions of TAK1 and JUN were expressed in NPCs, which were stimulated with BMP7. Wild type TAK1 and JUN expression augmented the BMP7-induced proliferative response, whereas kinase dead variants reduced it, confirming that the phosphorylation of pathway components is essential for the prolif-

eration of NPCs (Figure 4.2C). Transfection efficiency was analyzed by expressing a GFP construct and by measuring the expression of *Tak1* and *Jun* transcript levels in transfected NPCs (Figures 4.2D,E).

To confirm that NPCs retained their phenotype in the experimental conditions, we measured the expression of CITED1, SIX2, and LEF1 as well as evaluated a panel of cap mesenchyme and cortical interstitium markers (Figures 4.3A,B). Based on our primary cell analysis, we conclude that BMP7 promotes NPC proliferation through activation of the TAK1-JNK-JUN signaling cascade.

4.2. Establishing a genetic interaction between *Bmp7* and *Tak1* in NPCs

To confirm the BMP7-TAK1 relationship *in vivo*, we utilized the $Bmp7^{+/cre}$ strain to inactivate one copy of *Tak1*. $Bmp7^{+/cre}$ is an inactivating mutation, and heterozygous animals express only one copy of the gene [41]. We reasoned that limiting the availability of TAK1 would exacerbate the effect of reduced BMP7 ligand availability if these molecules operate in the same pathway.

Although the body weight of $Bmp7^{+/cre}$ embryos appeared slightly smaller than wild type, no significant difference could be detected between $Bmp7^{+/cre}$ and $Bmp7^{+/cre}$;$Tak1^{+/c}$ mice (Figures 4.4A,B). Morphometric analysis at E14.5 and P0 revealed significant reductions in size and weight of $Bmp7^{+/cre}$;$Tak1^{+/c}$ kidneys compared to $Bmp7^{+/cre}$, supporting the notion that BMP7 indeed does signal through TAK1 *in vivo* (Figures 4.4B-E).

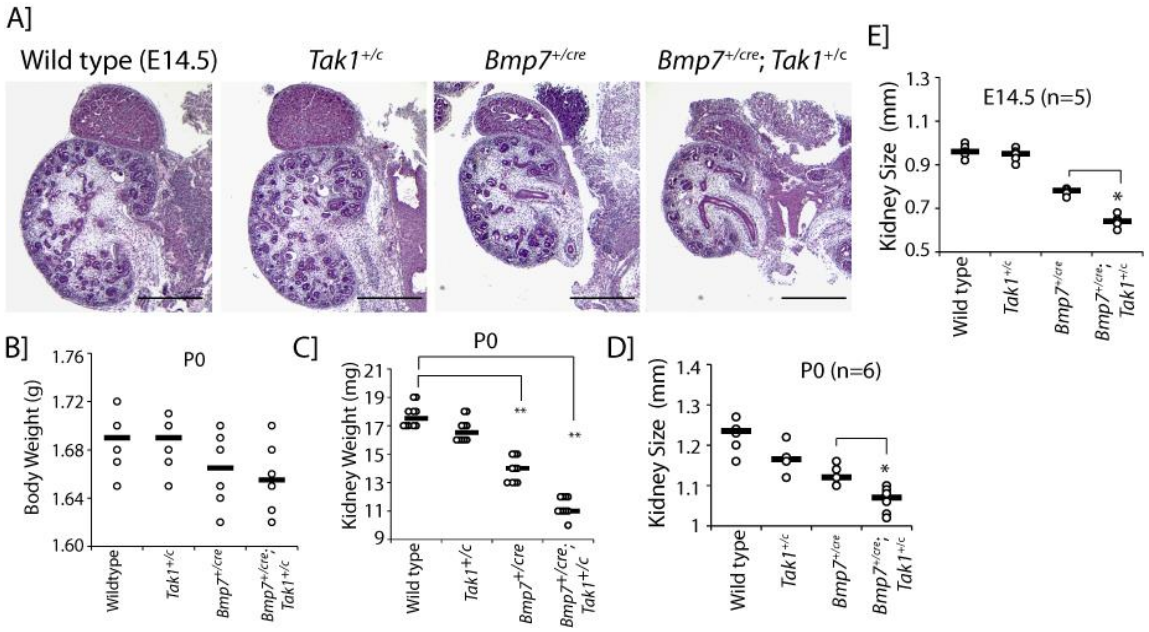

Figure 4.4: *Bmp7* and *Tak1* interact to control NPC self-renewal: (A) H&E staining of E14.5 wild type, $Tak1^{+/c}$, $Bmp7^{+/cre}$, and $Bmp7^{+/cre};Tak1^{+/c}$ kidneys. Scale bars, 500 µM. (B) Body and kidney weights and kidney size of E14.5 and P0 wild type, $Tak1^{+/c}$, $Bmp7^{+/cre}$ and $Bmp7^{+/cre};Tak1^{+/c}$ kidneys. **P*<0.01, ***P*<0.005 and **P*<0.05, Student's t-test. Number of mice analyzed per genotype (n) is shown on the panels.

To verify the loss of *Tak1* and *Jun* in mutant kidneys, we measured the expression of *Tak1*, *Jun* and their downstream target *Myc* in isolated NPCs from P0 wild type, $Tak1^{+/c}$, $Bmp7^{+/cre}$ and $Bmp7^{+/cre};Tak1^{+/c}$. *Tak1*, *Jun,* and *Myc* were reduced by approximately 60% in $Bmp7^{+/cre};Tak1^{+/c}$ compared to wild type (Figure 4.5A).

Activated pJUN levels were decreased in the cap mesenchyme but not in the ureteric bud tips of $Bmp7^{+/cre};Tak1^{+/c}$ kidneys compared to $Bmp7^{+/cre}$ and wild type, confirming that compound heterozygosity for *Bmp7* and *Tak1* results in reduced activation of JNK-JUN signaling specifically in NPCs (Figures 4.5B,C).

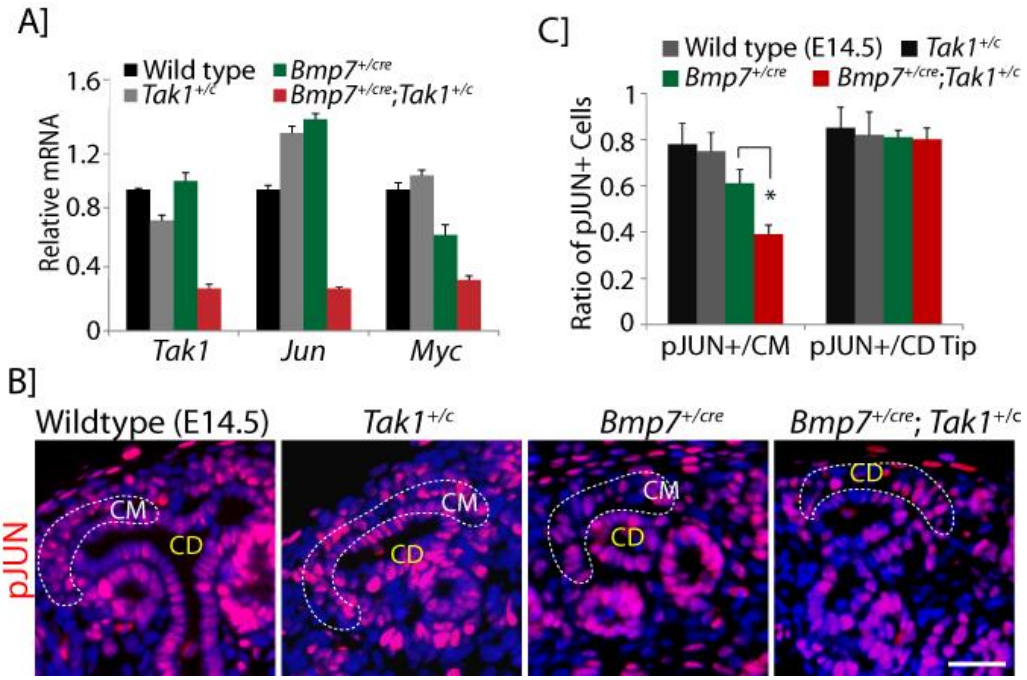

Figure 4.5: JNK-JUN signaling is reduced in *Bmp7*;*Tak1* compound mutants: (A)RT-qPCR of NPCs from P0 kidneys for *Tak1*, *Jun,* and *Myc* in mutants and wild type controls. Error bars represent S.D. Two biological replicates analyzed per genotype, n = 2. (B) pJUN immunostaining in E14.5 wild type, $Tak1^{+/c}$, $Bmp7^{+/cre}$ and $Bmp7^{+/cre}$;$Tak1^{+/c}$ kidneys. (C) Ratio of pJUN+ cells to the total number of cells per cap mesenchyme and collecting duct tip is represented in the graph. Between 10-15 collecting duct tips and cap mesenchymes were analyzed per kidney per genotype. *P<0.05, Student's t-test. Scale bars, 50 µM.

Cell death in the nephrogenic zone and premature loss of NPCs are hallmarks of *Bmp7* null mutants[33,34]. We therefore measured proliferation and cell death in NPCs of single and compound mutants. Using SIX2 with the proliferation marker Ki67, we observed a significant reduction in Ki67+/SIX2+ cells at E14.5 (15%) and P0 (10%) and a concomitant decrease in the number of SIX2+ cells per kidney in the $Bmp7^{+/cre}$;$Tak1^{+/c}$ kidneys relative to the $Bmp7^{+/cre}$ mutant (Figures 4.6A-H).

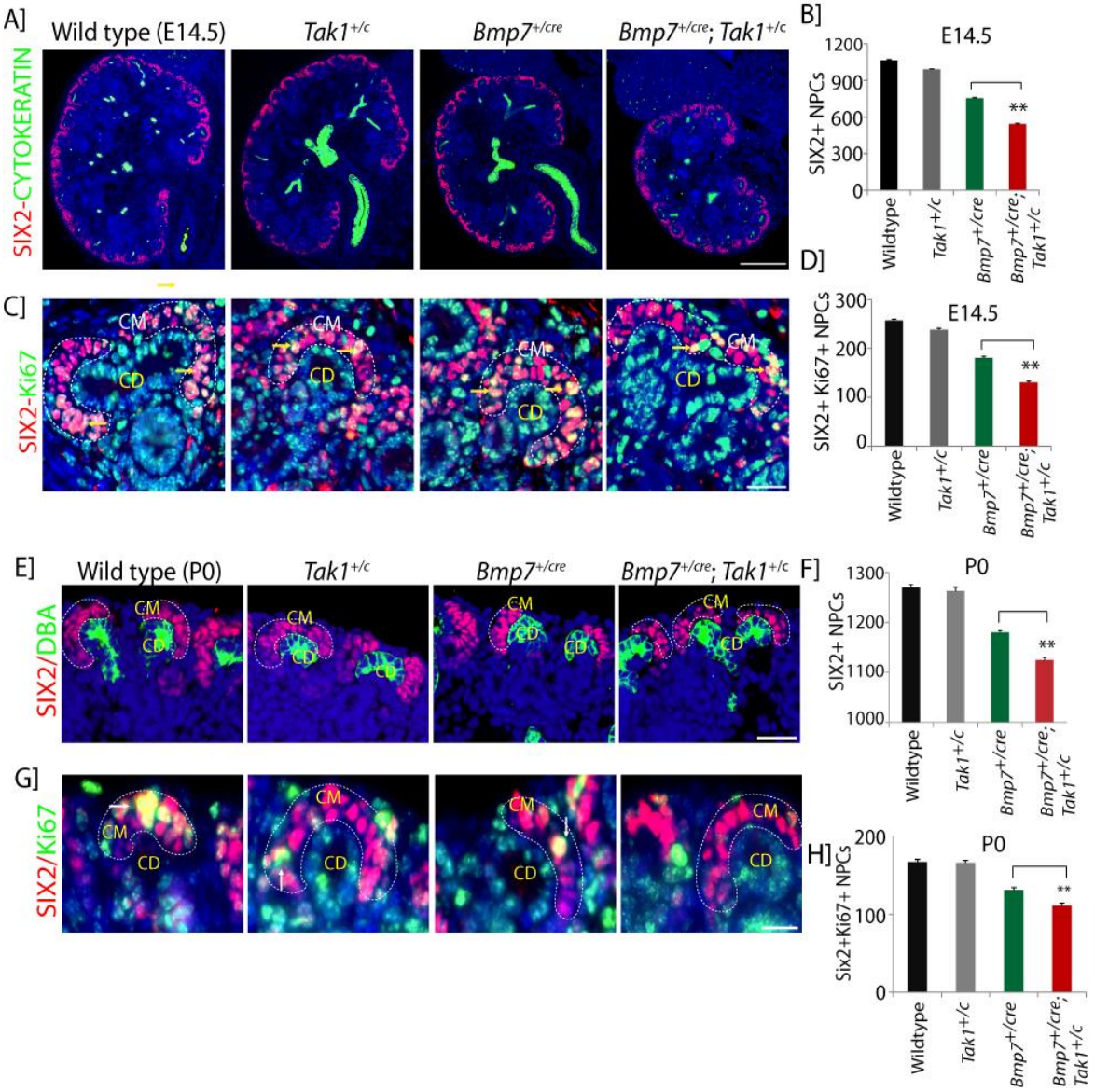

Figure 4.6: *Tak1* controls NPC proliferation downstream of BMP7: (A-D) SIX2 (red, cap mesenchyme) and Cytokeratin8 (green, collecting duct) immunostaining of E14.5 whole kidney sections. Scale bars, 500 µM. Co-immunostaining of SIX2 and the proliferation marker Ki67. Scale bars, 50 µM. Quantification of SIX2+, SIX2+/Ki67+, and collecting duct tips from 5-10 serial sections per kidney per genotype. Arrows point to Ki67+/SIX2+ cells in the cap mesenchyme, which is highlighted by white dashed lines. Error bars represent S.D. $**P<0.005$ and $*P<0.05$, Student's t-test. (E-G) SIX2 (red, cap mesenchyme), DBA Lectin (green, collecting duct) and Ki67 staining in P0 wild type, $Tak1^{+/c}$, $Bmp7^{+/cre}$ and $Bmp7^{+/cre};Tak1^{+/c}$ kidneys. Number of SIX2+ NPCs and Ki67+/SIX2+ cells (white arrows) per kidney section for the indicated genotypes. Error bars indicate S.D. $**P<0.005$, Student's t-test. Scale bars, 100µM and 50 µM.

Apoptosis analysis showed no evidence of increased cell death in the E14.5 *Bmp7*$^{+/cre}$;*Tak1*$^{+/c}$ or *Bmp7*$^{+/cre}$ kidneys, suggesting that *Tak1* is involved only in the proliferative response of NPCs to BMP7 (Figure 4.7A).

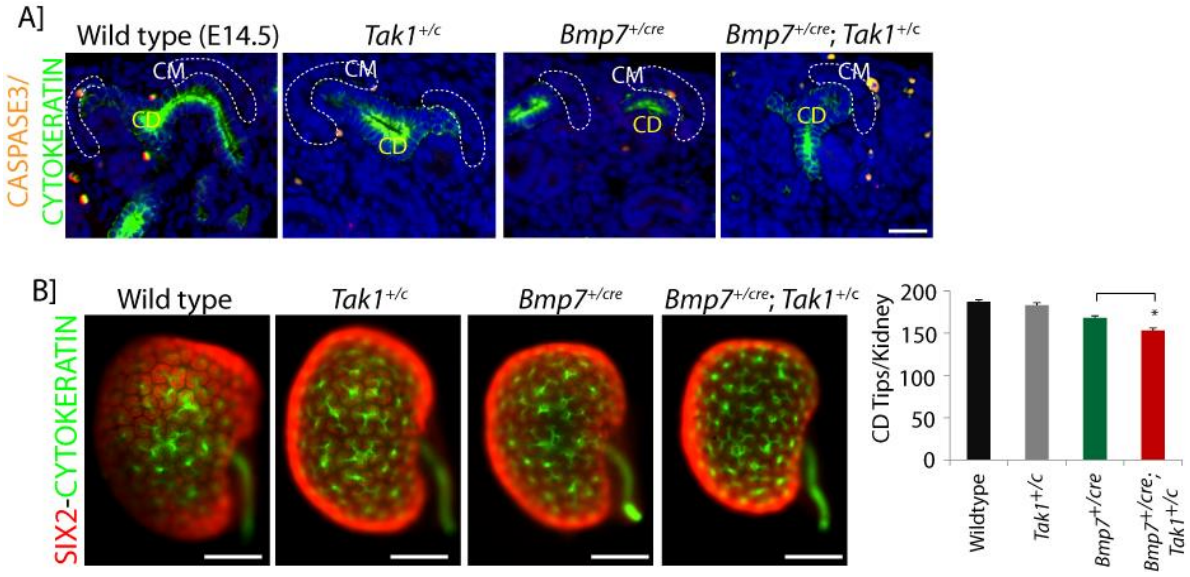

Figure 4.7: Reduction in collecting duct tips in *Bmp7*;*Tak1* compound mutants: A) Caspase3 (red, apoptosis marker) and Cytokeratin8 (green, collecting duct) staining in the conditional mutants. Scale bars, 50 μM. (B) Whole mount immunostained images showing SIX2 + NPCs and Cytokeratin8+ collecting duct tips in the conditional mutants. Number of collecting duct tips scored per kidney per genotype (n = 3) is shown in the graph. Error bars represent S.D. *P<0.05, Student's t-test. Scale bars, 500 μM.

Growth and branching of the ureteric bud is controlled by factors secreted by NPCs. To determine if ureteric bud branching was secondarily affected in *Bmp7*$^{+/cre}$;*Tak1*$^{+/c}$ kidneys, we quantified the number of collecting duct tips. *Bmp7*$^{+/cre}$ kidneys show reduced branching relative to wild type, which strongly suggests an effect of diminished NPC numbers in this mutant, considering that the reduction of *Bmp7* caused by heterozygosity is predicted to promote ureteric bud outgrowth and branching[99,100]. Compared to *Bmp7*$^{+/cre}$, *Bmp7*$^{+/cre}$;*Tak1*$^{+/c}$ kidneys showed a further reduction of ureteric bud branching

proportional to the reduction in NPC number (Figure 4.7B). Overall, our genetic interaction study supports the control of NPC renewal by BMP7 signaling through TAK1 in the developing kidney.

3.3. Conditional deletion of *Tak1* and *Jun* in NPCs

To stringently determine the requirement for the components of the BMP7-TAK1-JNK-JUN pathway in NPCs *in vivo*, we inactivated *Tak1* and *Jun* using *Six2-cre*. Both $Tak1^{NPC}$ (*Six2-cre*;$Tak1^{c/c}$) and Jun^{NPC} (*Six2-cre*;$Jun^{c/c}$) P0 kidneys showed significant reduction in kidney weight (50%) and size (30% to 40%) compared to $Tak1^{het}$ (*Six2-cre;*$Tak1^{+/c}$) and Jun^{het} (*Six2-cre;*$Jun^{+/c}$) kidneys, confirming that these genes are essential in the *Six2* lineage, which is limited to NPCs and their derivatives (Figures 4.8A-D)[16]. Body weights of these different strains did not show significant differences (Figure 4.8B).

To verify loss of *Tak1* and *Jun*, we measured the expression of *Tak1*, *Jun* and their target *Myc* in NPCs isolated at E17.5 ($Tak1^{NPC}$ and $Tak1^{het}$) or E14.5 (Jun^{NPC} and Jun^{het}). *Tak1* and *Jun* were reduced by 80% and *Myc* by approximately 50% to 60% in $Tak1^{NPC}$ and Jun^{NPC} NPCs, respectively (Figures 4.8E,F).

pJUN and MYC protein levels were also reduced in mutant kidneys, confirming that inactivation of *Tak1* and *Jun* results in reduced activation of JNK-JUN signaling and downstream targets in NPCs (Figure 4.8H).

Morphological analysis of $Tak1^{NPC}$ and Jun^{NPC} kidneys revealed several atypically organized cap mesenchymes containing few NPCs (Figure 4.9A). SIX2+ cells were reduced

by approximately 50% in mutant kidneys, suggesting that *Tak1* and *Jun* inactivation results in premature loss of NPCs (Figures 4.9A,B,E).

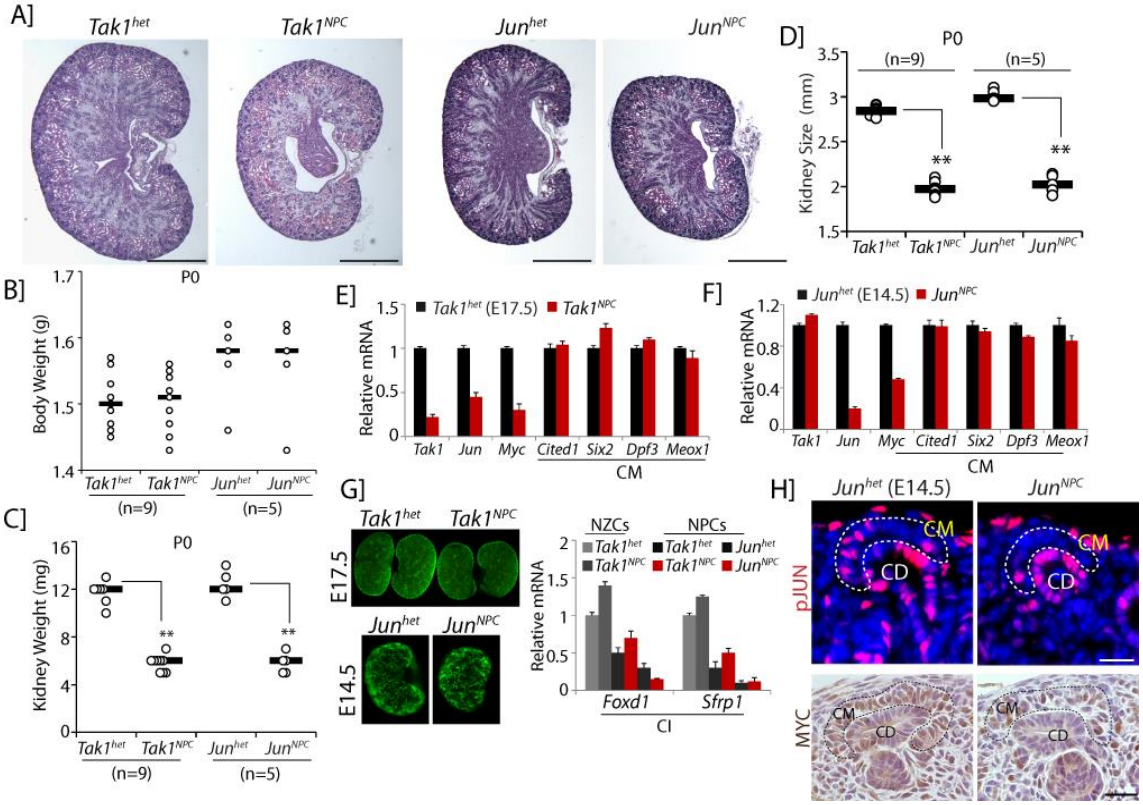

Figure 4.8: *Tak1* and *Jun* are essential for NPC proliferation**:** (A) H&E staining of P0 *Tak1*^{het}, *Tak1*^{NPC}, *Jun*^{het}, and *Jun*^{NPC} kidneys. Scale bars, 500 µM. (B-D) Kidney and body weights and kidney size of P0 *Tak1*^{het}, *Tak1*^{NPC}, *Jun*^{het} and *Jun*^{NPC} kidneys. Number of mice analyzed per genotype (n) is noted in the graphs. ***P*<0.005, Student's t-test. (E,F) Transcriptional analysis of *Tak1*, *Jun*, *Myc*, and cap mesenchyme markers in NPCs isolated from E17.5 *Tak1*^{het} and *Tak1*^{NPC} and E14.5 *Jun*^{het} and *Jun*^{NPC} kidneys. (G) E17.5 *Tak1*^{het} and *Tak1*^{NPC} and E14.5 *Jun*^{het} and *Jun*^{NPC} whole kidneys showing GFP fluorescence. RT-qPCR of the cortical interstitial markers *Foxd1* and *Sfrp1* in NZCs and NPCs isolated from the indicated genotypes. Error bars represent S.D. Two biological replicates per group, n = 2. (H) pJUN and MYC immunostaining in E14.5 *Jun*^{het} and *Jun*^{NPC} kidneys. Cap mesenchyme marked by white/black dotted lines. Scale bars, 50 µM.

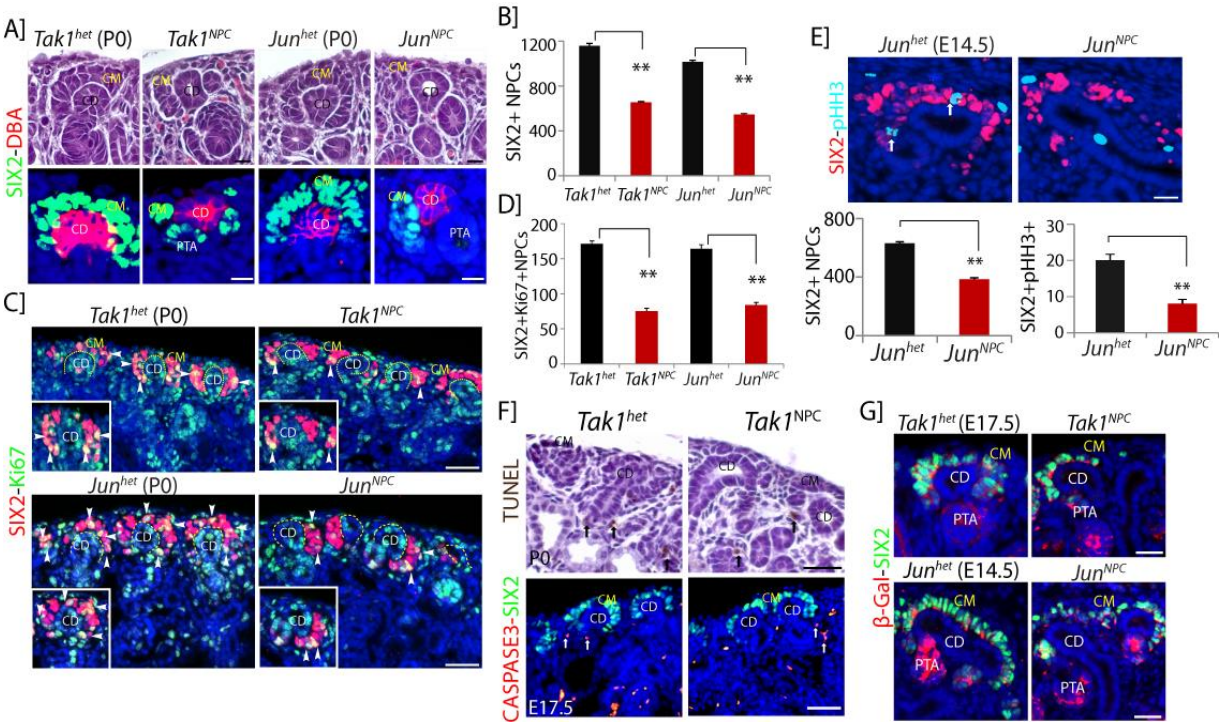

Figure 4.9: Premature depletion of NPCs in *Tak1* and *Jun* conditional mutants: (A) H&E and co-immunostaining of SIX2 (green, cap mesenchyme) and DBA lectin (red, collecting duct) in P0 $Tak1^{NPC}$ and Jun^{NPC} kidneys. Scale bars, 25 µM. (B) Average number of SIX2+ NPCs per kidney section per genotype. Number of mice (n) analyzed per group is noted in the graph. Error bars indicate S.D. $^{**}P<0.005$, Student's t-test. (C) Ki67 (green) and SIX2 (red) co-immunostaining of P0 $Tak1^{het}$, $Tak1^{NPC}$, Jun^{het}, and Jun^{NPC} kidneys. Insets show magnifications of cap mesenchymes with arrows pointing to Ki67+ cells. Scale bars, 100 µM. (D) Number of SIX2+/Ki67+ cells per kidney section. Error bars indicate S.D. $^{**}P<0.005$, Student's t-test. (E) SIX2 (red, cap mesenchyme) and pHH3 (blue, proliferation marker) co-immunostaining in E14.5 Jun^{het} and Jun^{NPC} kidneys. Number of SIX2+ NPCs and pHH3+/SIX2+ cells (white arrows) per kidney section is represented in the graph. Error bars indicate S.D. $^{**}P<0.005$, Student's t-test. Scale bars, 50 µM. (F) TUNEL (black arrows) and Caspase3 (red, apoptosis marker/white arrows) and SIX2 (green, cap mesenchyme) immunostaining in P0 and E17.5 $Tak1^{het}$ and $Tak1^{NPC}$ kidneys. Scale bars, 100 µM. (G) β -galactosidase (red) and SIX2 (green) co-immunostaining of E17.5 $Tak1^{het}$ (*Six2*$^{+/cre}$;*Tak1*$^{+/c}$;*R26RLacZ*) and $Tak1^{NPC}$ (*Six2*$^{+/cre}$;*Tak1*$^{c/c}$;*R26RLacZ*) kidneys. Three mice were analyzed per genotype at E14.5 and E17.5 (n = 3). Abbreviations: CD, Collecting duct; CM, Cap mesenchyme; PTA, Pretubular aggregate.

To understand if this was due to reduced proliferation, we measured the coexpression of Ki67 or pHH3 and SIX2 in $Tak1^{NPC}$ (P0) and Jun^{NPC} (E14.5 and P0) kidneys. We observed a 50% reduction of Ki67+/SIX2+ cells and pHH3+/SIX2+ cells in the $Tak1^{NPC}$ (P0) and Jun^{NPC} (E14.5, P0) kidneys (Figures 4.9C,D). TUNEL and Caspase3 staining showed no evidence of cell death in the $Tak1^{NPC}$ kidneys, suggesting that loss of NPCs was strictly due to reduced proliferation (Figure 4.9F).

To rule out the possibility that *Tak1* and *Jun* mutant NPCs may take on a cortical interstitial fate, we analyzed $Tak1^{NPC}$ (E17.5) and Jun^{NPC} (E14.5) NPCs for markers of cap mesenchyme (*Cited1*, *Six2*, *Dpf3*, *and Meox1*) and cortical interstitium (*Foxd1* and *Sfrp1)*. Cap mesenchyme markers either remained unchanged or showed a slight increase in $Tak1^{NPC}$ (E17.5) and Jun^{NPC} (E14.5). However, neither *Foxd1* nor *Sfrp1* were elevated in $Tak1^{NPC}$ or Jun^{NPC}, indicating that the cellular identity of NPCs was unaltered (Figure 4.9E,F,G).

To confirm that *Tak1* and *Jun* mutant NPCs retain their cellular identity *in vivo*, we performed lineage tracing analysis by crossing the $Six2^{+/cre};Tak1^{+/c}$ and $Six2^{+/cre};Jun^{+/c}$ mice with the *R26RLacZ* reporter. β-galactosidase and SIX2 immunostaining revealed that tagged cells were confined to the SIX2+ cap mesenchyme and its derivatives in both $Tak1^{NPC}$ and Jun^{NPC} kidneys (Figure 4.9G). Thus, inactivation of *Tak1* and *Jun* in NPCs partially phenocopies the *Bmp7* null phenotype, suggesting that they operate in the same pathway to regulate NPC self-renewal.

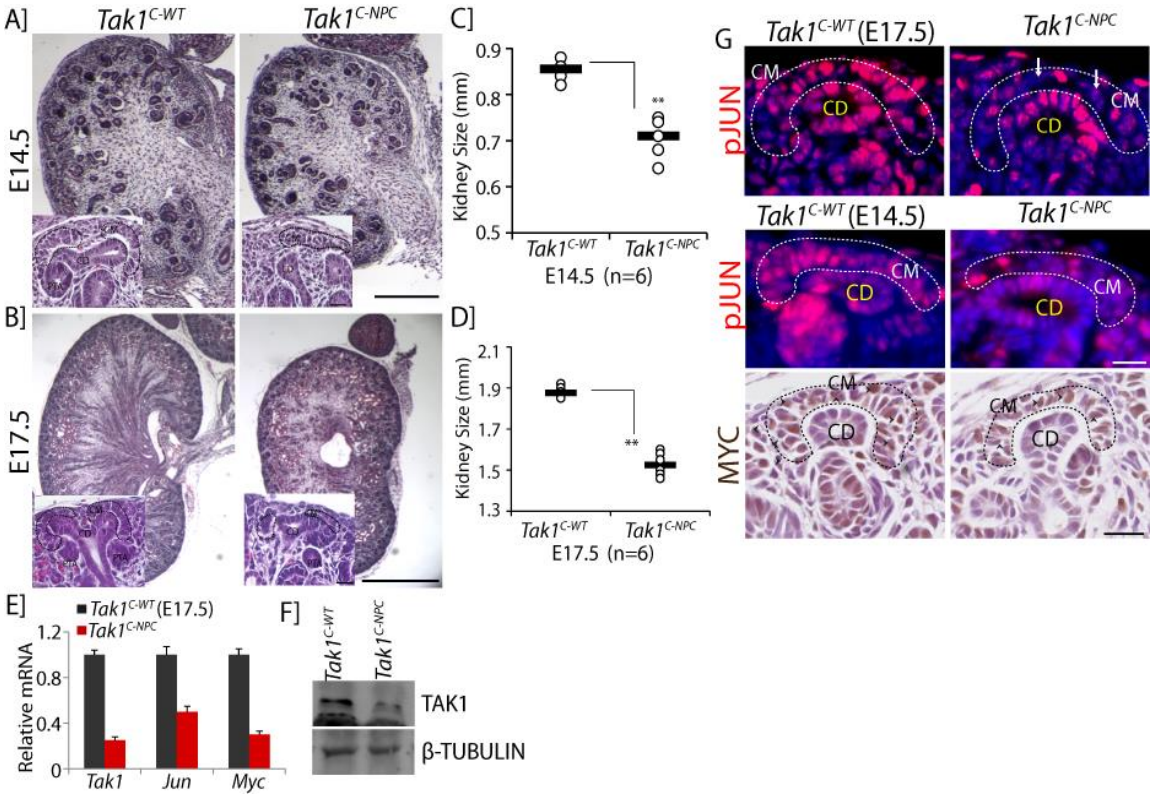

Figure 4.10: *Tak1* is essential for renewal of the early CITED1+ NPCs: (A-D) H&E staining of E14.5 and E17.5 whole *Tak1*$^{C\text{-}WT}$ and *Tak1*$^{C\text{-}NPC}$ kidneys. Insets show nephrogenic units in which cap mesenchymes are outlined with black dashed lines. (C,D) Kidney size. Number of mice analyzed per genotype (n) is noted in the graphs. $^{**}P<0.005$, Student's t-test. Scale bars, 500 μM, 50 μM and 1 mm. (E) RT-qPCR of *Tak1*, *Jun,* and *Myc* in NPCs isolated from E17.5 *Tak1*$^{C\text{-}WT}$ and *Tak1*$^{C\text{-}NPC}$ kidneys. Error bars indicate S.D. Two biological replicates analyzed per genotype (n = 2). (F) Immunoblot of TAK1 and β-Tubulin in NPCs isolated from E17.5 *Tak1*$^{C\text{-}WT}$ and *Tak1*$^{C\text{-}NPC}$ kidneys. (G) pJUN and MYC immunostaining of E14.5 and E17.5 *Tak1*$^{C\text{-}WT}$ and *Tak1*$^{C\text{-}NPC}$ kidneys. Scale bars, 50 μM. Abbreviations: CM, cap mesenchyme; CD, collecting duct.

The few Ki67+/SIX2+ NPCs we observed in *Tak1*^{NPC} kidneys localized predominantly to the distal cap mesenchyme under the collecting duct tips, where CITED1 expression is normally lost (See insets in Figure 4.9C). To understand if the *Tak1*^{NPC} phenotype results from gene inactivation specifically in the CITED1+ compartment, we used the *Cited1-creER*^{T2} strain. *Cited1-creER*^{T2};*Tak1*$^{c/c}$ (*Tak1*$^{C\text{-}NPC}$) and *Tak1*$^{c/c}$ (*Tak1*$^{C\text{-}WT}$, littermate control) mice were tamoxifen-injected at either E11.5 or E14.5 and harvested after 72 hours.

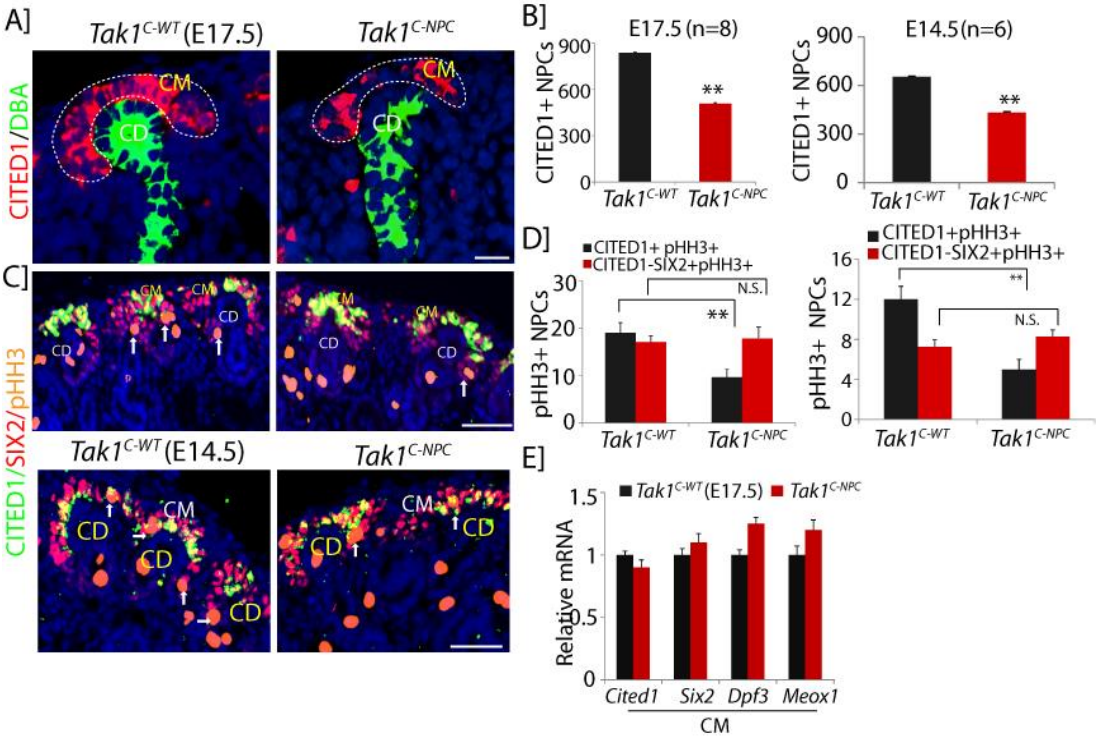

Figure 4.11: Reduced proliferation of CITED1+ NPCs in *Tak1* mutant: (A) CITED1 (red, cap mesenchyme) and DBA lectin (green, collecting duct) staining of E17.5 $Tak1^{C\text{-}WT}$ and $Tak1^{C\text{-}NPC}$ kidneys. Scale bars, 50 μM. (B) Quantification of numbers of CITED1+ cells per E14.5 and E17.5 kidney section per genotype. Number of mice (n) per genotype is noted in the graph. Error bars represent S.D. $^{**}P<0.005$, Student's t-test. (C,D) CITED1 (green), SIX2 (red), and pHH3 (orange/proliferation marker) staining in $Tak1^{C\text{-}WT}$ and $Tak1^{C\text{-}NPC}$ kidneys. Scale bars, 150 μM. Quantification of the number of pHH3+CITED1+SIX2+ and pHH3+CITED1-SIX2+ cells per kidney section per genotype. Error bars indicate S.D. $^{**}P<0.005$ and $P = 0.03$ (N.S, not significant), Student's t-test. (E) RT-qPCR of cap mesenchyme markers in NPCs isolated from E17.5 kidneys. Error bars indicate S.D. Two biological replicates per condition, n = 2.Cap mesenchymes highlighted with black or white dotted lines. Abbreviations: CD, Collecting Duct; CM, Cap mesenchyme.

$Tak1^{C\text{-}NPC}$ kidneys were significantly smaller than $Tak1^{C\text{-}WT}$ at both time points, and their cap mesenchymes were depleted (Figures 4.10A-D). *Tak1* transcript was reduced by 80%, and both *Jun* and *Myc* were reduced in mutant NPCs (Figure 4.8E). Immunoblotting confirmed the reduction of TAK1 in mutant NPCs (Figure 4.10D). pJUN and MYC

were also reduced, indicating that *Tak1* inactivation results in reduced JNK-JUN signaling in NPCs (Figure 4.10G).

To understand if *Tak1* is required to maintain NPCs in the CITED1+/SIX2+ state, we analyzed cap mesenchyme markers in $Tak1^{C\text{-}NPC}$ NPCs. *Tak1*-inactivated NPCs maintained *Cited1* and *Six2* expression at levels similar to wild type, indicating that they retained the appropriate cellular identity. However, the number of CITED1+ NPCs was reduced by 25% to 30% at both E14.5 and E17.5 (Figures 4.11A,B,E).

Coimmunostaining for CITED1, SIX2 and pHH3 confirmed decreased pHH3 staining in CITED1+/SIX2+ cells of $Tak1^{C\text{-}NPC}$ kidneys relative to $Tak1^{C\text{-}WT}$ but no significant difference in the CITED1-/SIX2+ compartment at both E14.5 and E17.5, validating our findings from the $Tak1^{NPC}$ mutants (Figures 4.11C,D). Collectively, our genetic analyses suggest that the BMP7-TAK1-JNK-JUN pathway is required for proliferation of the early CITED1+/SIX2+ compartment *in vivo*.

3.5. Defining cell cycle control mechanisms regulated by BMP7 in NPCs

Having defined the requirements for the components of the BMP7-TAK1-JNK-JUN signaling cascade in NPCs, we wanted to understand how this pathway interfaces with cellular proliferation control mechanisms. We have shown that the BMP7-TAK1-JNK-JUN pathway activates *Jun* and *Myc* transcription in NPCs (Figures 4.1 and 4.10). JUN and MYC are key transcriptional regulators of the cell cycle that modulate the expression of genes involved in the G1 to S phase transition[82,101].

To test how the BMP7-TAK1-JNK-JUN pathway controls NPC proliferation, we investigated the effects of inhibiting pathway components on the G1 to S transition in BMP7-stimulated NPCs. Immunostaining for specific markers of G1 (CCNE1) and S (PCNA) phase was performed to calculate the percentages of G1 and S phase cells in each experimental condition. After 24 hours of stimulation, BMP7 robustly promoted G1 to S transition in both E14.5 and E17.5 NPCs. TAK1 or JNK inhibition significantly reversed this effect, confirming that BMP7 promotes proliferation by controlling G1 to S transition in NPCs through TAK1-JNK signaling (Figures 4.12A-D).

To understand the mechanism underlying the effect of BMP7-TAK1-JNK-JUN signaling on the G1 to S transition, we set out to define the repertoire of G1 phase cell cycle regulatory genes modulated by the pathway in NPCs. Several cell cycle regulators containing AP-1 binding sites are JUN targets, including *Ccnd1*, *Ccnd3*, *p21*, *p16*, *Jun,* and *Myc* [82,83].

Like JUN, MYC regulates the cell cycle by controlling G1 phase genes. Although a number of targets are shared, MYC also has a unique repertoire, including *Ccne1*, *Cdc25a*, *p27,* and *Ccna2*[101]. BMP7 may therefore control G1-S cell cycle regulators not only through JUN but also through MYC. Conditional gene inactivation shows that *Myc* is required for NPC renewal at E15.5-E18.5 but not earlier in nephrogenesis, suggesting that the contribution of MYC to cell cycle control by BMP7 might be limited to later stages of nephrogenesis[84].

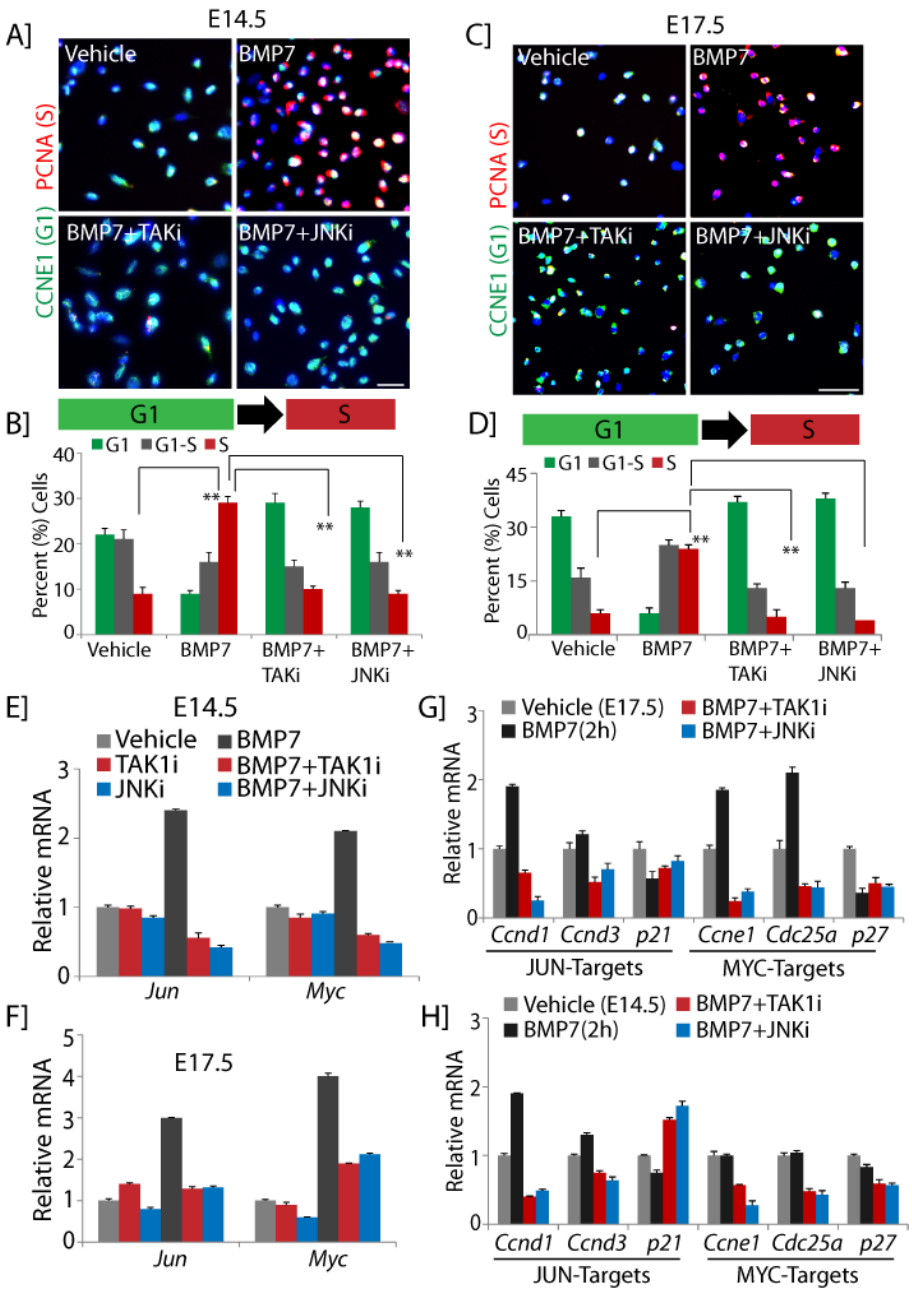

Figure 4.12: BMP promotes G1 to S cell cycle progression in NPCs: (A-D) CCNE1 (G1 phase) and PCNA (S phase) immunostaining of E14.5 and E17.5 NPCs treated for 24 hours with BMP7, TAK1, and JNK inhibitors. Graphs show the percentage of G1, G1-S and S phase cells per condition. Three biological replicates analyzed per condition (n=3). Error bars represent S.D. $^{**}P<0.005$ and $^{**}P<0.001$, Student's t-test. (E,H) RT-qPCR of JUN and MYC and their targets in E14.5 and E17.5 NPCs treated with vehicle, BMP7, TAK1, and JNK inhibitors for 2 hours. Error bars indicate S.D. Three biological replicates analyzed per condition (n=3).

To understand if this is the case, we compared the responsiveness of MYC and JUN targets to BMP7 in NPCs at E14.5 and E17.5. The JUN targets *Ccnd1*, *Ccnd3,* and *p21* were regulated by BMP7 in a TAK1- and JNK-dependent manner in both E14.5 and E17.5 NPCs (Figures 4.12E-H). However, the MYC targets *Ccne1*, *Cdc25a,* and *p27* were regulated by BMP7 in a TAK1- and JNK-dependent manner only in E17.5 NPCs (Figures 4.12E-H).

Our analysis indicates that the BMP7-TAK1-JNK-JUN pathway regulates JUN cell cycle targets including *Myc* throughout nephrogenesis, but that the contribution of MYC itself to the control of G1 targets is limited to later stages of nephrogenesis.

To confirm these observations *in vivo*, we first measured target gene activation in NPCs isolated from E14.5 Jun^{NPC} and E17.5 $Tak1^{NPC}$ kidneys. As expected, JUN targets were misregulated in mutant NPCs at both E14.5 and E17.5, whereas MYC targets were misregulated only at E17.5 (Figure 4.13A,B). Next, we immunostained *Bmp7* null, Jun^{NPC} and $Tak1^{C\text{-}NPC}$ kidneys for the JUN-activated target CCND1 and the MYC-activated target CCNE1 at E14.5 and E17.5. CCND1 has been used as a marker of the distal tubule. Therefore, we first verified its expression in cap mesenchyme using two different antibodies[102].

CCND1 was expressed in a salt-and-pepper distribution in wild type cap mesenchyme. This was expected, considering that its expression is limited to the G1 phase of the cell cycle (Figure 4.13C). CCND1 expression was reduced in the cap mesenchymes of all mutants, suggesting that the BMP7-TAK1-JNK-JUN pathway indeed controls CCND1 *in vivo* and regulates JUN targets both early and late in nephrogenesis (Figure 4.13C).

To understand if this could represent a general reduction in the expression of G1 cell cycle genes in the NPCs of mutant kidneys, we also measured the expression of *Ccnd3*, which is expressed in a temporally overlapping manner to *Ccnd1*. Although RNA expression was reduced by 20%, protein expression was not significantly altered in mutants, supporting the notion that CCND1 is specifically misregulated in BMP7-TAK1-JNK-JUN pathway mutants *in vivo* (Figure 4.13D).

Expression of the MYC-activated target CCNE1 was reduced in the E17.5 mutant kidneys but not in the E14.5 mutants, confirming our previous observation that MYC targets are regulated by the BMP7-TAK1-JNK-JUN pathway preferentially at later stages of nephrogenesis (Figure 4.13E).

From these analyses, we conclude that the BMP7-TAK1-JNK-JUN pathway controls cellular proliferation of NPCs by regulating different G1 phase cell cycle regulators in early and later phases of nephrogenesis (Figure 4.14).

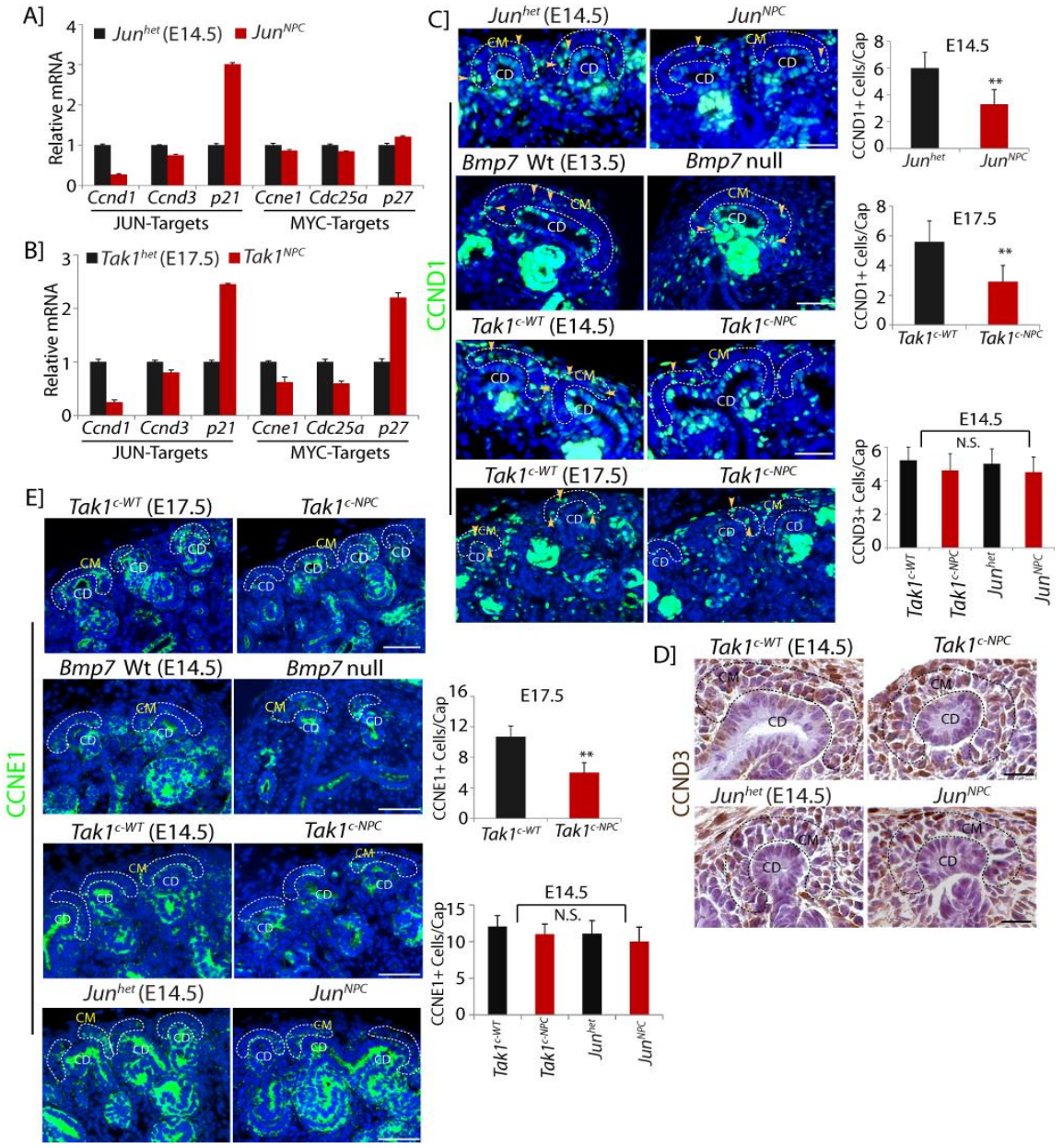

Figure 4.13: BMP7 controls JUN- and MYC-activated targets in NPCs (A,B) RT-qPCR of JUN and MYC targets in NPCs isolated from E14.5 *Jun*$^{\text{het}}$ and *Jun*^{NPC} and E17.5 *Tak1*$^{\text{het}}$ and *Tak1*^{NPC} kidneys. Error bars represent S.D. Two biological replicates analyzed per genotype (n=2). (C-E) CCND1, CCND3 and CCNE1 immunostaining in E14.5 *Jun*^{het} and *Jun*^{NPC} and E17.5 *Tak1*$^{C\text{-}WT}$ and *Tak1*$^{C\text{-}NPC}$ kidneys. Scale bars, 150 µM, 100 µM and 50 µM. Quantification of CCND1+, CCND3+ and CCNE1+ cells per cap mesenchyme was calculated by scoring at least 30 random cap mesenchymes per kidney section per genotype for a total of five sections from each experimental group. Number of mice (n) is indicated in the graphs. Error bars indicate S.D. $^{**}P<0.005$, N.S indicates not-significant ($P>0.05$), Student's t-test.

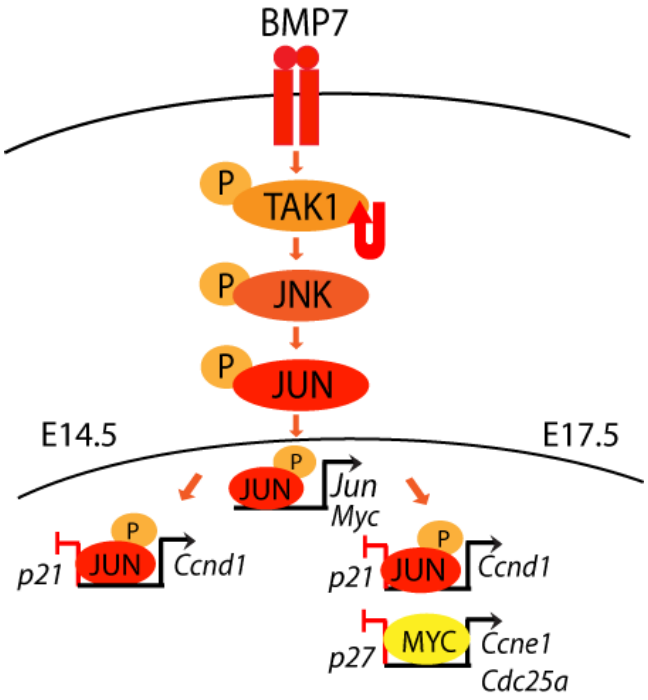

Figure 4.14: Model of BMP7 regulation of the cell cycle in NPCs.

CHAPTER 5

IDENTIFYING POINTS OF INTERSECTION BETWEEN THE NPC RENEWAL PATHWAYS

5.1. Control of NPC proliferation by combinatorial BMP7 and FGF9 signaling

FGF9 synergizes with BMP7 to promote the maintenance of isolated metanephric mesenchyme *in vitro*. However, the molecular mechanism(s) underlying this cross-talk remains unknown [35,55]. Metanephric mesenchyme consists of a mixture of cell types, and we first analyzed proliferation in BMP7 and FGF9 treated purified E17.5 NPCs to understand if the pathways intersect in this cell type.

Using EdU (5'-Ethynyl-2'deoxy-uridine) to label the S-phase and pHH3 to mark cells undergoing mitosis (M), we measured the overall proliferation of NPCs stimulated with BMP7, FGF9, or BMP7+FGF9. BMP7 or FGF9 stimulation showed a significant increase in EdU+ and pHH3+ nuclei compared to vehicle, and this effect was further augmented in BMP7+FGF9 stimulated cultures (Figure 5.1A).

Quantification of the number of EdU+ and pHH3+ nuclei revealed a significant increase in S and M phase cells in BMP7+FGF9 treated cultures relative to either BMP7 or FGF9 stimulation, suggesting that these growth factors indeed collaboratively promote NPC proliferation (Figure 5.1B). Immunostaining and transcriptional analysis of cap mesenchyme markers showed that BMP7+FGF9 stimulated cultures remained in the CITED1+ state following treatment (Figures 5.1C,D).

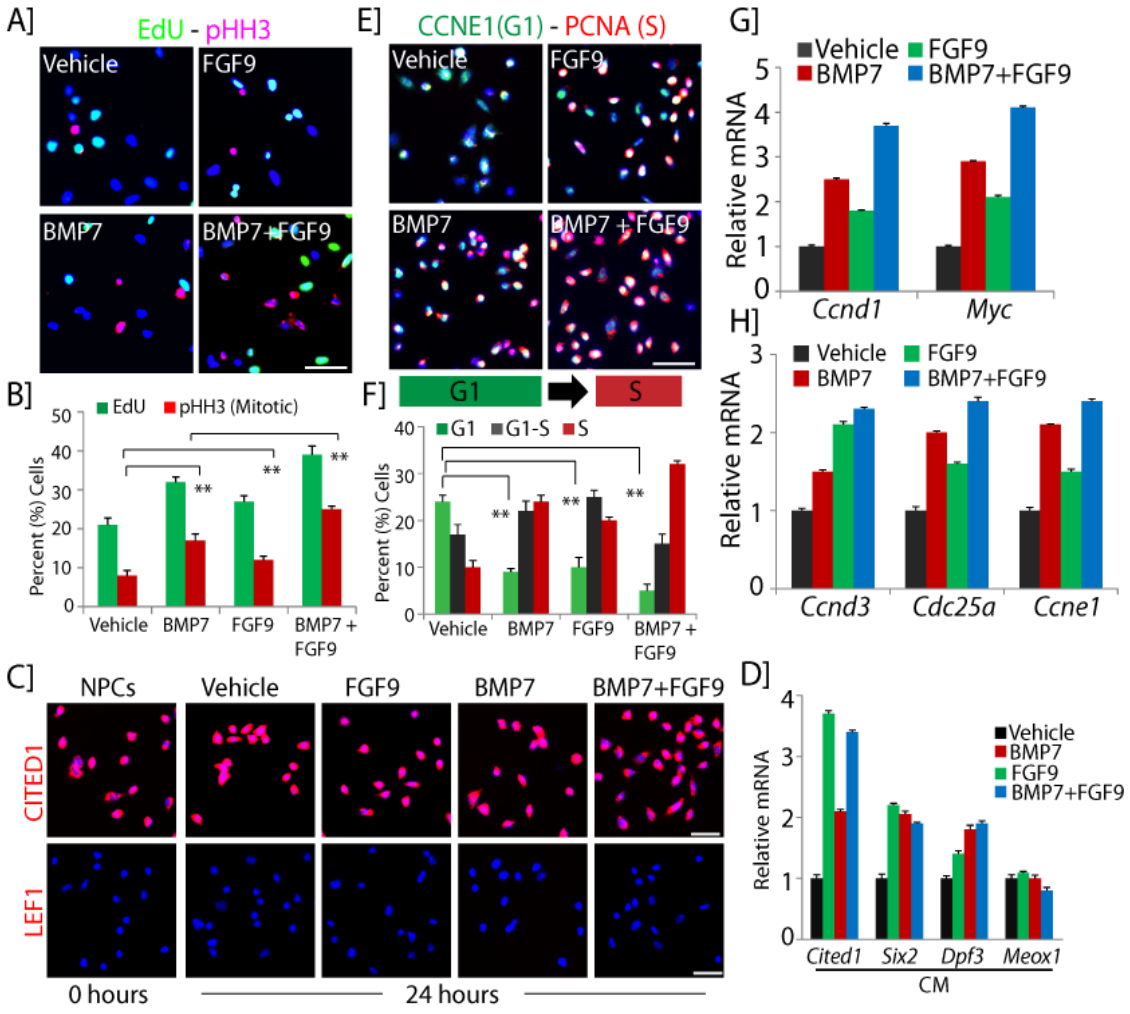

Figure 5.1: BMP7 and FGF9 combinatorially control NPC proliferation: (A,B) EdU (S phase) and pHH3 (M phase) immunostaining in E17.5 NPCs stimulated with vehicle, BMP7, FGF9, or BMP7+FGF9 for 24 hours. Graph shows the percentage of EdU+pHH3+ cells in each condition. Error bars represent S.D. $^{**}P<0.005$ (Student's t-test). Two biological replicates analyzed per condition (n = 2). (C) CITED1 and LEF1 immunostaining in freshly purified E17.5 NPCs treated with vehicle, FGF9 or BMP7 for 24 hours. Scale bars, 50 µM. (D) RT-qPCR of cap mesenchyme markers in NPCs treated with BMP7 and FGF9 for 24 hours. Error bars indicate S.D. Three biological replicates per condition, n=3. (E,F) CCNE1 (G1 phase) and PCNA (S phase) immunostaining of E17.5 NPCs stimulated with vehicle, BMP7, FGF9, or BMP7+FGF9 for 24 hours. Scale bars, 50 µM. Graph shows the percentage of G1, G1-S and S phase cells in each condition. Error bars represent S.D. $^{**}P<0.001$ (Student's t-test). Three biological replicates analyzed per condition (n=3). (G,H) RT-qPCR of cell cycle genes (*Ccnd1* and *Myc*, *Ccnd3*, *Cdc25a*, and *Ccne1*) in NPCs stimulated with vehicle, BMP7, FGF9, or BMP7+FGF9 for 2 hours. Error bars represent S.D. Three biological replicates analyzed per condition, n=3.

To understand if FGF9 interfaces with BMP7 to regulate G1 to S cell cycle progression, we labeled NPCs treated with BMP7, FGF9, or BMP7+FGF9 with CCNE1 and PCNA to distinguish cells in G1 and S phases respectively. BMP7+FGF9 stimulation resulted in approximately 50% fewer G1 and G1-S cells and 30% more S phase cells compared to BMP7 or FGF9 treatment, suggesting that BMP7 and FGF9 promote NPC proliferation by accelerating the G1 to S cell cycle progression (Figure 5.1E,F).

To determine how FGF9 and BMP7 control the G1-S transition, we analyzed the expression of G1 phase cell cycle regulatory genes (*Ccnd1*, *Ccnd3*, *Myc*, *Ccne1*, *Cdc25a*) controlled by the BMP7-TAK1-JNK-JUN pathway in response to either growth factor or combinatorial stimulation. Expression of all five transcripts was up-regulated by BMP7. Interestingly, FGF9 stimulation also increased their transcription, indicating that FGF9 contributes to the regulation of AP-1 targets. BMP7+FGF9 combinatorial stimulation showed an additive effect on these targets, indicating that BMP7 and FGF9 coordinately control transcription of G1 phase cell cycle regulators (Figures 5.1G,H).

5.2. Distinct control of AP-1 transcription factors by BMP7 and FGF9

AP-1 function is regulated by dimer composition as well as the phosphorylation status of its constituents, and activated JUN-FOS heterodimers activate targets more efficiently than JUN homodimers[77-80]. Given that BMP7 and FGF9 combinatorial stimulation increased the transcription of G1 phase cell cycle regulators containing AP-1 binding elements, we speculated that FGF9 may modulate the transcription and phosphorylation of JUN or its dimeric partner FOS concomitantly with BMP7 to regulate AP-1 function.

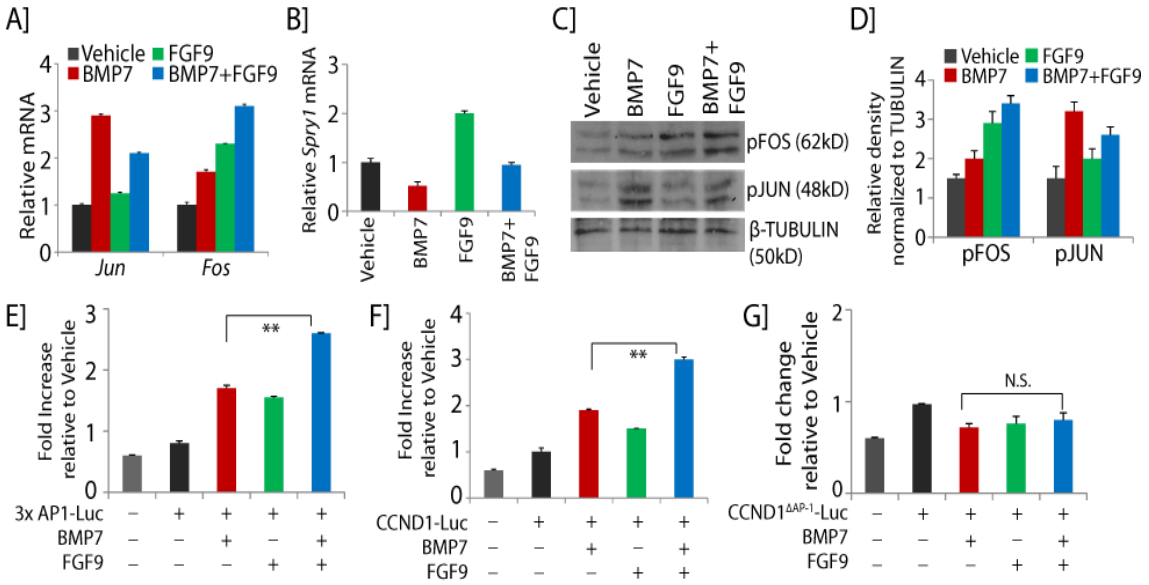

Figure 5.2: BMP7 and FGF9 distinctly control JUN and FOS activation: (A,B) RT-qPCR of *Jun* and *Fos* and *Spry1* (FGF-Target) in NPCs stimulated with vehicle, BMP7, FGF9, or BMP7+FGF9 for 2 hours. Error bars represent S.D. Three biological replicates analyzed per condition, n=3. (C,D) pJUN and pFOS immunoblot of NPCs stimulated with vehicle, BMP7, FGF9, or BMP7+FGF9 for 20 minutes. Graph shows the relative density of pJUN and pFOS normalized to β-tubulin in each condition. (E-G) Bars in the graphs represent the average fold change in luciferase activity of 3XAP1-Luc, CCND1-Luc, and CCND1$^{\Delta AP\text{-}1}$-Luc in NPCs stimulated with BMP7 and FGF9 relative to vehicle treatment for 24 hours. Three biological replicates analyzed per condition (n=3). Error bars represent S.D. ***P*<0.005, N.S, non-significant, Student's t-test.

We first measured the effects of FGF9 and BMP7 stimulation on *Jun* and *Fos* transcription. As expected, *Jun* transcription was up-regulated by BMP7, but surprisingly it was unaffected by FGF9 (Figure 5.2A). FGF9 stimulation of cells was verified by measuring the expression of the FGF-target gene *Spry1* (Figure 5.2B).

Fos transcription, on the other hand, was strongly induced by FGF9 compared to BMP7, and this effect was further enhanced by combined stimulation with BMP7. Thus, while FGF9 and BMP7 cooperatively promote *Fos* transcription, the obligate DNA-binding partner *Jun* is controlled by BMP7 alone (Figure 5.2A).

Examination of JUN and FOS phosphorylation showed that BMP7 robustly activates JUN (3.15-fold), whereas FGF9 activates FOS (2.85 fold) (Figure 5.2C). BMP7+FGF9 stimulation resulted in simultaneous phosphorylation of FOS and JUN, suggesting that AP-1 transcriptional activation may be potentiated (Figure 5.2D). To test this, we transfected the AP-1 luciferase reporter (3XAP1-Luc) and measured reporter activity in response to BMP7 and FGF9 stimulation[96]. BMP7 or FGF9 treatment resulted in less than a 2-fold luciferase response, but combined treatment caused more than a 2.5-fold increase, indicating that simultaneous JUN and FOS activation promotes AP-1 transcriptional activity (Figure 5.2E).

To test this in a gene that directly influences proliferation in NPCs, we compared activation of a *Ccnd1* luciferase reporter (CCND1-Luc) with a variant in which the AP-1 binding site has been mutated (CCND1$^{\Delta AP\text{-}1}$-Luc)[97]. BMP7 or FGF9 treatment alone showed a less than 2-fold luciferase response, whereas BMP7+FGF9 stimulation resulted in a 3-fold increase, demonstrating that concurrent BMP7 and FGF9 signaling strongly promotes AP-1 function compared to either factor alone (Figure 5.2F).

Dependence on the AP-1 element for this transcriptional activity was confirmed by the finding that the *Ccnd1* promoter with a mutated AP-1 binding site was unresponsive to BMP7 and/or FGF9 stimulation (Figure 5.2H). These findings suggest that BMP7 and FGF9 distinctly control the activation of JUN and FOS and regulate AP-1 transcriptional activity in NPCs.

5.3. Inhibition of FGF signaling *in vivo* by conditional overexpression of the *Spry1* transgene

We previously reported that transgenic expression of the FGF feedback regulator *Spry1* in NPCs results in increased apoptosis in cap mesenchyme[21,89]. To confirm the contribution of FGF signaling to FOS regulation *in vivo,* we generated the *Six2-cre*;*Spry1-Tg* (*Spry1-Tg*) strain. Kidneys were severely hypoplastic at P0. Body weight was also reduced compared to wild type littermate controls (Figures 5.3A-D).

Spry1-Tg kidneys displayed a thin nephrogenic zone with depleted cap mesenchymes and distended tubules (Insets in Figures 5.3A). SIX2 immunostaining confirmed the premature loss of NPCs in *Spry1-Tg* kidneys, with approximately 65% reduction in NPC number (Figures 5.3E-G).

Spry1 expression increased 7-fold in *Spry1-Tg* NPCs, whereas the FGF target gene *Pea3* was reduced by 55%, confirming the inhibition of FGF signaling. *Fos* transcript diminished by 70%, whereas *Jun* and its upstream regulator *Tak1* remained unchanged, suggesting that FGF signaling distinctly controls *Fos* transcription in NPCs (Figure 5.3H).

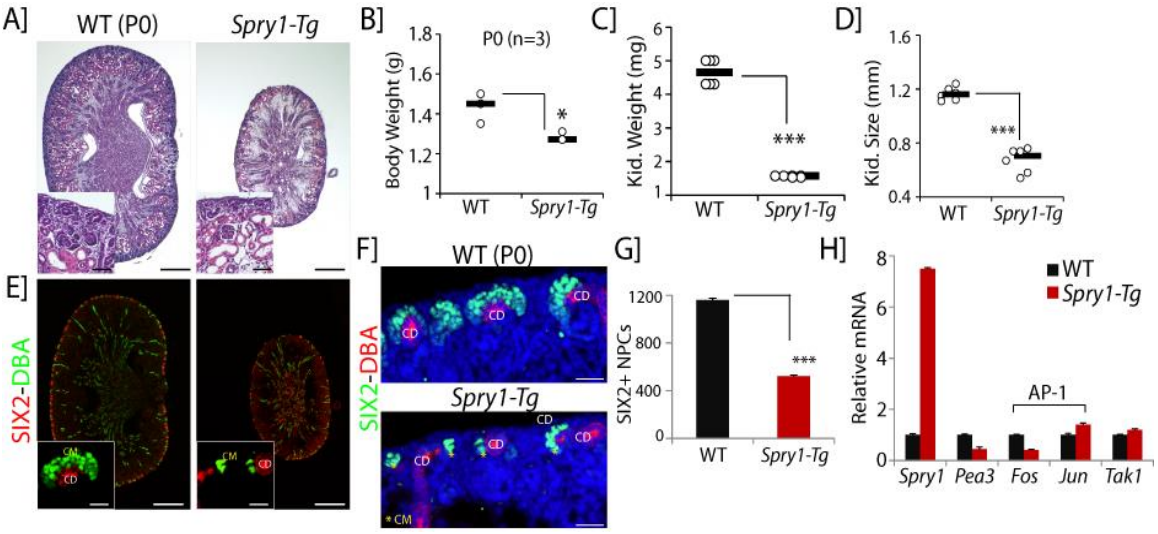

Figure 5.3: *Spry1*-Tg kidneys display premature depletion of NPCs: (A-D) H&E staining of P0 wild type/WT (*Six2-cre* or *Spry1-Tg* littermate controls) and *Spry1-Tg* (*Six2-cre*;*Spry1-Tg*) kidneys. Insets show higher magnification images of the nephrogenic zone. Scale bars, 500 µM and 50 µM. Scatter plots show body and kidney weights, and kidney sizes of P0 WT and *Spry1-Tg* kidneys. * $P<0.05$, ** $P<0.0005$, Student's t-test. Number of mice (n) per genotype is indicated in the graph. (E-G) SIX2 (green, cap mesenchyme) and DBA lectin (red, collecting duct) immunostaining of *Spry1-Tg* kidneys. Scale bars, 500 µM, 200 µM and 25 µM (d) Number of SIX2+ NPCs per section in P0 WT and *Spry1-Tg* kidneys. Error bars represent S.D. *** $P<0.0005$, Student' t-test. (H) RT-qPCR of *Spry1*, *Pea3* (FGF target), *Fos* and *Jun* (AP-1 components) and *Tak1* in E17.5 WT and *Spry1-Tg* NPCs. Two biological replicates analyzed per genotype (n=2). Error bars represent S.D.

5.4. Comparative analysis of AP-1 function in *Jun* mutant and *Spry1-tg* NPCs

To determine if the *Spry1*- mediated attenuation of FGF signaling strictly results in reduced activation of FOS, we compared pFOS and pJUN expression in cap mesenchymes of P0 WT and *Spry1-Tg* versus Jun^{het} and Jun^{NPC} kidneys. Expression of pFOS was reduced, whereas pJUN levels remained intact in cap mesenchymes of *Spry1-Tg* kidneys. Reciprocally, pFOS levels were unperturbed, while pJUN was strongly reduced in the cap mesenchymes of Jun^{NPC} kidneys (Figure 5.4A)

We next asked if reduced activation of JUN and FOS in *Jun*^{NPC} and *Spry1-Tg* NPCs respectively decreases AP-1 transcriptional activity in response to BMP7 or FGF9 stimulation and whether this effect can be rescued by expressing JUN or FOS in mutant NPCs. We treated 3XAP-1Luc-transfected E17.5 NPCs isolated from *Jun*^{het}, *Jun*^{NPC}, WT and *Spry1-Tg* kidneys with BMP7 and/or FGF9. Interestingly, *Jun*-deficient NPCs failed to activate the AP-1 reporter in response to both BMP7 and FGF9 treatment. *Spry1-Tg* NPCs only showed a slight reduction in AP-1 reporter activity in response to BMP7 but were completely unresponsive to FGF9 (Figures 5.4B,C).

Expression of a wild type JUN construct (pCMV-JUN) rescued AP-1 reporter activation in both BMP7 and FGF9 stimulated *Jun*-deficient NPCs, and the expression of a FOS phosphorylation-mimic construct (pcDNA-FOSDD) rescued AP-1 reporter activity in FGF9 stimulated *Spry1-Tg* NPCs (Figures 5.4B,C)[94,95]. This suggests that JUN is essential for AP-1 activation by both growth factors, and the availability of FOS determines the amplitude of AP-1 activity.

To determine whether JUN and FOS are required for the proliferative response of NPCs to BMP7 and FGF9, we performed EdU labeling of NPCs isolated from E17.5 *Jun*^{het}, *Jun*^{NPC}, WT and *Spry1-Tg* kidneys and stimulated with BMP7 and/or FGF9. *Jun*-deficient NPCs failed to respond to both BMP7 and FGF9 stimulation.

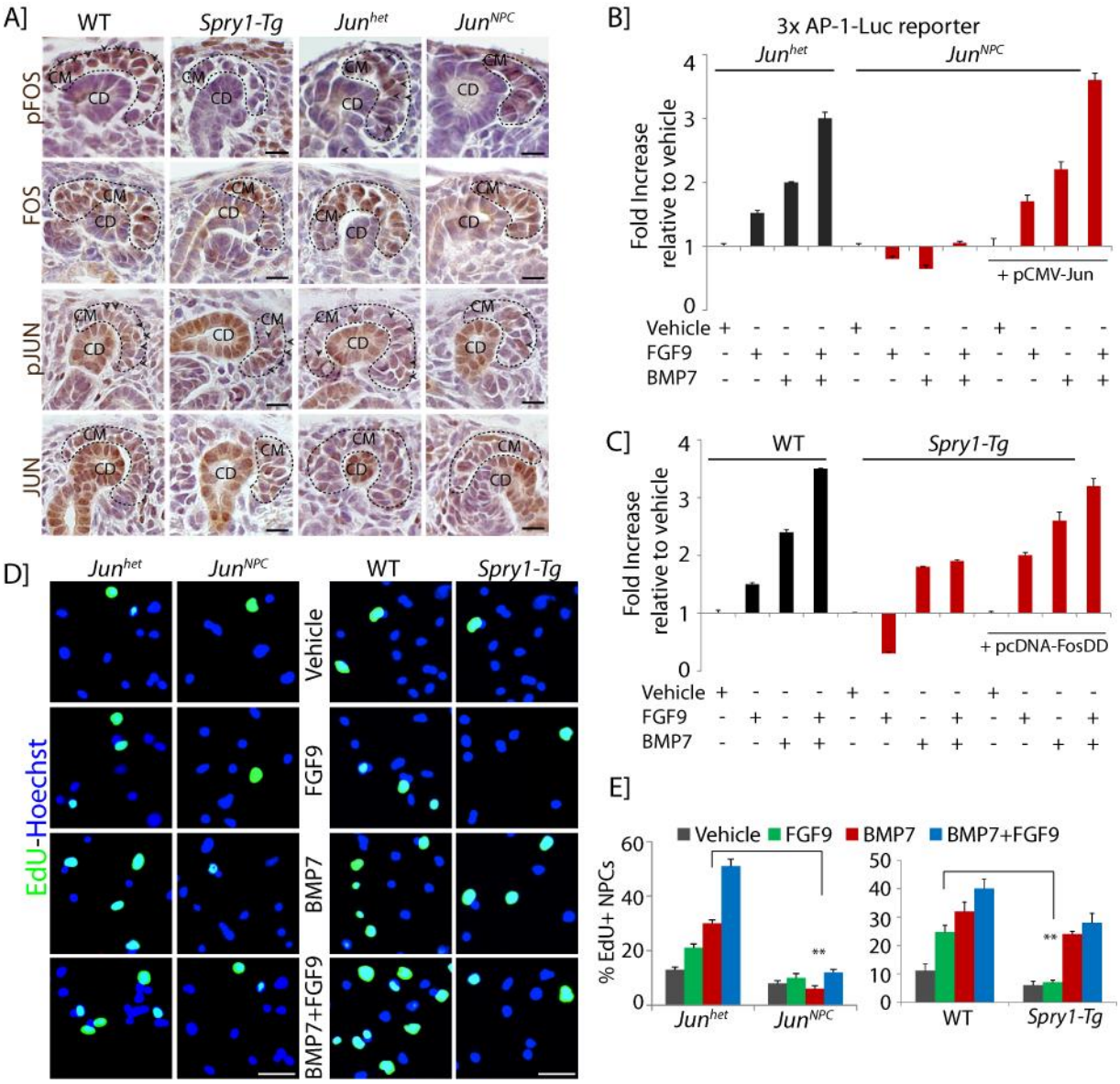

Figure 5.4: BMP7 and FGF9 cooperatively regulate AP-1 function in NPCs: (A) pFOS, FOS, pJUN and JUN (black arrows) immunostaining in P0 WT, *Spry1-Tg* and Jun^{het}, Jun^{NPC} kidneys. Scale bars, 50 µM. (B,C) Luciferase activity relative to vehicle treatment in E17.5 Jun^{het}, Jun^{NPC}, WT, and *Spry1-Tg* NPCs transfected with 3XAP1-Luc and pCMV-JUN or pcDNA-FOSDD and treated with BMP7, FGF9, and BMP7+FGF9 for 24 hours. Error bars represent S.D. Three biological replicates analyzed per condition (n=3). (D,E) EdU-labeling (green, proliferation marker) of E17.5 NPCs isolated from Jun^{het}, Jun^{NPC}, WT and *Spry1-Tg* kidneys and treated with vehicle, BMP7, FGF9, and BMP7+FGF9 for 24 hours. Average number of EdU+ NPCs scored in each condition. Two biological replicates analyzed per condition (n = 2). Error bars represent S.D. $^{**}P<0.005$, Student's t-test. Scale bars, 50 µM.

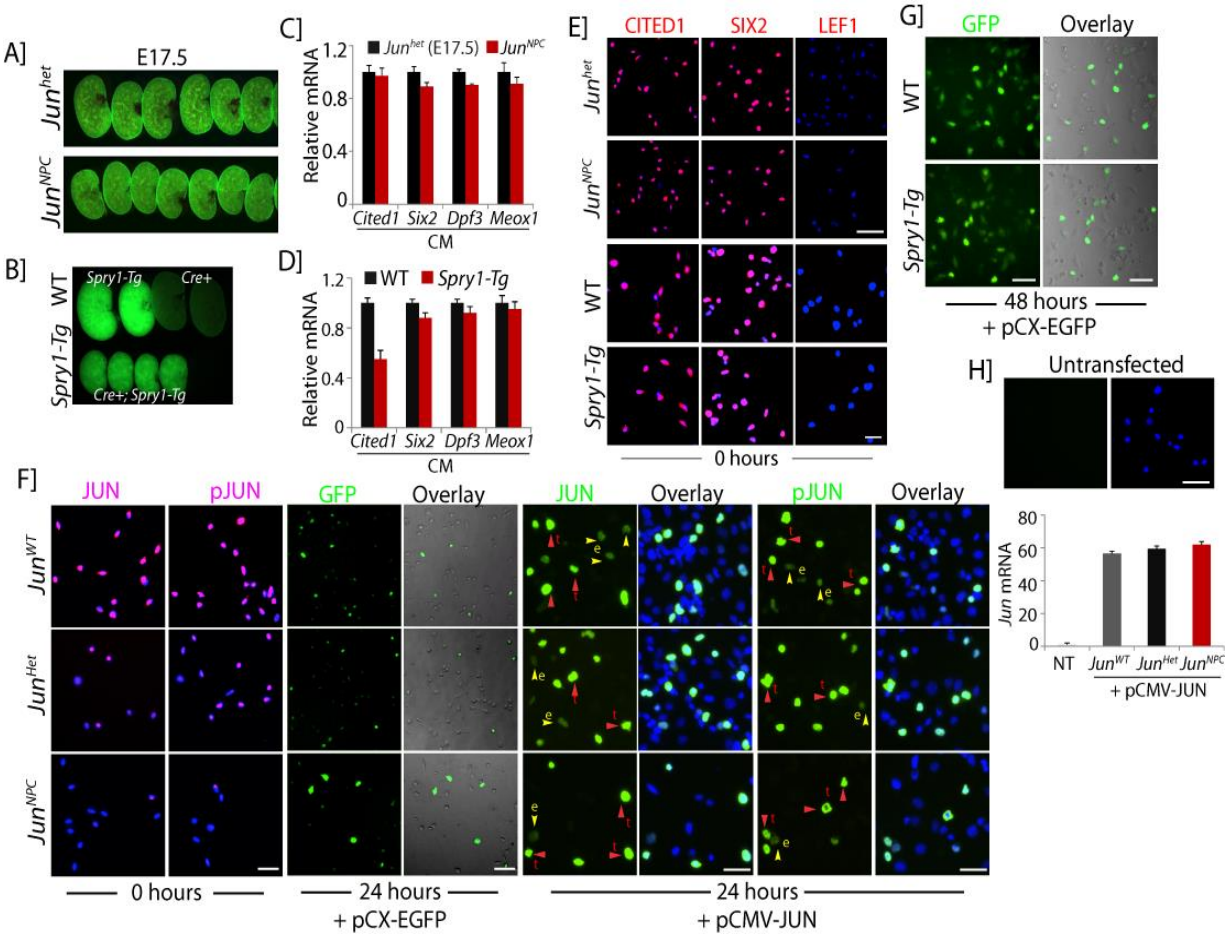

Figure 5.5: Marker analysis of *Spry1*-Tg and *Jun* conditional mutant kidneys: (A,B) E17.5 WT, *Spry1-Tg, Jun*^{het} and *Jun*^{NPC} whole kidneys showing GFP fluorescence. (C,D) Transcriptional analysis of cap mesenchyme (CM) markers in E17.5 WT, *Spry1-Tg, Jun*^{het} and *Jun*^{NPC} kidneys. (E) CITED1, SIX2 and LEF1 immunostaining in E17.5 NPCs isolated from WT, *Spry1-Tg, Jun*^{het} and *Jun*^{NPC} kidneys. Scale bars, 50 µM. (F) JUN and pJUN immunostaining in freshly purified NPCs isolated from E17.5 *Jun*^{het} and *Jun*^{NPC} kidneys. NPCs transfected with pCX-EGFP showing GFP expression at 24 hours. pJUN and JUN immunostaining in pCMV-JUN transfected NPCs showing endogenous (e, yellow arrows) and over-expressed JUN (t, red arrows) 24 hours after transfection. Scale bars, 50 µM. (G) GFP expression at 48 hours in pCX-EGFP transfected E17.5 NPCs isolated from WT and *Spry1-Tg* kidneys. Scale bars, 50 µM. (H) DAPI staining of untransfected cells. RT-qPCR of *Jun* expression in NPCs transfected with pCMV-JUN for 24 hours. Error bars represent S.D. Two biological replicates per condition, n=2.

However, proliferation of *Spry1-Tg* NPCs in response to FGF9 was severely attenuated but only slightly reduced in response to BMP7, suggesting that *Jun* is essential for the proliferative response of NPCs to both BMP7 and FGF9 (Figures 5.4D,E). Cellular identity of isolated E17.5 *Jun* mutant and *Spry1-Tg* NPCs was verified by examining cap mesenchyme and pre-tubular aggregate markers, which revealed that NPCs are retained in the CITED1+ state in mutant NPCs (Figures 5.5A-D). The transfection efficiency of NPCs was estimated by expression of a GFP construct, JUN and pJUN immunostaining and RT-qPCR analysis of *Jun* transcript levels in transfected cells (Figures 5.5E-H). Based on these studies, we propose that BMP7 and FGF9 cooperatively control the composition of AP-1 dimers in NPCs and that AP-1 composition influences the strength of activation of cell cycle regulators such as *Ccnd1* (Figure 5.6).

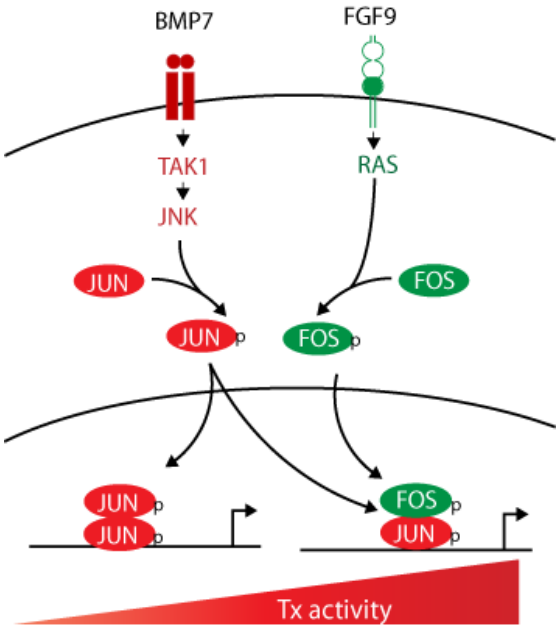

Figure 5.6: Model of BMP7 and FGF9 combinatorial control of NPC renewal.

CHAPTER 6

DISCUSSION AND FUTURE DIRECTIONS

6.1. BMP7-SMAD1/5 signaling in NPC differentiation

BMP7 is essential for NPC maintenance and self-renewal in the developing kidney[33,34]. In this study, we identified an important role for BMP7-mediated SMAD signaling in priming NPCs for differentiation. We demonstrate that a SIX2-only sub-compartment resides between the early CITED1+SIX2+ progenitor compartment and the differentiated LEF1+ PTA compartment within the CM. We also show that the SIX2-only sub-compartment represents a functionally distinct progenitor state, and the transition from the CITED1+ progenitor state to the SIX2-only state requires BMP7 signaling.

Previous studies indicated that low-level SMAD signaling occurs in the CM[42,45]. Here, we clearly show that activated phospho-SMAD1/5 is localized to the SIX2-only compartment in the distal region of the CM underneath the CD tips. We find that BMP7 promotes the transition between compartments through activation of SMAD1/5 signaling, in contrast to the progenitor renewal effect mediated through the MAPK pathway in CITED1+ cells[43]. In E14.5 *Bmp7* null mutants, in addition to a reduction in CITED1+ NPCs, we also see a loss of the SIX2-only compartment with a concomitant reduction in pSMAD1/5 in the region, supporting a role for BMP7-mediated SMAD signaling in NPC differentiation. However, we cannot rule out that this effect could be due to premature depletion of progenitors rather than a differentiation defect due to loss of SMAD1/5 signaling. Conditional inactivation of SMAD1/5 transcription factors specifically in the

NPCs would be important to distinguish these effects and to confirm the role of SMAD signaling in NPC differentiation *in vivo*.

A previous study suggested that the anti-differentiation factor SIX2 interacts with β-catenin/LEF/TCF complex in CITED1+ NPCs, preventing the activation of pro-differentiation genes. However, in a subset of progenitors with low SIX2 activity, β-catenin/LEF/TCF signaling induces NPC differentiation through activation of *Fgf8* and *Wnt4*[68,69]. Our findings indicate that BMP7-SMAD1/5 signaling synergizes with β-catenin to induce the pro-differentiation program via *Wnt4* activation. Whether SMAD1/5 transcription factors interact in the SIX2/β-catenin/LEF/TCF complex in SIX2-only NPCs to promote the pro-differentiation program remains to be determined.

Several molecular cross-talk mechanisms can be found in the literature supporting a direct or indirect involvement of SMADs in the regulation of β-catenin transcriptional activity. SMAD transcription factors interact with β-catenin and form a transcriptional complex on target genes such as *c-Myc, Slug,* and *Msx2*[103-105]. Therefore, SMAD1/5 could directly bind to β-catenin to drive the expression of *Wnt4* in differentiating NPCs. Alternatively; SMAD1/5 could be involved in the recruitment of co-activators necessary for β-catenin to induce transcription[103-106]. Future biochemical studies will be required to elucidate the mechanistic bases for this synergistic interaction in NPC differentiation. Based on our findings, we propose that the compartmentalization of the CM into a series of functionally distinct progenitor cell sub-compartments might be necessary to ensure that CITED1+ NPCs are prevented from undergoing premature induction and are retained for future rounds of nephrogenesis.

Cessation of nephrogenesis occurs shortly after birth between P2 and P3, resulting in the terminal differentiation and exhaustion of all undifferentiated CITED1+ NPCs[8]. What causes the shift in balance between self-renewal and differentiation during this terminal phase of nephrogenesis has not been determined. We find that activated pSMAD1/5 signaling, which is initially restricted to the distal region of the CM until E18.5, expands into the cortical aspect between P0 and P1. Pharmacological inhibition of pSMAD1/5 signaling in newborn pups retained the NPCs in the CITED1+ state and increased nephron endowment, indicating that increased pSMAD1/5 signaling between P0 and P1 skews the balance towards NPC differentiation. Whether the expansion in activated SMAD1/5 signaling domain is accompanied by a reduction in pro-renewal MAPK signaling in the CM is yet to be determined.

The mechanisms by which activated SMAD1/5 signaling is suppressed in CITED1+ NPCs are currently less well understood. However, a recent work indicated that FGF signaling may negatively regulate SMAD signaling, providing an explanation for the lack of SMAD signaling seen in the CITED1+ compartment[107]. Extracellular modifiers of BMP7 signaling such as CV2 and TWSG regulate SMAD1/5 signaling in the CM during the embryonic period[45]. However, their effects on MAPK signaling were not studied.

How BMP7 differentially activates MAPK versus SMAD1/5 signaling in the CM is not known. It is also not clear whether MAPK activation displays an inverse relationship to SMAD1/5 activation. One possible mechanism by which SMAD1/5 signaling increases during the terminal stages of nephrogenesis could be due to an increase or a reduction in the levels of extracellular modifiers that regulate the activation of MAPK versus SMAD signaling. Further studies to investigate if the levels of CV2, TWSG and possibly other

modifiers change during the different stages of nephrogenesis, influencing the activation of MAPK and SMAD1/5 signaling in response to BMP7 will be essential to understand the mechanisms affecting NPC renewal versus differentiation.

Previous studies have proposed two distinct models to explain the premature exhaustion of NPCs during the cessation of nephrogenesis. The first model postulates that changes in gene expression within the CM or other cell types in the niche caused by changes in oxygen tension during parturition could serve as a trigger to end NPC renewal[108]. However, it is not clear how the changes in gene expression skew the balance towards NPC differentiation. A *de novo* parturition-based trigger also does not support the reported cessation of nephrogenesis in humans that occurs at 36th week of pregnancy[109]. An alternative model suggested that the termination of nephrogenesis occurs due to a gradual depletion of the renewing population of NPCs within the CM due to a shift in growth factors within the niche[110]. Our finding that SMAD1/5 signaling increases in the CM after P0, possibly due to the altered equilibrium between growth factors and their modifiers expressed within the niche, supports the second model of a progressive loss of renewing progenitors. Taken together, our data suggests that BMP7-mediated SMAD1/5 signaling is essential for NPC differentiation.

6.2. BMP7-TAK1-JNK-JUN signaling in NPC proliferation

Previously, we showed that BMP7 promotes proliferation of NPCs through MAPK signaling[43]. Here, we have defined the molecular components of the signaling cascade through which BMP7 promotes proliferation of NPCs. The signaling cascade is initiated by the activation of the MAPKKK TAK1 in response to BMP7 stimulation. Although

TAK1 can be activated by numerous stimuli, the finding that *Bmp7* and *Tak1* interact to regulate NPC renewal *in vivo* indicates an essential role for TAK1 specifically in the BMP7 pathway[75].

TAK1 activates JNK, which in turn phosphorylates the transcription factor JUN, and the kinase activity of each of these components is essential for the proliferation of NPCs. Kidneys lacking *Tak1* or *Jun* in the cap mesenchyme display identical phenotypes characterized by premature depletion of NPCs, indicating that JUN may be the sole essential mediator downstream of TAK1 in this signaling process. This is unanticipated, as a previous study demonstrated a role for p38 in SMAD-independent signaling downstream of the BMP receptor ALK3 in the developing kidney[39]. However, *Alk3* was inactivated throughout the kidney with the exception of the collecting duct in this experiment, and it is probable that SMAD-independent signaling in cell types other than NPCs accounts for the difference. We show that *Myc* is a transcriptional target of the BMP7-TAK1-JNK-JUN pathway in NPCs. *Myc* is essential for cap mesenchyme proliferation *in vivo* and undergoes complex posttranslational regulation by the EYA1 phosphatase[84,111]. Together with JUN, MYC activates G1 phase cell cycle regulators in NPCs, explaining the proliferative effect of BMP7 stimulation.

NPCs display different average cell cycle lengths during early (E13.5) and later (E17.5) stages of nephrogenesis. Proliferation profiles of cap mesenchymes at these stages suggest that they are heterogeneous, containing both slowly and rapidly dividing cells[112]. An interpretation consistent with models of other stem/progenitor cell populations is that the slowly-dividing subset may represent the self-renewing CITED1+/SIX2+ population, whereas the rapidly-dividing subset represents the CITED1-/SIX2+ population that is dif-

ferentiating[113,114]. Our finding that the CITED1+/SIX2+ population is reduced following conditional inactivation of *Tak1* using *Six2-cre* and *Cited1-creER^{T2}* drivers without a significant effect on the proliferation of the CITED1-/SIX2+ population indicates that the BMP7-TAK1-JNK-JUN pathway is utilized primarily by the slowly-dividing, self-renewing cells in the CM.

The cycle length of NPCs increases as the embryo ages, indicating that control mechanisms are added as development progresses[112]. Interestingly, targets of MYC are primarily regulated late in nephrogenesis, which is consistent with the observation that conditional *Myc* inactivation slows cap mesenchyme proliferation only after E15.5[85]. Whether cell cycle control through MYC late in nephrogenesis represents the addition of a control mechanism or simply redundancy with N-MYC, whose expression is lost late in nephrogenesis, will need to be answered by comparing the conditional inactivation of both factors[84,85].

6.3. BMP7 regulation of NPC survival

In addition to reduced proliferation in the CM, loss of *Bmp7* causes ectopic cell death within the nephrogenic zone of the developing kidney[33,34,43]. However, we do not see any effects on survival in kidneys in which *Tak1* or *Jun* have been inactivated in the CM. However, inactivation of *Smad4* using *Bmp7-cre* results in ectopic cell death within the nephrogenic zone of mutant kidneys, indicating that cell survival may be regulated through the SMAD pathway[41].

Our findings show that SMAD signaling is limited to the CITED1-/SIX2+ compartment of the cap mesenchyme and that it is this specific compartment that is lost in the *Bmp7* null. Based on this, we hypothesize that SMAD signaling promotes cell survival once they have exited the CITED1+ compartment. The gene encoding the anti-apoptotic regulator *Bcl-2* is highly expressed in NPCs, and its inactivation results in the development of a hypomorphic kidney[86]. The metanephric kidney forms in both *Bcl-2* and *Bmp7* null mutants, and growth is noticeably retarded at approximately E12 in both, suggesting that they may operate in the same pathway[33,34]. Studies aimed at understanding how SMAD signaling integrates with the upstream regulators of *Bcl-2* such as PAX2 and p53 will be needed to test this hypothesis[87].

6.4. BMP7 and FGF9 combinatorial regulation of AP-1 function

JUN, FOS and ATF proteins comprise the AP-1 transcription factor family, with JUN and FOS constituting the prototypical form of the AP-1 dimer[77-81]. Composition of the AP-1 dimer is a critical factor in determining cellular fates such as proliferation, apoptosis and differentiation[80]. We find that BMP7 robustly controls transcription and activation of JUN, whereas FGF9 strongly induces transcription and phosphorylation of FOS. Analyses of the *Six2-cre*;*Spry1-Tg* mouse strain in which the FGF feedback inhibitor SPRY1 is expressed in NPCs and primary cell transcriptional reporter assays indicate that the activation of JUN and FOS by simultaneous BMP7 and FGF9 signaling potentiates AP-1 transcription[89]. We propose that co-regulation of the AP-1 transcription factor is one basis for the cooperative effect of BMP7 and FGF9 in kidney development[35,55]. While we have defined the signaling cascade between BMP7 and *Jun*, the pathway between FGF9 and

Fos is less clear. The inhibitory effect of *Spry1* indicates that RAS is essential, and a recent report showing that NPC self-renewal is dependent on PI3K suggests that FGF9-RAS-PI3K may be the pathway governing *Fos* expression[115].

Although JUN can form homodimers to activate target transcription, these bind to AP-1 elements less tightly than JUN-FOS heterodimers and have weaker transcriptional activity[80]. In the case of BMP7 stimulation alone, the ratio would be skewed toward homodimer formation, whereas concurrent FGF9 signaling would skew the ratio toward JUN-FOS heterodimers, thus amplifying target transcription. Combinatorial BMP7 and FGF9 stimulation promotes the robust transcription of the G1 regulator *Ccnd1* in an AP-1 dependent manner, and we propose that control of AP-1 targets by combinatorial BMP7 and FGF9 signaling promotes G1-S transition, providing a mechanism for the cooperative effects of these growth factors on NPC proliferation.

Our current findings identify AP-1 as a specific point of interaction of the BMP and FGF pathways in NPCs. We have previously shown that WNT and FGF activate common targets in NPCs[21]. WNT9b-β-catenin signaling could converge with BMP7 and FGF9 on the regulation of AP-1 in CITED1+ NPCs. Signaling cross-talk between BMP, FGF, and WNT pathways is a recurring theme in organogenesis, and WNT/β-catenin signaling can ββregulate the transcription of AP-1 targets such as *Myc, Ccnd1* and *Ccnd2*[74,116]. Understanding this point of intersection further could explain the molecular basis for the combinatorial effects of these three distinct pathways on NPC proliferation.

6.5. Future directions

Our understanding of the growth factor signaling involved in the regulation of NPC maintenance, self-renewal and differentiation has significantly expanded over the years, but several questions are still unanswered. We have yet to fully understand how the distinct growth factor signaling pathways integrate to combinatorially regulate these disparate cellular events. Given the array of candidate cross-talk mechanisms available in the literature, a systematic approach is required to map individual components of the signal transduction cascade and identify mechanisms involved in regulating the balance between renewal and differentiation of NPCs.

The molecular and biochemical tools developed in this study along with the primary NPC culture system will allow us to investigate the pathway interactions and test them *in vivo* using conditional gene inactivation approaches. Understanding the developmental signaling mechanisms that balance NPC renewal and differentiation will be essential to develop an *in vitro* culture system for the simultaneous propagation and generation of nephrons from embryonic stem (ES) cell-derived NPCs and for clinical applications.

In the current study, we have mapped the MAPK components downstream of BMP7 in NPCs. However, it is not clear which type I and type II receptors are expressed and required for activation of the TAK1-JNK-JUN pathway in CITED1+ NPCs. The GUDMAP database shows expression for all three type I (*Alk2/3/6*) and type II (*Bmpr2, Acvr2a/b*) BMP-receptors in the CM[81]. Of these receptors, kidney phenotypes have been reported for *Alk3*, *Acvr2a* and *Acvr2b*[39,40]. However, their potential role and requirement in the

activation of MAPK and SMAD signaling in NPC renewal and differentiation has not been explored.

Differential receptor expression, oligomerization and utilization in different CM compartments could be a potential mechanism by which BMP7 bimodally activates MAPK versus SMAD pathways in CITED1+ and SIX2-only NPCs[117,118]. Preliminary unpublished findings indicate that BMP7 activates TAK1 and SMAD pathways in a dose-dependent manner (data not shown). It will be interesting to see if co-expression of a specific receptor switches the activation of MAPK versus SMAD by BMP7 in CITED1+ NPCs. Additionally, the role of extracellular modifiers such as CV2 or TWSG or other proteins should be examined in this setting to see if they affect the response to BMP7 in skewing the activation of TAK1 versus SMAD signaling[45].

SMAD and TAK1 pathways act redundantly to regulate the development of different organ systems[119-121]. However, our preliminary data show that activated SMAD1/5 signaling increases in *Tak1* mutants, suggesting an inverse relationship between TAK1 and SMAD in CITED1+ NPCs (data not shown). In addition to other reported mechanisms, TAK1 suppression of pSMAD1/5 signaling may explain the lack of activated SMAD signaling in CITED1+ NPCs[107].

Conditional inactivation of the common-mediator co-SMAD *Smad4* only partially recapitulates the *Bmp7* null phenotype, with premature cessation of nephrogenesis and cell death in the nephrogenic zone[41]. Given that SMAD4 is shared by the TGF-β pathway, conditional inactivation of the receptor-SMADs *Smad1* and *Smad5* will be required to clearly demonstrate the role of BMP7-mediated SMAD1/5 signaling in NPC differentia-

tion[75]. Global *Smad1* and *Smad5* knockouts are embryonic lethal and die by E11.5 before the onset of metanephric kidney development[122,123]. Hence, single and compound inactivation of *Smad1* and *Smad5* specifically in NPCs should be carried out to accommodate the effects of redundancy between these factors and to define the specific R-SMADs involved in control of NPC differentiation.

An important feature of the *Smad4* mutant is the improper segregation of CM and CI cells that is distinct from *Bmp7* null and *Tak1* mutants. However, this phenotype is recapitulated by compound inactivation of *Cv2* and *Bmp7,* indicating that SMAD4-dependent BMP7 signaling is essential for NPC segregation from the CI. The molecular mechanism underlying this phenotype is not clear. *Kif26b* and *Itga8* are implicated in the regulation of CM adhesion and the segregation of NPCs from the CI[124,125]. Preliminary studies indicate that SMAD signaling regulates *Kif26b* expression in NPCs (data not shown). Further experiments will be needed to understand this interaction and elucidate the role of SMAD1/5 signaling in CM adhesion and the segregation of NPCs from the CI. Because conditional mutants of *Tak1* and *Smad4* do not fully recapitulate the *Bmp7* null phenotype, compound inactivation of *Tak1* and *Smad4* in NPCs and comparison with single mutants should shed light on their specific roles downstream of BMP7 in NPC adhesion, survival, self-renewal and differentiation.

BMP7 and FGF9 synergistically promote NPC maintenance in organ culture experiments[35,55]. Our findings suggest that BMP7 and FGF9 co-operatively control AP-1 activation and NPC proliferation, indicating that additional cross-talk mechanisms may underlie their synergistic interaction during kidney development.

The intracellular signal transduction mechanisms utilized by FGF9/20 in NPCs are still not understood. RAS and PI3K pathways play an essential role in the maintenance of NPCs[31]. A recent study reported that PI3K has dose-dependent effects on NPC self-renewal and differentiation through regulation of β-catenin signaling *in vitro*[115]. However, the function of the ERK/MAPK pathway downstream of FGF signaling remains to be elucidated. Our preliminary findings indicate that both ERK and PI3K pathways may be involved in the regulation of AP-1 transcription and NPC proliferation downstream of FGF9 (data not shown). Generating conditional mutants of these key pathway components will uncover their putative functions in the regulation of NPC renewal and differentiation.

Recent work indicates that FGF20 through the ERK/MAPK pathway antagonizes BMP-SMAD activation in the CM to promote NPC survival[107]. ERK/MAPK regulates SMADs through linker modification, resulting in their degradation. However, linker phosphorylation and degradation of SMADs can be regulated by several kinases, including TAK1 and GSK3β, implying that BMP7-TAK1 and WNT signaling may also be involved in regulating SMAD activation in CITED1+ NPCs[126,127].

WT1, an anti-apoptotic factor in NPCs, was shown to modulate both FGF-ERK and BMP-SMAD activity in the CM. More recently, WT1 was shown to regulate FGF-PI3K signaling via activation of a novel modulator of FGF signaling called Growth arrest-specific 1 (GAS1) in NPCs. Kidney development proceeds normally in *Gas1* mutants until E15.5. However, proliferation is then reduced in NPCs leading to their premature depletion by E18.5 and indicating that *Gas1* is required for the regulation of FGF signaling and NPC proliferation during the late stages of nephrogenesis[128].

Our findings on BMP7 regulation of the cell cycle in NPCs also indicates that different cell cycle regulatory mechanisms are utilized during early and late phases of nephrogenesis. Comprehensive analyses of conditional mutants of genes essential to kidney development at different stages of nephrogenesis will be needed to fully understand and delineate their specific functions in NPC renewal and differentiation.

The receptors involved in the activation of β-catenin signaling downstream of WNT9b in NPCs have not yet been identified. The amplitude of β-catenin activity is a determining factor in maintaining the undifferentiated state of NPCs and for the induction of a pro-differentiation program[56,69]. A cross-talk mechanism between BMP-SMAD and WNT signaling at the level of receptor regulation has been demonstrated in other cellular contexts[129]. Determining if such regulatory mechanisms are utilized in the context of NPC differentiation is important to understand the molecular mechanism driving the nephron induction program.

An essential role for stroma-derived signals in regulation of NPC self-renewal and differentiation has been demonstrated over the years. The earliest evidence came from *Foxd1* null mutants that displayed large clusters of undifferentiated CM cells in their kidneys[22]. The proliferative index of the CM cells in the mutants was comparable to the wild type, indicating that a block in differentiation caused the accumulation of CM cells. Work from our laboratory has shown that Decorin, small leucine-rich proteoglycan, is regulated by FOXD1 and antagonizes BMP7 activation of SMAD signaling, thereby blocking NPC differentiation[130]. Other studies have highlighted a role for the stromal-derived protocadherin FAT4 in the regulation of WNT9b-β-catenin signaling in NPC self-renewal and differentiation[131]. Several models have been proposed for FAT4 interaction with NPCs.

However, the downstream components activated by FAT4 are unclear [142,143]. Microanatomical and histological analyses show that as kidney development proceeds towards the final phase, cortical stromal progenitors reduce in numbers and differentiate into mature cell types by P3.

One possible trigger for the initiation of terminal nephron differentiation could be that stroma-derived signals necessary for NPC renewal (FAT4) or inhibitors of NPC differentiation (Decorin) are altered in the terminal phase of nephrogenesis, skewing the balance towards differentiation. Understanding the changes in the molecular and cellular landscape of the nephrogenic niche during the cessation of nephrogenesis can have important clinical ramifications.

Building an integrated model of NPC self-renewal and differentiation will require a complete understanding of the molecular underpinnings governing these interactions at specific stages of nephrogenesis. Future work aimed at teasing out these signaling networks and cross-talk mechanisms will significantly expand our knowledge of renal organogenesis.

REFERENCES

1. Smith, H.W. (1951) The Kidney: Structure and Function in Health and Disease. New York: Oxford Univ. Press

2. Saxen, L. (1987). Organogenesis of the Kidney. Developmental and Cell Biology Series. Cambridge University Press

3. Boundless (2015) "Kidney Structure." Boundless Biology. Boundless

4. Bertram, F.G., Douglas-Denton, R.N., Diouf, B., Hughson, M.D., and Hoy, W.E. (2011). Human nephron number: implications for health and disease. *Pediatr Nephrol* 26, 1529-1553

5. Hershkovitz, D., Burbea, Z., Skorecki, K., and Brenner, B.M. (2007). Fetal programing of adult kidney disease: cellular and molecular mechanisms. *Clin J Am Soc Nephrol* 2, 334-342

6. Hokke, S.N., Armitage, J.A., Puelles, V.G., Short, K.M., Jones, L., Smyth, I.M., Bertram, J.F., and Cullen-McEwen, L.A. (2013). Altered Ureteric Branching Morphogenesis and Nephron Endowment in offspring of Diabetic and Insulin treated Pregnancy. *PLos ONE* 8:3

7. Fong, D., Denton, K.M., Moritz, K.M., Evans, R., and Singh, R.R. (2014). Compensatory responses to nephron deficiency: adaptive or maladaptive? *Nephrology*. 19, 119-128

8. Hartman, H.A., Lai, H.L., and Patterson, L.T. (2007) Cessation of renal morphogenesis in mice. *Dev. Bio*. 310, 379-387

9. Dressler, G.R. (2006). The cellular basis of kidney development. *Annu. Rev. Cell Dev. Biol.* 22, 509–529

10. Dressler, G.R. (2009). Advances in early kidney specification, development and patterning. *Development*. 136, 3863-3874

11. Little, M.H., and McMahon, A.P. (2012). Mammalian Kidney Development: Principles, Progress and Projections. *Cold Spring Harb Perspect Biol.* 4

12. Carroll, T. J., Park, J. S., Hayashi, S., Majumdar, A. and McMahon, A. P. (2005). Wnt9b plays a central role in the regulation of mesenchymal to epithelial transitions underlying organogenesis of the mammalian urogenital system. *Dev. Cell* 9, 283-29

13. Constantini, F., and Kopan, R. (2010). Patterning a complex organ: Branching Morphogenesis and Nephron Segmentation in Kidney Development. *Dev.Cell.* 18, 698-712

14. Boyle, S., and de Caestecker, M. (2006). Role of transcription factors in control of kidney development. *Am. J. Physiol. Renal. Physiol*. 291, F1-F8

15. Self, M., Lagutin, O. V., Bowling, B., Hendrix, J., Cai, Y., Dressler, G. R. and Oliver, G. (2006). Six2 is required for suppression of nephrogenesis and progenitor renewal in the developing kidney. *EMBO J.* 25, 5214-5228

16. Kobayashi, A., Valerius, M. T., Mugford, J. W., Carroll, T. J., Self, M., Oliver, G. and McMahon, A. P. (2008). Six2 defines and regulates a multipotent self-renewing nephron progenitor population throughout mammalian kidney development. *Cell Stem Cell* 3, 169-181

17. Boyle, S., Shioda, T., Perantoni, A.O., and de Caestecker, M. (2007). Cited1 and Cited2 are differentially expressed in the developing kidney but are not required for nephrogenesis. *Dev. Dyn*. 236, 2321–2330

18. Boyle, S., Misfeldt, A., Chandler, K. J., Deal, K. K., Southard-Smith, E. M., Mortlock, D. P., Baldwin, H. S. and de Caestecker, M. (2008). Fate mapping using Cited1-CreERT2 mice demonstrates that the cap mesenchyme contains self-renewing progenitor cells and gives rise exclusively to nephronic epithelia. *Dev. Biol.* 313, 234-245

19. Brunskill, E. W., Aronow, B. J., Georgas, K., Rumballe, B., Valerius, M. T., Aronow, J., Kaimal, V., Jegga, A. G., Yu, J., Grimmond, S. *et. al.*, (2008). Atlas of gene expression in the developing kidney at microanatomic resolution. *Dev. Cell* 15, 781-791

20. Mugford, J.M., Yu J, Kobayashi, A and McMahon, A.P. (2009). High-resolution gene expression analysis of the developing mouse kidney defines novel cellular compartments within the nephron progenitor population. *Dev. Bio* 333, 312-323

21. Brown, A.C., Adams, D., Caestecker, M., Yang, X., Friesel, R., and Oxburgh, L. (2011). FGF/EGF signaling regulates the renewal of early nephron progenitors during embryonic development. *Development* 138, 5099–5112

22. Hatini, V., Huh, S. O., Herzlinger, D., Soares, V. C. and Lai, E. (1996). Essential role of stromal mesenchyme in kidney morphogenesis revealed by targeted disruption of Winged Helix transcription factor BF-2. *Genes Dev.* 10, 1467-1478

23. Mendelsohn, C., Batourina, E., Fung, S., Gilbert, T. and Dodd, J. (1999). Stromal cells mediate retinoid-dependent functions essential for renal development. *Development* 126, 1139-1148

24. Levinson, R. S., Batourina, E., Choi, C., Vorontchikhina, M., Kitajewski, J. and Mendelsohn, C. L. (2005). Foxd1-dependent signals control cellularity in the renal capsule, a structure required for normal renal development. *Development* 132, 529-539

25. Humphreys, B.D., Lin, S.L., Kobayashi, A. Hudson,T.E., Nowlin, B.T., Bonventre, J.V. *et al.,* (2010). Fate tracing reveals the pericyte and not epithelial origin of myofibroblasts in kidney fibrosis. *Am J Pathol*. 176:85–97

26. Kobayashi, A., Mugford, J.W., Krautzberger, A.M., Naiman, N., Liao, J. and McMahon, A.P. (2014). Identification of a multipotent self-renewing stromal progenitor population during mammalian kidney organogenesis. *Stem Cell Rep*. 3, 650–62

27. Little, M.H. (2015). Kidney Development, Disease, Repair and Regeneration. Elsevier Academic press

28. Gao, X., Chen, X., Taglienti, M., Rumballe, B., Little, M. H. and Kreidberg, J. A. (2005). Angioblast-mesenchyme induction of early kidney development is mediated by Wt1 and Vegfa. *Development* 132, 5437-5449

29. Cain, J.E., Hatwig, S., Bertram, J.F. and Rosenblum, N.D. (2008). Bone morphogenetic protein signaling in the developing kidney: present and future. *Differentiation.* 76, 831-842

30. Derynck, R. and Zhang, Y. E. (2003). Smad-dependent and Smad-independent pathways in TGF-beta family signalling. *Nature* 425, 577-584

31. Shore, E.M., and Kaplan, F.S. (2010). Inherited human diseases of heterotropic bone formation. *Nat Rev Rheum*. 6,518-527

32. Dudley, A.T., and Robertson, E.J. (1997). Overlapping expression domains of bone morphogenetic protein family members potentially account for limited tissue defects in BMP7 deficient embryos. *Dev Dyn*. 208, 349–62

33. Dudley, A.T., Lyons, K. M. and Robertson, E. J. (1995). A requirement for bone morphogenetic protein-7 during development of the mammalian kidney and eye. *Genes Dev.* 9, 2795-2807

34. Luo, G., Hofmann, C., Bronckers, A. L. J. J., Sohocki, M., Bradley, A. and Karsenty, G. (1995). BMP-7 is an inducer of nephrogenesis, and is also required for eye development and skeletal patterning. *Genes Dev.* 9, 2808-2820

35. Dudley, A. T., Godin, R. E. and Robertson, E. J. (1999). Interaction between FGF and BMP signaling pathways regulates development of metanephric mesenchyme. *Genes Dev.* 13, 1601-1613

36. Godin, R.E, Takaesu, N.T, Robertson, E.J, Dudley, A.T. (1998). Regulation of BMP7 expression during kidney development. *Development.* 125:3473–82

37. Park, J.S., Ma, W., O'Brien, L.L., Chung, E., Guo, J.J., Cheng, J.G., et. al., (2012). Six2 and Wnt regulate self-renewal and commitment of nephron progenitors through shared gene regulatory networks. *Dev Cell*. 23(3):637–51

38. Tomita, M., Asada, M., Asada, N., Nakamura, J., Oguchi, A., Higashi, A.Y. *et. al.,* (2013). Bmp7 maintains undifferentiated kidney progenitor population and determines nephron numbers at birth. *PLoS One.* 8(8):e73554

39. Di Giovanni, V., Alday, A., Chi, L., Mishina, Y., and Rosenblum, N.D. (2011). Alk3 controls nephron number and androgen production via 4lineage-specific effects in intermediate mesoderm. *Development*. 138,2717–2727

40. Oh, S.P., Yeo, C.Y., Lee, Y., Schrewe, H., Whitman, M., and Li, E. (2002). Activin type IIA and IIB receptors mediate Gdf11 signaling in axial vertebral patterning. *Genes Dev*. 16, 2749–54

41. Oxburgh, L., Chu, G.C., Michael, S.K. and Robertson, E.J. (2004). TGF-β superfamily signals are required for morphogenesis of the kidney mesenchyme progenitor population. *Development* 131, 4593-4605

42. Blank, U., Seto, M.L., Adams, D.C., Wojchowski, D.M., Karolak, M.J., and Oxburgh, L. (2008). An in vivo reporter of BMP signaling in organogenesis reveals targets in the developing kidney. *BMC Dev Biol*. 8:86

43. Blank, U., Brown, A.C., Adams, D.C., Karolak, M.J. and Oxburgh, L. (2009). BMP7 promotes proliferation of nephron progenitor cells via a JNK-dependent mechanism. *Development* 136, 3557–3566

44. Kazama, I., Mahoney, Z., Miner, J.H., Graf, D., Economides, A.N., and Kreidberg, J.A. (2008). Podocyte-derived BMP7 is critical for nephron development. J. *Am. Soc. Nephrol.* 19, 2181–2191

45. Ikeya, M., Fukushima, K., Kawada, M., Onishi, S., Furuta, Y., Yonemura, S. *et. al.*, (2010). Cv2, functioning as a pro-BMP factor via twisted gastrulation, is required for early development of nephron precursors. *Dev Biol.* 337,405–14

46. Wu, J.W, Fairman, R., Penry, J., and Shi, Y. (2001). Formation of a stable heterodimer between Smad2 and Smad4. *J Biol Chem*. 276, 20688–94

47. Chacko, B.M., Qin, B.Y., Tiwari, A., Shi, G., Lam, S., Hayward, L.J. *et. al.*, (2004). Structural basis of heteromeric smad protein assembly in TGF-beta signaling. *Mol Cell*.15, 813–23

48. Dorey, K., and Amaya, E. (2010). FGF signaling: diverse roles during early vertebrate embryogenesis. *Development*. 137,3731-3742

49. Perantoni, A.O., Dove, L.F., and Karavanova, I. (1995). Basic fibroblast growth factor can mediate the early inductive events in renal development. *PNAS*. 92, 4696–700.

50. Barasch, J., Qia, J., McWilliams, G., Chen, D., Oliver, J.A., and Herzlinger, D. (1997). Ureteric bud cells secrete multiple factors, including bFGF, which rescue renal progenitors from apoptosis. *Am J Physiol*. 273, F757–67

51. Celli, G., LaRochelle, W.J., Mackem, S., Sharp, R., and Merlino, G. (1998). Soluble dominant-negative receptor uncovers essential roles for fibroblast growth factors in multi-organ induction and patterning. *EMBO J*. 17,1642–55

52. Poladia, D.P., Kish, K., Kutay, B., Hains, D., Kegg, H., Zhao, H., and Bates, C.M. (2006). Role of fibroblast growth factor receptors 1 and 2 in the metanephric mesenchyme. *Dev. Biol*. 291, 325–339

53. Ortega, S., Ittmann, M., Tsang, S.H., Ehrlich, M., and Basilico, C. (1998). Neuronal defects and delayed wound healing in mice lacking fibroblast growth factor 2. *PNAS*. 95, 5672–7.

54. Colvin, J.S., Green, R.P., Schmahl, J., Capel, B., and Ornitz, D.M. (2001). Male-to-female sex reversal in mice lacking fibroblast growth factor 9. *Cell*.104, 875–89.

55. Barak, H., Huh, S.H., Chen, S., Jeanpierre, C., Martinovic, J., Parisot, M. *et. al.*, (2012). FGF9 and FGF20 maintain the stemness of nephron progenitors in mice and man. *Dev Cell.* 22,1191–207

56. Karner, C.M., Das, A., Ma, Z., Self, M., Chen, C. Lum, L. *et. al.*, (2011). Canonical Wnt9b signaling balances progenitor cell expansion and differentiation during kidney development. *Development*. 138, 1247–57

57. Perantoni, A.O., Timofeeva, O., Naillat, F., Richman, C., Pajni-Underwood, S., Wilson, C., Vainio, S., Dove, L.F., and Lewandoski, M. (2005). Inactivation of FGF8 in early mesoderm reveals an essential role in kidney development. *Development*. 132, 3859–3871

58. Grieshammer, U., Cebrian, C., Ilagan, R., Meyers, E., Herzlinger, D. and Martin, G. R. (2005). FGF8 is required for cell survival at distinct stages of nephrogenesis and for regulation of gene expression in nascent nephrons. *Development* 132, 3847-3857

59. Sims-Lucas, S., Cusack, B., Baust, J., Eswarakumar, V.P., Masatoshi, H.,Takeuchi, A., et al. (2011). Fgfr1 and the IIIc isoform of Fgfr2 play critical roles in the metanephric mesenchyme mediating early inductive events in kidney development. *Dev Dyn.* 240,240–9

60. Weinstein, M., Xu, X., Ohyama, K., and Deng, C.X. (1998). FGFR-3 and FGFR-4 function cooperatively to direct alveogenesis in the murine lung. *Development.* 125, 3615–23

61. Yayon, A., Klagsbrun, M., Esko, J.D., Leder, P., and Ornitz, D.M.(1991). Cell surface, heparin-like molecules are required for binding of basic fibroblast growth factor to its high affinity receptor. *Cell*. 64, 841–8

62. Bullock, S.L., Fletcher, J.M., Beddington, R.S., and Wilson, V.A. (1998). Renal agenesis in mice homozygous for a gene trap mutation in the gene encoding heparan sulfate 2-sulfotransferase. *Genes Dev*. 12,1894–906

63. Ahn, S.Y., Kim, Y., Kim, S.T., Swat, W., and Miner, J.H. (2013). Scaffolding proteins DLG1 and CASK cooperate to maintain the nephron progenitor population during kidney development. *J Am Soc Nephrol*. 24, 1127–38

64. Cohen, A.R., Woods, D.F. Marfatia, S.M., Walther, Z., Chishti, A.H., and Anderson, J.M. (1998). Human CASK/LIN-2 binds syndecan-2 and protein 4.1 and localizes to the basolateral membrane of epithelial cells. *J Cell Biol*. 142(1):129–38

65. Hsueh, Y.P., Yang, F.C., Kharazia, V., Naisbitt, S., Cohen, A.R., et al. (1998). Direct interaction of CASK/LIN-2 and syndecan heparan sulfate proteoglycan and their overlapping distribution in neuronal synapses. *J Cell Biol*.142, 139–51

66. Maiga, O., Philippe, M., Kotelevets, L., Chastre, E., Benadda, S., Pidard, D., et al. (2011). Identification of mitogen-activated protein/extracellular signal-responsive kinase kinase 2 as a novel partner of the scaffolding protein human homolog of disc-large. *FEBS J*. 278, 2655–65

67. Habas, R., and David, I.B. (2005). Dishevelled and Wnt signaling: is the nucleus the final frontier? *J.Biol*. 4, 2-5

68. Park, J. S., Valerius, M. T. and McMahon, A. P. (2007). Wnt/beta-catenin signaling regulates nephron induction during mouse kidney development. *Development* 134, 2533-2539

69. Park, J.S., Ma, W., O'Brien, L.L., Chung, E., Guo, J., Cheng, J., Valerius, M.T., McMahon, J.A., Wong, W.H., and McMahon, A.P. (2012). Six2 and Wnt regulate self-renewal and commitment of nephron progenitors through shared gene regulatory networks. *Dev Cell*. 23,637–51

70. McMahon, A. P., Aronow, B. J., Davidson, D. R., Davies, J. A., Gaido, K. W., Grimmond, S., Lessard, J. L., Little, M. H., Potter, S. S., Wilder, E. L., et al. (2008). GUDMAP: the genitourinary developmental molecular anatomy project. *J. Am. Soc. Nephrol.* 19, 667-67

71. Stark, K., Vainio, S., Vassileva, G., and McMahon, A.P. (1994). Epithelial transformation of metanephric mesenchyme in the developing kidney is regulated by Wnt-4. *Nature* 372, 679–83

72. Tanigawa, S., Wang, H., Yang, Y., Sharma, N., Tarasova, N., Ajima, R., et al. (2011). Wnt4 induces nephronic tubules in metanephric mesenchyme by a non-canonical mechanism. *Dev Biol*. 352, 58–69

73. Burn, S.F., Webb, A., Berry, R.L., Davies, J.A., Ferrer-Vaquer, A., Hadjantonakis, A.K., et al. (2011). Calcium/NFAT signalling promotes early nephrogenesis. *Dev Biol.* 352, 288–98

74. Saadeddin, A., Babaei-Jabidi, R., Spencer-Dene ,B. and Nateri, A.S. (2009). The links between transcription, β -catenin/JNK signaling and carcinogenesis. *Mol. Cancer Res.* 7, 1189-1196

75. Guo, X. and Wang, X.F. (2009). Signaling crosstalk between TGF- β /BMP and other pathways. *Cell Res.* 19, 71-88

76. Iavarone, C., Catania, A., Marinissen, M.J., Visconti, R., Acunzo, M., *et al*. (2003).The platelet-derived growth factor controls c-myc expression through a JNK- and AP-1-dependent Signaling pathway. *J. Biol. Chem.* 278, 50024-50030

77. Karin, M., Liu, Z. and Zandi, E. (1997). AP-1 function and regulation. *Curr. Opin. Cell. Biol*. 9, 240-246

78. Shaulian, E. and Karin, M. (2001).AP-1 in cell proliferation and survival. *Oncogene*. 20, 2390

79. Jochum, W., Passegue, E and Wagner, E.F. (2001). AP-1 in mouse development and tumorigenesis. *Oncogene*. 20, 2401-2412

80. Hess, J., Angel, P. and Schorpp-Kistner, M. (2004). AP-1 subunits, quarrel and harmony among siblings. *J. Cell. Sci*. 117, 5965-5973

81. Angel, P., Hattori, K., Smeal, T. & Karin, M. (1998). The Jun proto-oncogene is positively autoregulated by its product, Jun/AP-1. *Cell.* 55, 875-885

82. Wisdom, R., Johnson, R.S. and Moore C. (1999). c-Jun regulates cell cycle progression and apoptosis by distinct mechanisms. *EMBO J.* 18,188–197

83. Schreiber, M. *et al*., (1999). Control of cell cycle progression by c-Jun is p53 dependent. *Genes Dev.* 13, 607-619

84. Couillard, M., and Trudel M. (2009). c-myc as a modulator of renal stem/progenitor cell population. *Dev. Dyn.* 238, 405-414

85. Bates, C.M., Kharzai, S., Erwin, T., Rossant, J. & Parada, L.F. (2000). Role of N-myc in the developing mouse kidney. *Dev. Bio.* 222, 317-325

86. Sorenson, C.M., Rogers, S.A., Korsmeyer, S.J., Hammerman, M.R. (1995). Fulminant metanephric apoptosis and abnormal kidney development in bcl2-deficienct mine. *Am J physiol Renal Phy.* 268, F73-81

87. Saifudeen, Z., Liu, J., Dipp, S., Yao, X., Li, Y., McLaughlin, N., Aboudehen, K., and El-Dahr, S.S. (2012). A p53-Pax2 pathway in kidney development: Implications for Nephrogenesis. *PLos One.* 7, 44869

88. Soriano, P. (1999) Generalized lacZ expression with the ROSA26 Cre reporter strain. *Nat. Genet.* 21, 70–71

89. Yang, X., Harkins, L.K., Zubanova, O, Harrington, A., Kovalenko, D., Nadeau, R.J., (2008). Overexpression of Spry1 in chondrocytes causes attenuated FGFR ubiquitination and sustained ERK activation resulting in chondrodysplasia. *Dev. Biol.* 321, 64

90. Liu, H., Xie, M., Schneider, M.D., & Chen, Z.J. (2006). Essential role of TAK1 in thymocyte development and activation. *PNAS.* 103, 11677-1168

91. Behrens, A., Sibilia, M., David, J., Möhle‐Steinlein, U., Tronche, F., Schütz, G., and Wagner. E.F. (2002). Impaired postnatal hepatocyte proliferation and liver regeneration in mice lacing c-jun in liver. *EMBO J*. 21, 1782-1790

92. Yamaguchi, K. *et al*., (1995). Identification of a member of MAPKKK Family as a potential mediator of TGF-β signal transduction. *Sci.* 270, 2088-2011

93. Okabe, M., Ikawa, M., Kominami, K., Nakanishi, T., and Nishimune, Y. (1997). 'Green mice' as a source of ubiquitous green cells. *FEBS Lett*. 407, 313–319

94. Aguilera, C. et al., (2011). c-Jun N-terminal phosphorylation antagonizes recruitment of the Mbd3/NuRD repressor complex. Nature. 13, 231-235

95. Murphy O.L., Smith, S., Chen, R., Fingar, C.D., and Blenis, J. (2002). Molecular interpretation of ERK signal duration by immediate early gene products. *Nat. Cell. Bio*. 2, 556-564

96. Vasanwala, F.H., Kusam, S., Toney, L.M. and Dent, A.L. (2002). Repression of AP-1 function: a mechanism for the regulation of Blimp-1 expression and B lymphocyte differentiation by the B cell lymphoma-6 protooncogene**.** *J Immunol.* 15,1922-1929

97. Tetsu, O. and McCormick, F. (1999). Beta-catenin regulates expression of cyclin D1 in colon carcinoma cells. *Nature.* 398, 422-426

98. Yu, P.B., Deng, D.Y., Lai, C.S., Hong, C.C., Cuny, G.D. et al. (2008). BMP type I receptor inhibition reduces heterotropic ossification. *Nat. Med*. 14, 1363-1369

99. Goncalves, A., & Zeller, R. (2011). Genetic analysis reveals an unexpected role of BMP7 in initiation of ureteric bud outgrowth in mouse embryos. *PLoS ONE*. 6,4

100. Davies, J., Hohenstein, P., Chang, C., Berry, R. (2014). A self-avoidance mechanism in patterning of the urinary collecting duct tree. *BMC Dev. Bio*. 14, 35

101. Dang, C.V. (1999). c-Myc target genes involved in Cell Growth, Apoptosis and Metabolism. *Mol. Cell. Biol*. 19, 1-11

102. Georgas, K. *et al*., (2009). Analysis of early nephron patterning reveals a role for distal RV proliferation in fusion to the ureteric tip via a cap mesenchyme-derived connecting segment. *Dev. Bio*. 332, 273-286

103. Hu, M.C., and Rosenblum, N.D. (2004). SMAD1, β-catenin and Tcf4 associate in a molecular complex with the Myc promoter in dysplastic renal tissue and cooperate to control Myc transcription. *Development*. 132, 215-225

104. Hussein, S.M., Duff, E.K. and Sirard, C. (2008). Smad4 and β-Catenin Co-activators Functionally Interact with Lymphoid-enhancing Factor to Regulate Graded Expression of Msx2. *J bio Chem*. 278, 48805–4881

105. Sakai, D., Tanaka, Y., Endo, Y., Osumi, N., Okamoto, H. and Wakamatsu, Y. (2005) Regulation of *Slug* transcription in embryonic ectoderm by β-catenin-Lef/Tcf and BMP-Smad signaling. Develop. *Growth Differ*. 47, 471–482

106. Teo, J., and Kahn, M. (2010) The Wnt signaling pathway in cellular proliferation and differentiation: A tale of two coactivators. *Adv. Drug. Deliv. Rev.* 62, 1149–1155

107. Motamedi, F.J. *et al*. (2014). WT1 controls antagonistic FGF and BMP-pSMAD pathways in early renal progenitors. *Nat Commun.* 17, 4444

108. Brunskill, E.W., Lai, H.L., Jamison, D.C., Potter, S.S., and Patterson, L.T. (2011). Microarrays and RNA-Seq identify molecular mechanisms driving the end of nephron production. *BMC Dev Biol* 11,15

109. Hinchliffe, S.A., Sargent, P.H., Howard, C.V., Chan, Y.F., and van Velzen, D. (1991). Human intrauterine renal growth expressed in absolute number of glomeruli assessed by the disector method and Cavalieri principle. *Lab Invest*. 64, 777–784

110. Rumballe, B., Georgas, K.M., Combes, A.N., Ju, A.L., Gilbert, T., and Little, M.H. (2011). Nephron formation adopts a novel spatial topology at cessation of nephrogenesis. *Dev Biol*. 360, 110-122

111. Xu, J., Wong, E.Y.M., Cheng, C., Li, J., Sharkar, M.T.K., Xu, C.Y., Chen, B., Sun, J., Jing, D., and Xu, P. (2014). Eya1 interacts with Six2 and Myc to regulate expansion of the nephron progenitor pool during nephrogenesis. *Dev. Cell.* 31, 434-447

112. Short, K.M. *et al*. (2014). Global Quantification of Tissue dynamics in the developing mouse kidney. *Dev. Cell.* 29, 188-202

113. Calegari, F., Haubensak, W., Haffner, C. and Huttner, W.B. (2005). Selective Lengthening of the cell cycle in the neurogenic subpopulation of neural progenitor cells during mouse brain development. *J Neurosci*. 25, 6533-6538

114. Mascré, G., Dekoninck, S., Drogat, B., Youssef, K.K., Brohée, S., Sotiropoulou, P.A., Simons, B.D., and Blanpain, C. (2012). Distinct contribution of stem and progenitor cells to epidermal maintenance. *Nature*. 489, 257-26

115. Lindstorm, N.O., Carragher, N.O., and Hohenstein, P. (2015). The Pi3K pathway balances self-renewal and differentiation of nephron progenitor cells through β -catenin signaling. *Stem cell Reports.* 4, 551-560

116. Itasaki, N., and Hoppler, S. (2010)**.** Crosstalk between WNT and BMP Signaling: A Turbulent Relationship. *Dev dyn* 239:16–33

117. Nohe, A., Hassel, S., Ehrlich, M., Neubauer, F., Sebald, W., Henis, Y.I., and Knaus, P. (2002). The mode of Bone Morphogenetic Protein (BMP) Receptor Oligomerization Determines Different BMP-2 signaling Pathways. *J biol Chem*. 277, 5330-5338

118. Guzman, A., Zelman-Femiak, M., Boergermann, J.h., Paschkowsky, S., Kreuzaler, P.A., Fratzl, P., Harmsn, G.S., and Knaus, P. (2012). SMAD versus non-SMAD signaling is determined by lateral mobility of BMP receptors. *J Biol Chem*. 287, 39492-39504

119. Xu, X., Han, J., Ito, Y., Bringas, P., Deng, C., and Chai, Y. (2008). Ectodermal Smad4 and p38 MAPK are functionally redundant in mediating TGF β /BMP signaling during tooth and palate development. *Dev. Cell*. 15, 322-329

120. Lane, J., Yumoto, K, Azhar, M., Ninomiya-Tsuji, J., Inagaki, M., Hu, Y., Deng, C., Kim J., Mishina, Y., and Kaartinen, V. (2015). Tak1, Smad4 and Trim33 redundantly regulate TGFβ-3signaling during palate development. *Dev bio*. 398, 231-241

121. Chang, H., Huylebroeck, D., Verschueren, K., Guo, Q., Matzuk, M.M., and Zwijsen, A. (1999). Smad5 knockout mice die at mid-gestation due to multiple embryonic and extra-embryonic defects. *Development.* 126, 1631-1642

122. Tremblay, K.D., Dunn, N.R., and Robertson, E.J. (2001). Mouse embryos lacking Smad1 signals display defects in extra-embryonic tissues and germ cell formation. *Development*. 128, 2609-21

123. Uchiyama, Y., Sakaguchi, M., Terabayashi, T., Inenaga, T., Inoue, S., Kobayashi, C., et al. (2010). Kif26b, a kinesin family gene, regulates adhesion of the embryonic kidney mesenchyme. *PNAS*. 107, 9240–5

124. Muller, U., Wang, D., Denda, S., Meneses, J.J., Pedersen, R.A., and Reichardt, L.F. (1997). Integrin alpha8beta1 is critically important for epithelial mesenchymal interactions during kidney morphogenesis. *Cell*. 88, 603-13

125. Massague, J. (2003). Integration of Smad and MAPK pathways: a link and a linker revisited. *Genes Dev*. 17, 2993-2997

126. Aubin, J., Davy, A., and Soriano, P. (2004). In vivo convergence of BMP and MAPK signaling pathways: impact of differential Smad1 phosphorylation on development and homeostasis. *Genes Dev*. 18, 1482-94

127. Kann, M., Bae, E., Lenz, M.O., Li, L., Trannguyen, B., Schumacher, V.A., Taglienti, M.E. et al., (2015). WT1 targets Gas1 to maintain nephron progenitor cells by modulating FGF signals. *Development.* 142, 1254-1266

128. Yang, Z., Yamasaki, K., Shirakata, Y., Dai, X., Tokumaru, S., Yahata, Y., Tohyama, M., Hanakawa, Y., Sayama, Y., and Hashimoto, K. (2006). Bone morphogenetic protein-2 modulates Wnt and frizzled expression and enhances the canonical pathway of Wnt signaling in normal keratinocytes. *J Dermatol Sci*. 42, 111-119

129. Fetting JL, Guay JA, Karolak MJ, Iozzo RV, Adams DC, Maridas DE, et al. (2014). FOXD1 promotes nephron progenitor differentiation by repressing decorin in the embryonic kidney. *Development* .141,17–27

130. Das, A., Tanigawa, S., Karner, C.M., Xin, M., Lum, L., Chen, C., Olson, E.N., Perantoni, A.O., and Carroll, T.J. (2013). Stromal-epithelial crosstalk regulates kidney progenitor differentiation. *Nat Cell Bio*. 15, 1035-1045

131. Bagherie-Lachidan, M., Reginensi, A., Pan, Q., Zaveri, H.P., Scott, D.A., Blencowe, B.J., Helmbacher, F., and McNeill, H. (2015). Stromal Fat4 acts non-autonomously with Dcsh1/2 to restrict the nephron progenitor pool. *Development*. 142, 2564-2573

132. Mao, Y., Francis-west, P., and Irvine, K.D. (2015). Fat4/Dchs1 signaling between stromal and cap mesenchyme cells influences nephrogenesis and ureteric bud branching. *Development*. 142, 2574-2585

BIOGRAPHY OF THE AUTHOR

Sree Deepthi Muthukrishnan was born in India. She graduated from high school in 2004. Following high school, Deepthi attended Stella Maris College and graduated with a Bachelor of Science degree in Plant Biology and Biotechnology in 2007. Upon graduation, she pursued a Master's degree in Molecular Biology and graduated on top of her class from the University of Madras in 2009. For her Master's degree, she performed her thesis work at the Indian Institute of Technology, Madras, and after graduation continued as a research assistant in the same laboratory to work on *Drosophila* models of Parkinson's disease until June 2010. Deepthi enrolled in the Graduate School of Biomedical Sciences and Engineering program at the University of Maine in August 2010. She joined Dr. Leif Oxburgh's laboratory for her dissertation work to study the role of growth factor signaling in the regulation of nephron progenitor cell self-renewal and differentiation using mouse models. Deepthi's thesis work has resulted in one first author and two co-author publications. She also has another manuscript under review. After graduation, Deepthi will join a post-doctoral fellowship position and continue to build her career in academic research. Deepthi is a candidate for the Doctor of Philosophy degree in Biomedical Sciences with a concentration in Cell and Molecular Biology from the University of Maine in May 2016.